



Master in Computational and Mathematical Engineering

Final Master Project (FMP)

# Simulation of the Mechanical Behaviour of a Historical Church

**Gerard Abril Sierra**
Simulation of Architectural Structures

**Montserrat Fernández Barta**
**Dr. Gerard Fortuny**

June of 2017

This work is subject to a licence of Recognition-NonCommercial- NoDerivs 3.0 Creative Commons

## INDEX CARD OF THE FINAL MASTER PROJECT

| | |
|---|---|
| **Title of the FMP:** | *Simulation of the Mechanical Behaviour of a Historical Church* |
| **Name of the author:** | *Gerard Abril Sierra* |
| **Name of the TUTOR:** | *Montserrat Fernández Barta* |
| **Name of the PRA:** | *Dr. Gerard Fortuny* |
| **Date of delivery:** | June/2017 |
| **Degree:** | *Master's Degree in Computer Engineering and Mathematics* |
| **Area of the Final Work:** | *Simulation of Architectural Structures* |
| **Language of the work:** | *English* |
| **Keywords** | *Finite Elements, homogenization, architecture* |


**Summary of the Work (maximum 250 words):** *With the purpose, context of application, methodology, results and conclusions of the work.*

This work is related to structural analysis by the finite element method.

The structure analysed is the upper part of the Church of San Bartolomé in Benicarló.

The analysis has been carried out by Salome-Meca, freeware software based on Linux Operative System.

Two models have been analysed, both models are equal except in their domes. In the model A, the dome is a half sphere while in the model B, the dome is a half dome but with nerves on its external face.

The loads applied to the model have been the own load and the superimposed load of the roofs.

Three structural analysis have been done. The first analysis has been a linear analysis, where all the loads have been applied to the model at the same time.

The second analysis has been a modal analysis, to find the five first modes of vibration of the structure.

Finally, the third analysis has been a non-linear analysis, where the loads have been applied incrementally taking into account second order effects.

The results obtained from these analyses show that the nerves of the dome allow to control stresses in the dome, reducing their values in the nerves and also vary the firsts modes of vibration of the structure.

As a complement to the study of the domes, the rest of structural parts have been analysed as well to know the behaviour of a masonry and brickwork structure.

**Abstract (in English, 250 words or less):**

The work has been organised starting with an introduction where the general notes about the work are gathered.

After this introduction there is a brief history of the church of San Bartolomé to follow with the description of the geometry of the church.

The following chapters are the scope of the work and the FEM model, where the two models are described and the materials and the loads are shown.

After the description of the analysis models, the results of the analysis are shown according to the analysis done, the linear analysis, the modal analysis and the non-linear analysis.

In this chapter where all the results are shown, it has been tried to show the maximum number of graphs of the stresses, reactions, deformations, etc. with their explanation.

At the end of the work some annexes contain the files to run the analysis and some intermediate steps of the non-linear analysis to understand better the evolution of the stresses in the models.

# Index

## List of figures

# 1. Introduction

## 1.1 Context and justification of the Work

Some historical buildings, and specifically, churches suffer deformations that go beyond the limits of the used materials.

To understand why the structure is in this state nowadays, it is necessary to study all the possible loads it has been under to find the reason of this deformations and cracks.

Due to these structures are historical monuments, studies of the materials are very difficult to do due to these tests imply destruction of the material or bore some structural elements.

The alternative is to do a structural analysis modelling the whole structure with finite elements and study the behaviour varying the inputs as the materials, loads, etc.

## 1.2 Aims of the Work

The aim of this work is to create two structural models with 3D finite elements and compare them to analyse the differences that appear if the structure is constructed with a dome as a half sphere or a dome as a half sphere with external nerves.

On the other hand, related to the analysis of the dome, it is the analysis of the rest of the structure.

Three analysis are planned, a linear analysis, a modal analysis and a non-linear analysis.

## 1.3 Approach and method followed

The method used to carry out this structural analysis has been to model the structures by the finite element modeller Salome and apply all the boundary conditions and loads by Code-Aster.

The mathematical calculation of the equation within the finite element method has been done by Code-Aster, creating files of commands telling the software what to do and what results they had to give.

Finally, the results have been displayed with Paraview, a visualization package integrated in Salome.

## 1.4 Planning of the Work

The analysis of a structure has a relative simple planning, once the dimensions of the structure are defined and set, the first step is to create the model (2D or 3D).

The second step is to mesh the volume of the structure.

After the mesh has been created, the model needs to be load with the actions that act over the structure (own load, superimposed loads, live loads, etc.).

Finally, when all the previous steps are finished, the stresses, the displacements and the reactions are calculated and the results analysed.

All these steps are linked in an only way, so it is not possible to change the order.

According to this the planning has been very simple to follow, knowing all the steps to do, the time has been able to be distributed according to the requirements of every step.

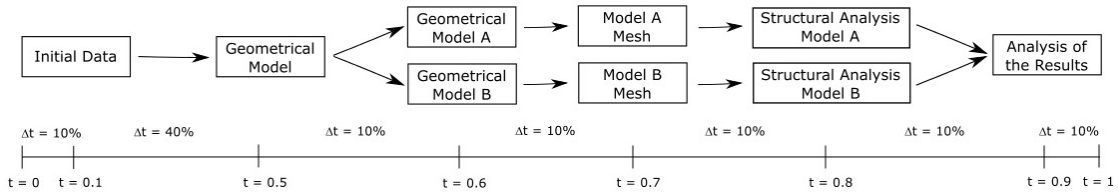


*Figure 1. Distribution of the work time.*

## 1.5 Brief summary of products obtained

The products obtained have been two structural models of the upper part of the church of San Bartolomé with only one different structural element, the dome.

In model A, the dome has no nerves and in the model B, the dome has nerves on its outer face.

## 1.6 Brief description of the others chapters of the memory

After this introduction there is a brief history of the church of San Bartolomé to follow with the description of the geometry of the church.

The following chapters are the scope of the work and the FEM model, where the two models are described and the materials and the loads are shown.

After the description of the analysis models, the results of the analysis are shown according to the analysis done, the linear analysis, the modal analysis and the non-linear analysis.

In this chapter where all the results are shown, it has been tried to show the maximum number of graphs of the stresses, reactions, deformations, etc. with their explanation.

At the end of the work some annexes contain the files to run the analysis and some intermediate steps of the non-linear analysis to understand better the evolution of the stresses in the models.

# 2. Emplacement & History

## 2.1 Emplacement

The church of Benicarló is placed in the town of Benicarló, a town in the East of Spain in the Comunitat Valenciana, in the province of Castelló, in the region of Baix Maestrat.

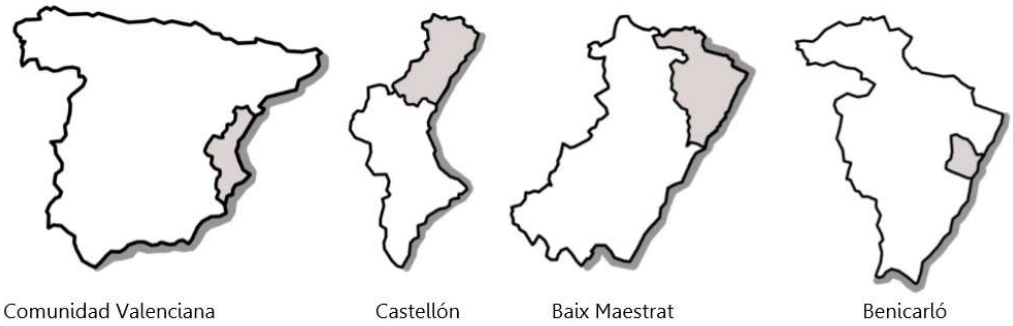


*Figure 2. Emplacement of Benicarló [b1].*

The church is located in the historic centre of the village, at the intersection of several streets as can be seen in the image 3. These streets are 1) San Bartolomé Square; 2) Ferreres Bretó Street; 3) Street of Alcalá de Xivert; 4) San Francesc Street; 5) Mare de Déu del Carme Street; 6) Ample Street; 7) Major Street 8) Sant Joaquim Street and 9) Street of the Pubill.

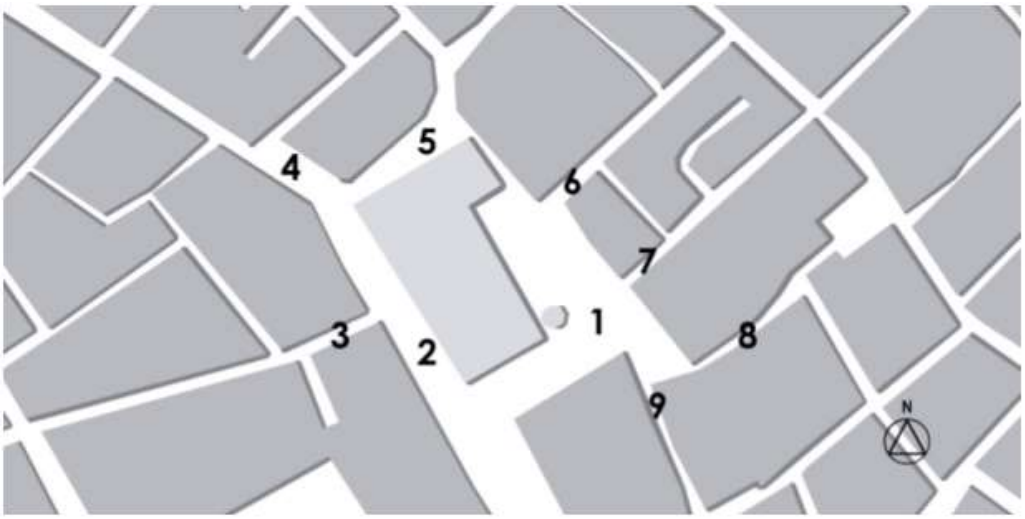


*Figure 3. Situation of the church [b1].*

## 2.2 Brief History of the Church of Benicarló

Before the current temple, in the same place, there was another which we know little. In 1392 the Council granted license to expand the bell tower. In 1473 the Valencian painter Pere Cabanes signs a contract to perform an altarpiece for the church. Between 1619 and 1633 works to widen the church are made.

The works of the present temple began on 25 May 1724 and concluded on 9 October 1743, although the altarpiece of the altar was not finished until 1818. Without any data of the architect, the foremen were Gaspar Castaruelles and Vicent Carbó. However, some features of the temple allow including the possibility that the works were started in the late seventeenth century, and after a break from work caused by the War of Succession, were continued in 1724.

During the first Carlina War became the main bastion of the city and it was affected in the roof and the side walls that were rebuilt from damage due to municipal initiative. During the Spanish Civil War all the furniture inside were burned.

In 2013 the church has been restored, on the occasion of being appointed as one view of the exhibition called "Pulchra Magistri. The splendour of the Maestrat". The restoring of the exterior has consisted to repair the roof and put again on place the blank edges of the central dome, cleaning facades, consolidation of masonry and driven segments, and recovering the original inner decoration

# 3. Geometry of the Church of Benicarló

## 3.1 Geometry of the Church

The church of Benicarló can be inscribed into a rectangle formed by a nave with lateral chapels on its short side, and on its long side 6 proportioned spans plus a 7th of smaller dimension. The proportions of the short side correspond to the central nave (with a module of 2A) and to the lateral chapels (with a module of A each).

The seven spans of the long side correspond: 4 of them to the lateral chapels (of module A each), 1 to the false cruise (of module 2A), 1 to the apse (of module 2A) and 1 dedicated to the present Sacristy (of module B).

Subsequently to this rectangle, another rectangle of smaller dimensions was attached to it, destined for the Communion Chapel, which does not correspond in modulation to the spans.

The church and the Chapel of the Communion were united through a volume, result of the extension of the Trasagrario. After the construction of each and every one of the volumes, the building was L-shaped, as it is today.

# 4. Scope of the FEM Analysis

## 4.1 Scope of the Analysis

The scope of this study is focused on the false cruiser of the church.

The false cruiser is a dome without lantern, supported over a blind octagonal drum supported on pendentives. There are two spaces at their laterals as continuation of the chapels on its sides. These spaces are covered by canyon vaults and blind lunettes to the interior and as the central nave to the exterior, with a gabled cover.

## 4.2 Description of the Dome and the Drum

The dome over the cruiser has been built with brickwork and it is leaned on four arches though a drum built with brickwork.

The construction process of the dome starts with four arches leaned on four columns.

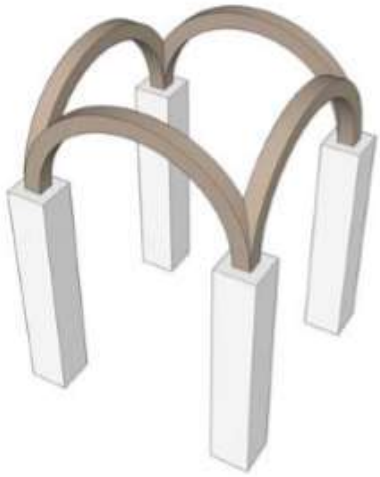

*Figure 4. Arches and columns [b1].*

On the corners of the arches, four pendentives are built with brickwork to receive the drum.

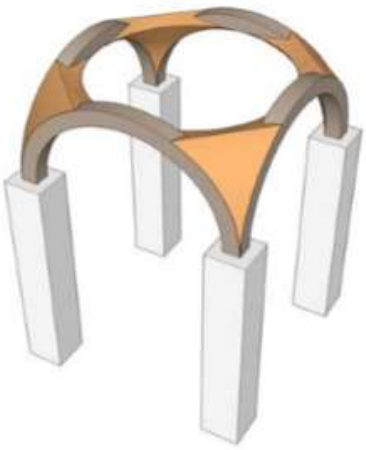

*Figure 5. Arches with pendentives [b1].*

The drum is composed of brickwork covered with mortar and over it a brickwork wall is built in conjunction with a mass to place the ring.

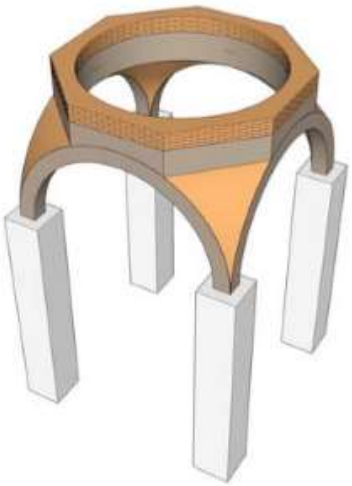

*Figure 6. Brickwork drum covered with mortar [b1].*

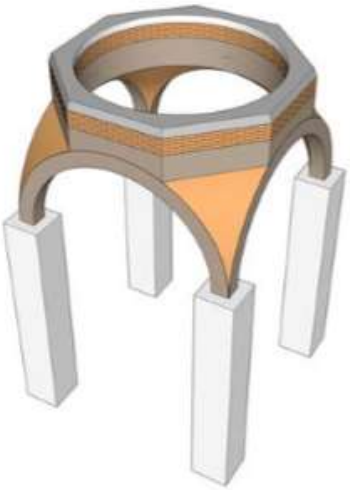

*Figure 7. Mass over the drum [b1].*

Over the drum a brickwork dome is constructed. Surrounding the dome a perimeter ring of wood is built to reduce the forces that the dome produces outwards due to its geometry.

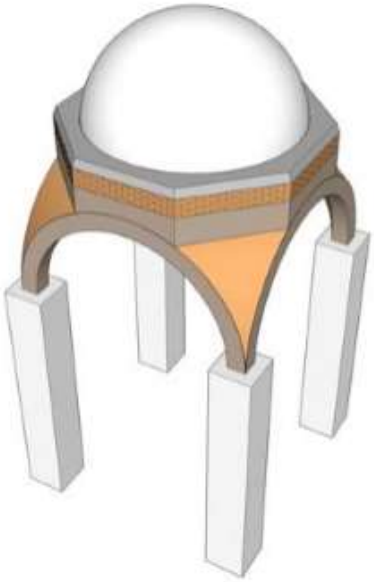

*Figure 8. Construction of the dome [b1].*

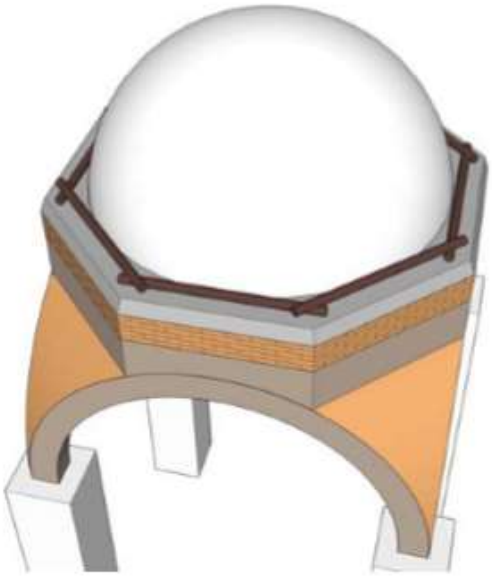

*Figure 9. Perimeter ring around the dome [b1].*

Over the dome the nerves are stacked out to later support the tiles of the roof.

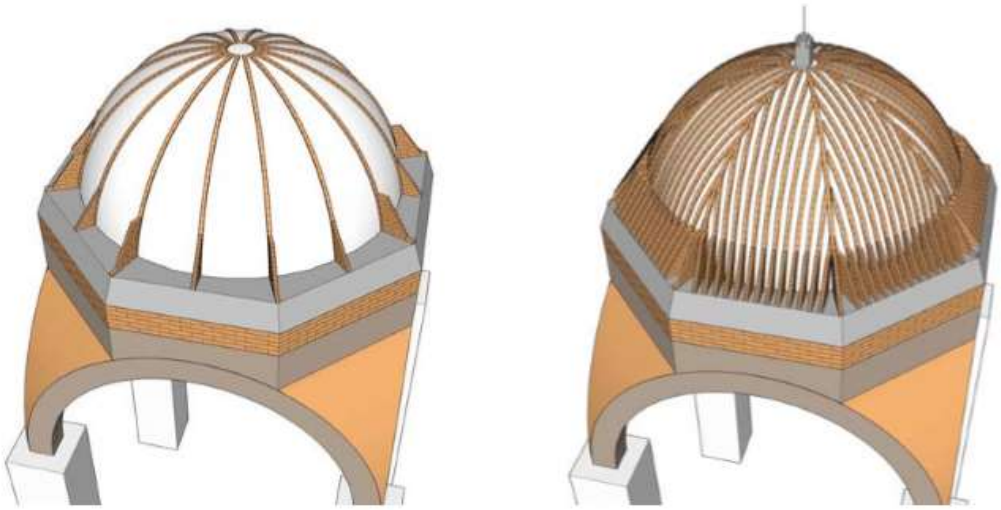

*Figure 10. Nerves of the dome [b1].*

The tiles are placed between the nerves of brickwork and are subjected with mortar. The dome is covered with blue and white tiles. Finally, the construction is finalized with a pinnacle.

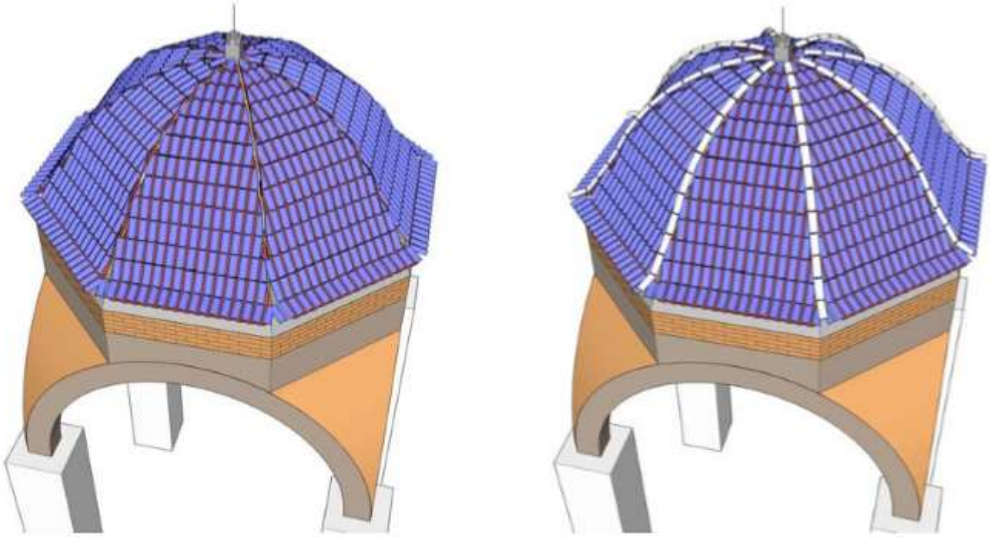

*Figure 11. Final view of the drum and the dome [b1].*

# 4. Analysis Model

## 4.1 Software Used

The software used is open-source software run on a Linux operative system, Ubuntu 16 [s1].

The geometry and the mesh has been created by Salome-Meca 2016.0_LGPL [s2], that provides a generic platform for Pre- and Post-Processing for numerical simulation.

The structural analysis through 3D finite elements has been carried out with Code-Aster [s3]. It is a software package for civil and structural engineering, finite element analysis, and numerical simulation in structural mechanics.

The code for run Code-Aster analysis has been written with Efficient [s4] or the wizard incorporated in the Code-Aster module for Salome, adapting the code when necessary by hand.

## 4.2 Geometry

### 4.2.1 Definition of the Models

The part of the church of Benicarló that has been analysed, as said before, is the false cruiser and the walls that it is connected to. The joint is composed by a dome, a ring under the dome, the connection of the ring with the columns through four arches, the lateral walls and the roof between these lateral walls.

The dimensions of the elements that will be analysed have been obtained by a topographical survey made with a 3D scanner.

Two models that are equal but the dome have been built. The first model (model A) has a dome without nerves, and the second model (model B) has a dome with external nerves that gives an additional rigidity.

The models are symmetric through axis X and Y. In the Figure 12 there is a 3D view of the whole model (Model A), in the Figure 13 a 3D view of the model B and in the Figure 14 a view of the model A and B upwards.

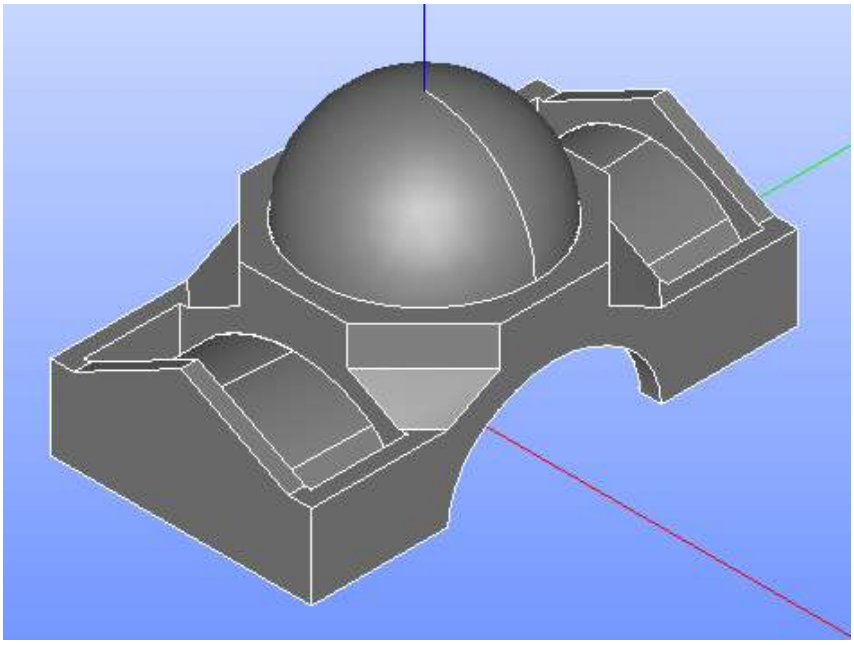

*Figure 12. 3D view of the model A*

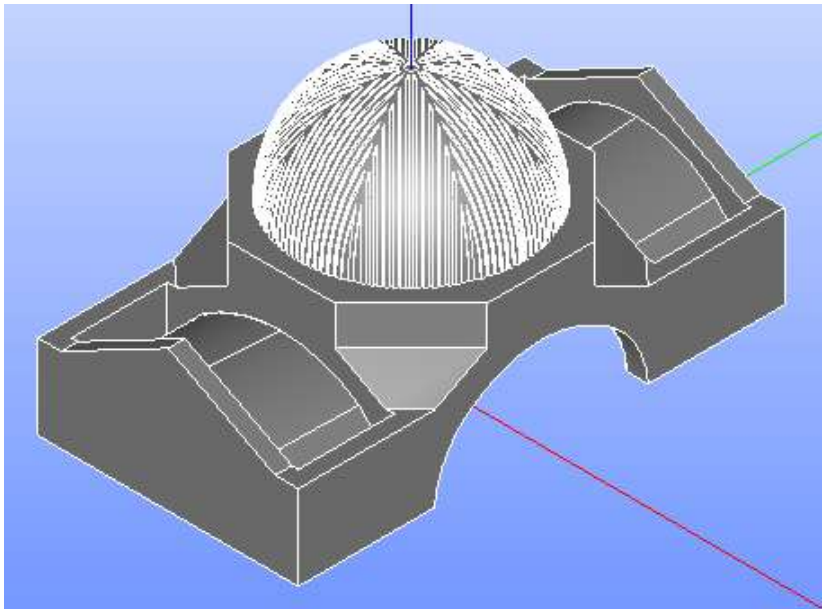

*Figure 13. 3D view of the model B*

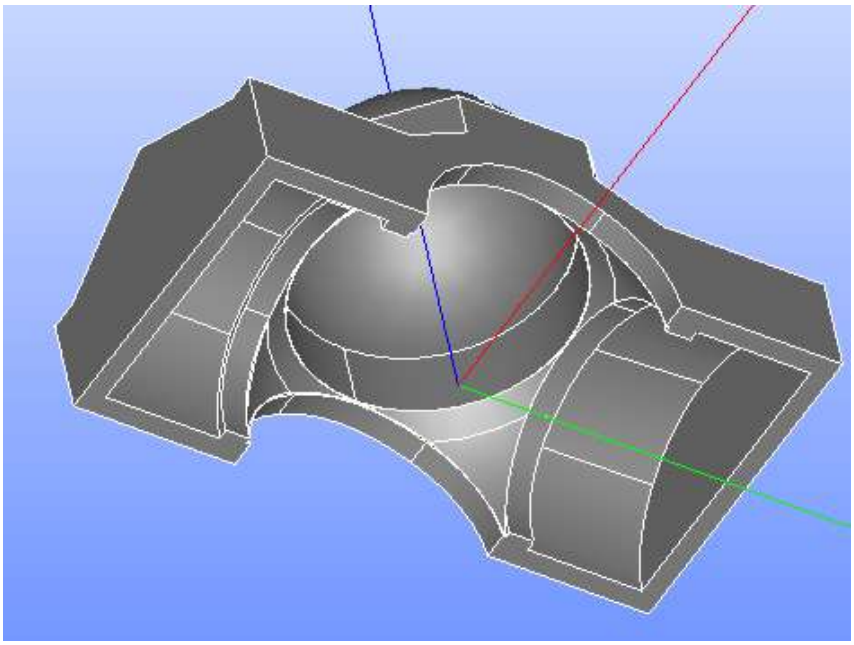

*Figure 14. Upwards view of the models A and B.*

### 4.2.2 Walls

The walls can be separated into two types, the first type is the transversal walls and the second type are the longitudinal walls. The two types of walls are shown at image 3.

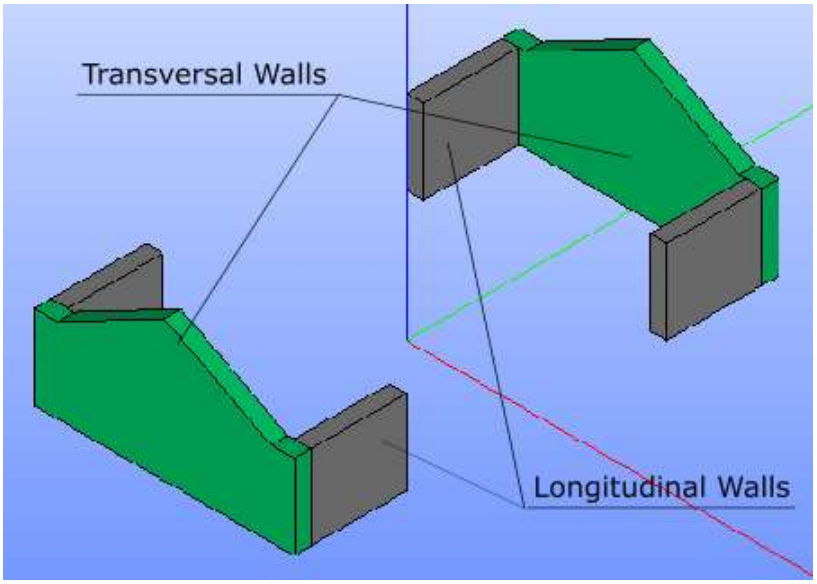


*Figure 15. Designation of the walls.*

The maximum height of the transversal walls is 8.01 m, with a total length of 14.84 m. The longitudinal walls have a height of 4.85 m with a length of 5.474 m. The distance between external faces of the transversal wall

is 27.69 m. The width of these walls varies slightly between 0.954 m for the longitudinal walls up to 0.95 m for the transversal walls. Figure 16 shows the dimensions.

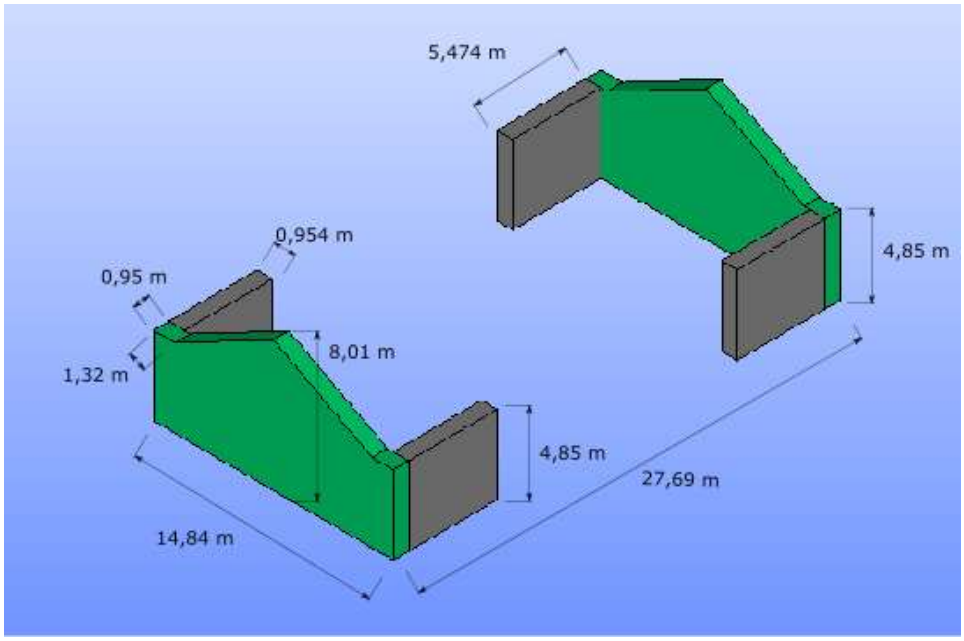


*Figure 16. Dimensions of the walls.*

### 4.2.3 Roofs

There are two roofs that lean on the longitudinal walls only with a width of 0.08 m placed symmetrically respect the centre of the drum. They have a slope towards the drum. The maximum height is 6.04 m at the inner face of the transversal walls and the minimum height is at the drum with a height of 5.68 m. The roofs only transmit forces to the longitudinal walls.

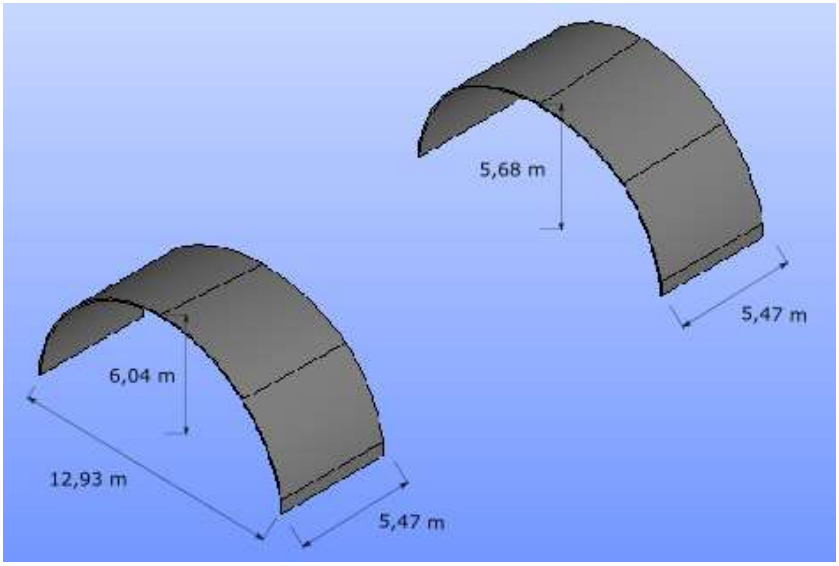


*Figure 17. Dimensions of the roofs.*

### 4.2.4 Drum

To simplify the names of the central part of the model, the ring under the dome and the part of the structure under this ring is gathered under the name of “drum”.

The bottom part of the drum can be defined as a box of 14.84 m x 14.84 m x 6.353 m. The ring has the same dimension in plan with a height of 2.20 m. The ring is the plan of the bottom part with a rotation of 45º. The centre hole has a diameter of 12.47 m.

The box that forms the bottom part of the drum is cut by three spheres that make the inner curvature. On its sides there are arcs with a height of 5.30 m and 5.22 m. All these dimensions can be seen in the Figure 18 and Figure 19.

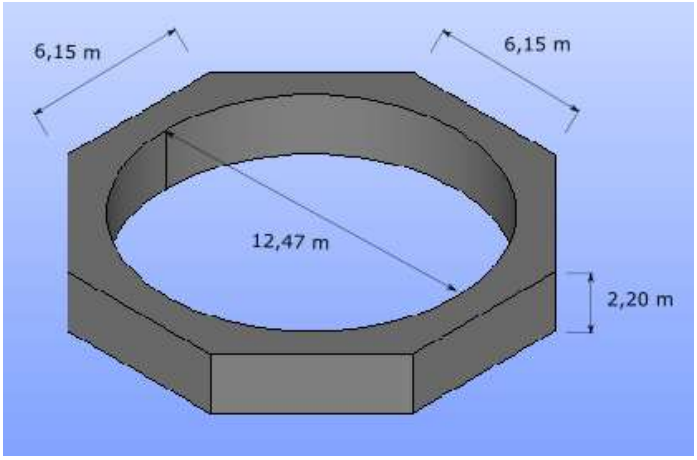


*Figure 18. Dimensions of the top part of the drum.*

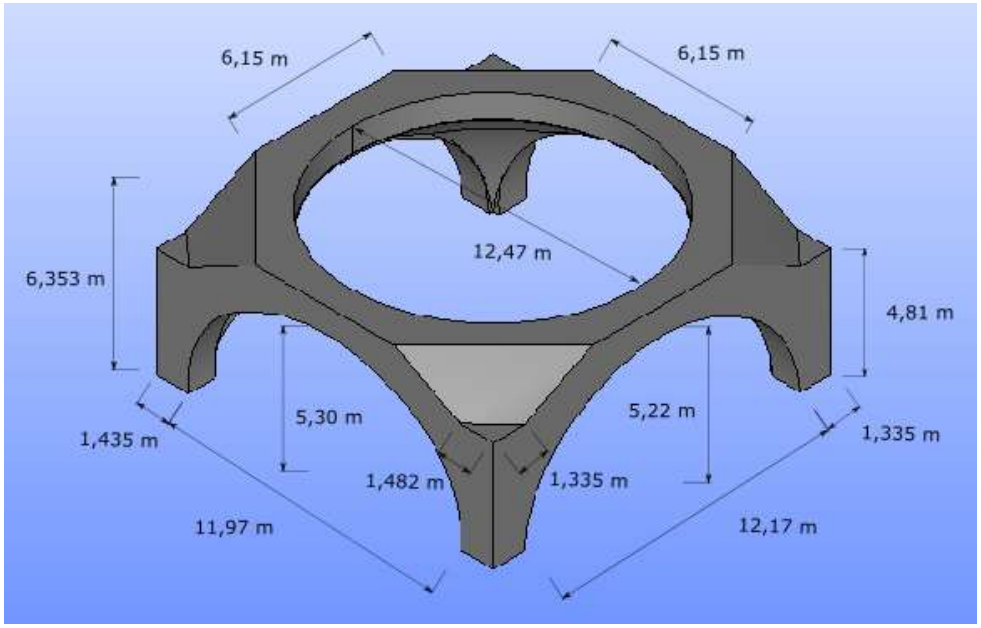


*Figure 19. Dimensions of the bottom part of the drum*

### 4.2.5 Dome

The dome is a half sphere of 12.63 m of outer diameter and a width of 0.08 m. The inner diameter is the same that the hole of the drum, 12.47 m. The dome without nerves is in Figure 20.

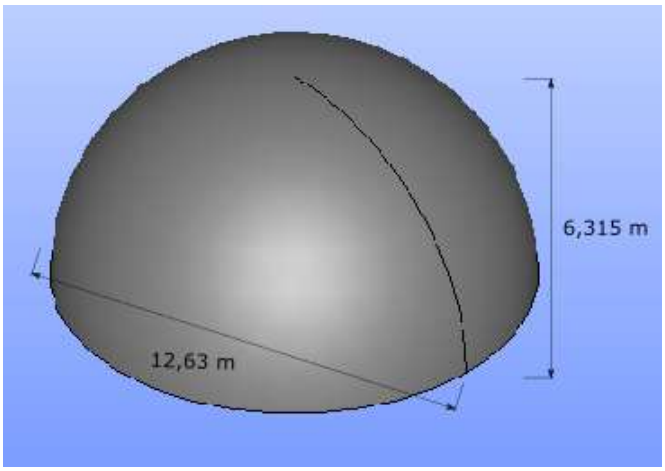


*Figure 20. Dome without nerves*

A second dome has been considered to study the effect of the nerves that the church has outside the dome. These nerves have a length of 20 cm, and a width of 7 cm increasing the diameter of the dome without nerves. These nerves are placed first in the corners of the ring dividing the dome in eight parts. Each part is divided by several nerves placed parallel with a distance between them of 12 cm. The Figure 21 and the Figure 22 show the dome with nerves and a detail of the nerves considered in the model.

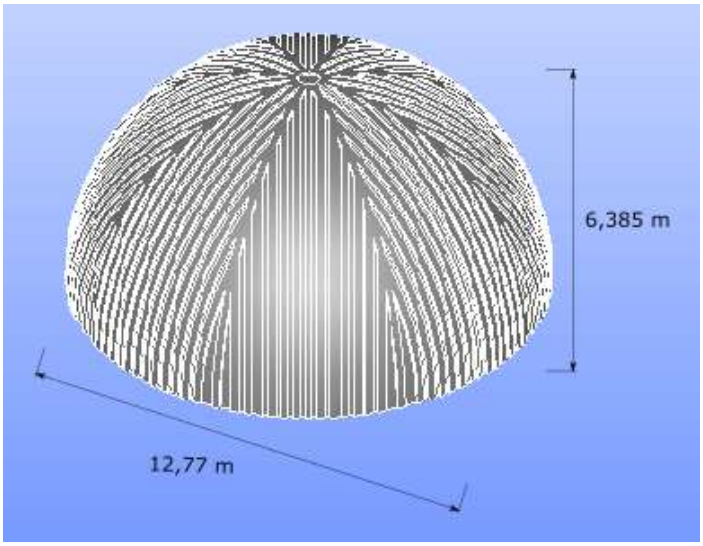


*Figure 21. Dome with nerves*

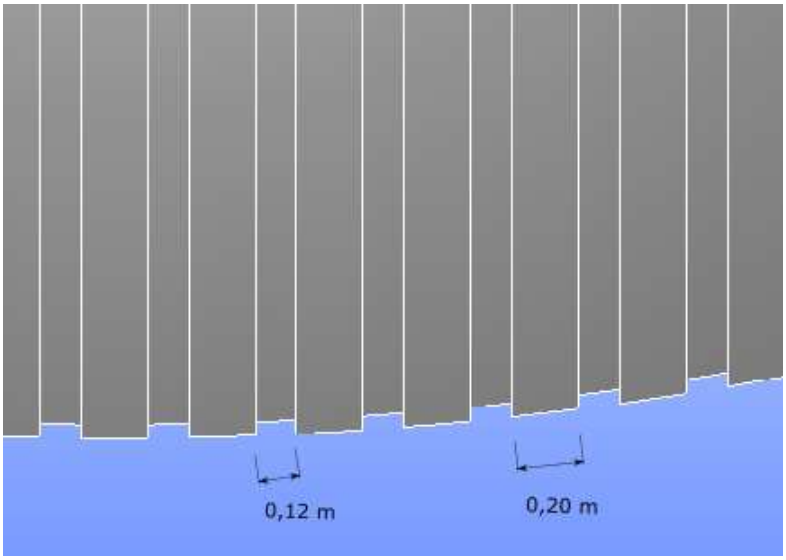


*Figure 22. Detail of the nerves of the dome.*

## 4.3 Materials

To analyse the structure, materials have been reduced to two kinds of materials. The first material considered is brickwork, which has been assigned to the dome and the lateral roofs. The second material is stone masonry and it has been assigned to the rest of the structure. Figure 23 shows the distribution of the materials.

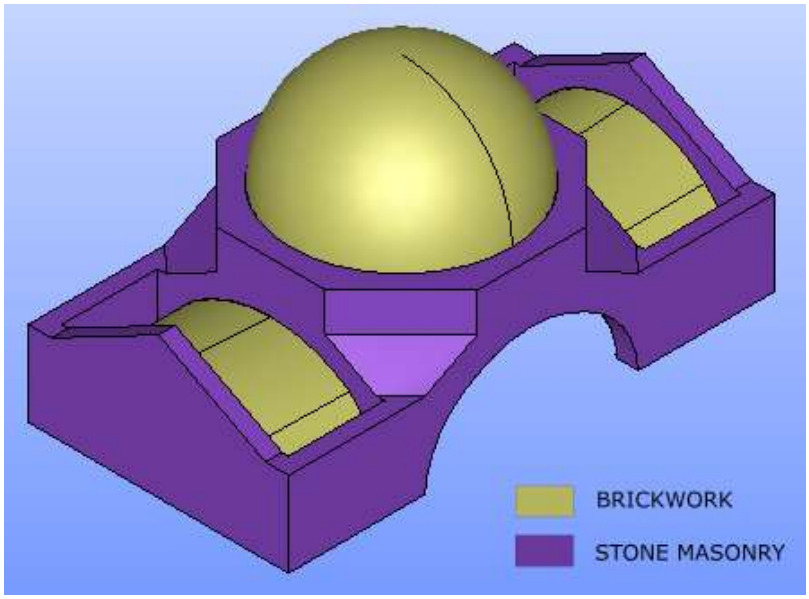


*Figure 23.Distribution of the materials*

As "in situ" tests have not been able to do, the characteristics of the materials have been taken from bibliography. The mechanical properties of these materials are gathered in the following table:

| | Elastic Modulus, E (MPa) | Poisson ratio, $\nu$ | Density, $\gamma$ (kN/m$^3$) | Tens. Str., $f_t$ (MPa) | Tens. Comp., $f_c$ (MPa) |
|---|---|---|---|---|---|
| Brickwork | 2000 | 0.20 | 17.00 | 0.07 | 1.00 |
| Stone Masonry | 5000 | 0.20 | 22.00 | 0.07 | 1.00 |

*Table 1. Mechanical Properties of the materials*

## 4.4 Loads

The loads considered are the own weights of the different construction materials, so the loads will be the own weight of the brickwork and the stone masonry and the superimposed loads of the roof.

On the lateral, the covering with wood structure and Arabic tiles lean on the longitudinal walls. On the dome, tiles are supported by brickwork nerves.

Own weights:

- Brickwork: 17.0 kN/m$^3$.
- Stone masonry: 22.0 kN/m$^3$.

Superimposed loads:

- Dome without nerves: 3.0 kN/m$^2$.
- Dome with nerves: 2.0 kN/m$^2$.
- Sloped lateral roofs: 3.0 kN/m$^2$.

## 4.5 Boundary Conditions

The boundary conditions applied to the model has been the restraint of the movements Ux, Uy and Uz of the base of the walls and the central part. In the Figure 24 the base that has its movements restrained is shown.

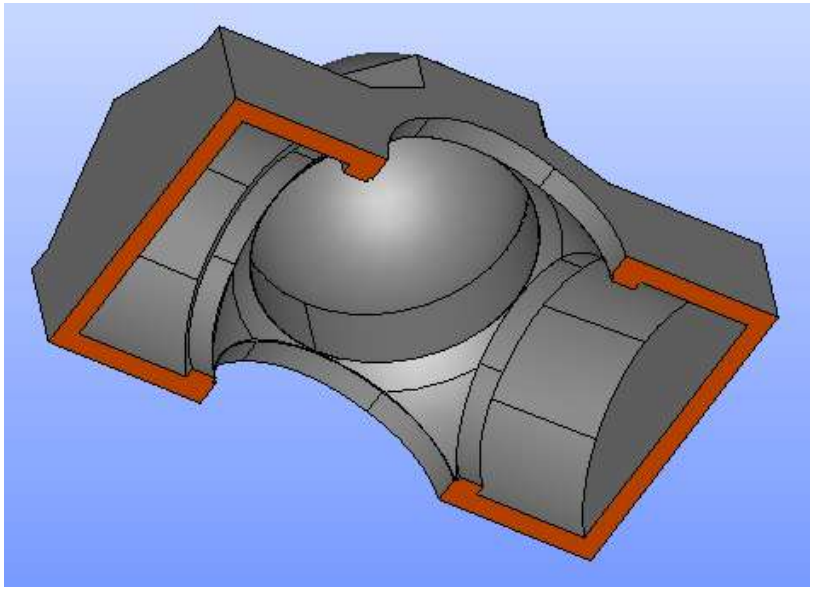

*Figure 24. Boundary conditions on the model*

## 4.6 Mesh

The mesh for these model have to be able to take into account the different widths of the elements and be denser where it is necessary to be able to model correctly the different geometries, especially the geometry of the dome with nerves.

For these reasons the type of mesh chosen is a mesh of tetrahedrons, using the 'Netgen 1D-2D-3D' algorithm. The adopted parameters to run this algorithm have been sized between 0.65 for the biggest and 0.045 for the smallest. Figure 25 shows the parameters considered to mesh the model.

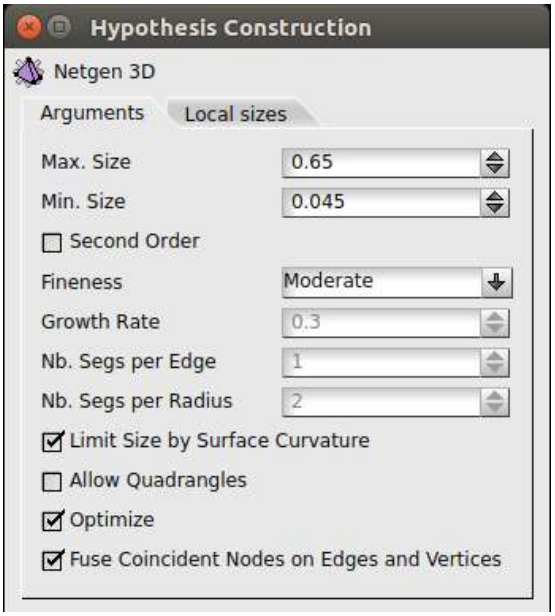


*Figure 25. Parameters used in the Netgen 1D-2D-3D algorithm*

At the moment of joining all the parts in the model, before meshing it, the lateral roofs have been separated from the transversal walls to avoid them to pass forces to the transversal walls.

### 4.6.1 Model A

This model supposes that the dome has not nerves that increase its stiffness. As the dome do not have nerves, the smallest tetrahedrons concentrates basically on the surface in contact with the drum.

After applying the algorithm, we obtain a model with 70,105 nodes and 256,894 tetrahedrons. In the Figure 26 there is the summary of the elements that compose the mesh. In the Figure 27 there is an image of the model meshed.

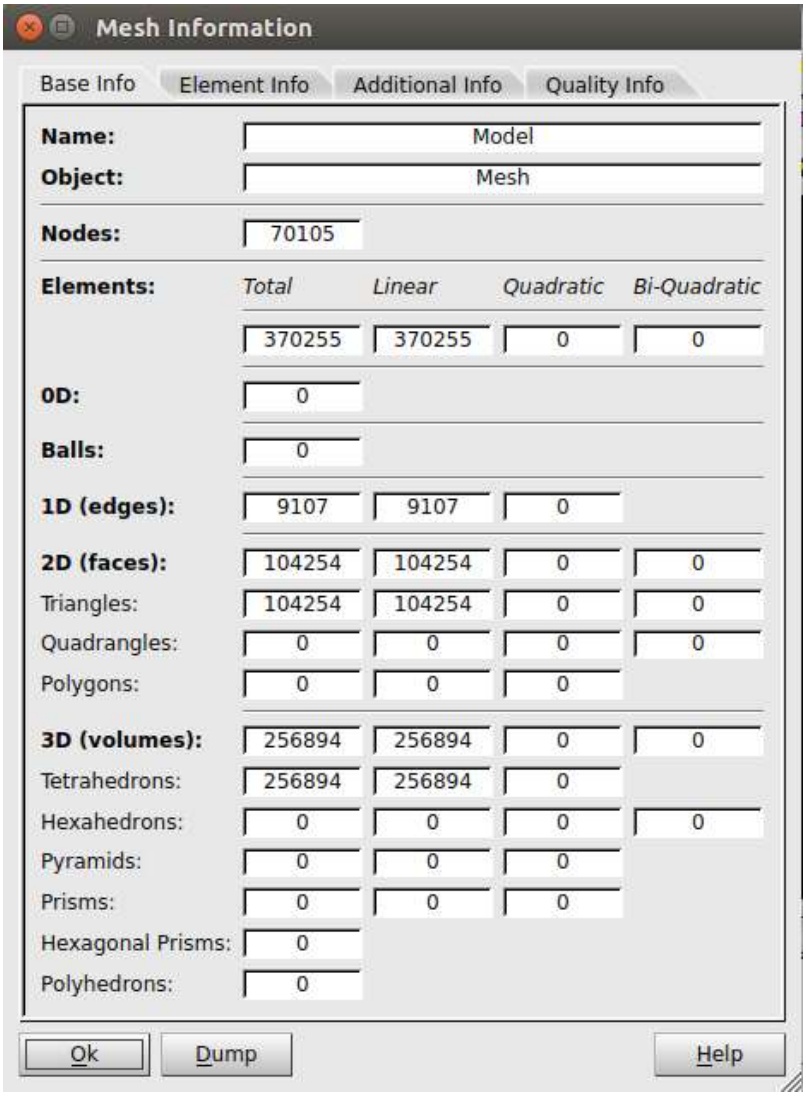


*Figure 26. Summary of the mesh computing of the model A*

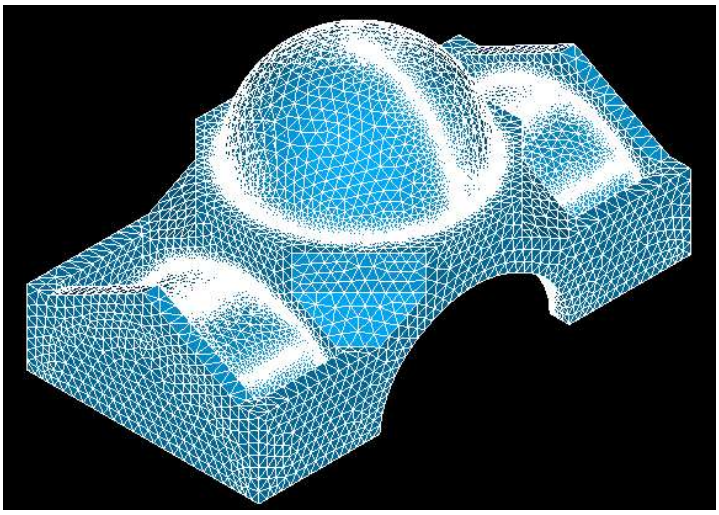

*Figure 27. Mesh of the model A*

### 4.6.2 Model B

This model supposes that the dome has nerves that increase its stiffness. As the dome has nerves, all the nerves have been meshed with the smallest tetrahedrons, as well as on the surface in contact with the drum.

After applying the algorithm, we obtain a model with 139,499 nodes and 467,675 tetrahedrons. It can be seen that the number of nodes has been multiplied by two respects to the first model and the number of tetrahedrons has been multiplied around 1.8 times respect to the first model. This is caused by the addition of the nerves.

In the Figure 29 there is the summary of the elements that compose the mesh. In the Figure 28 there is an image of the model meshed and in the Figure 30 there is a zoom showing the mesh of the nerves.

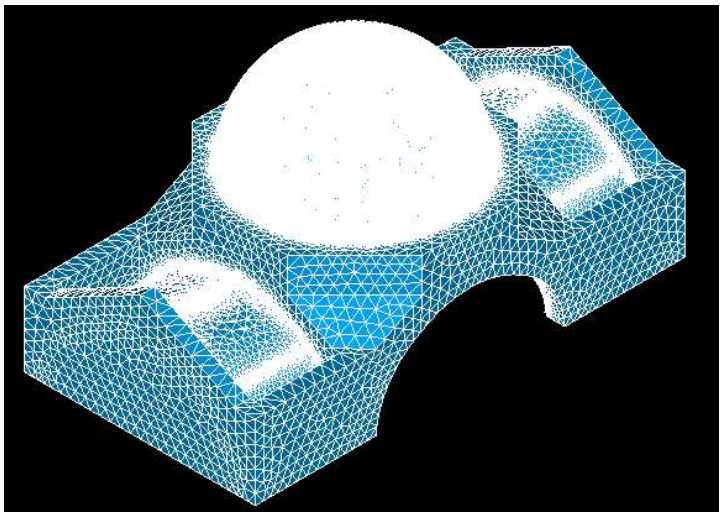

*Figure 28. Mesh of the model B*

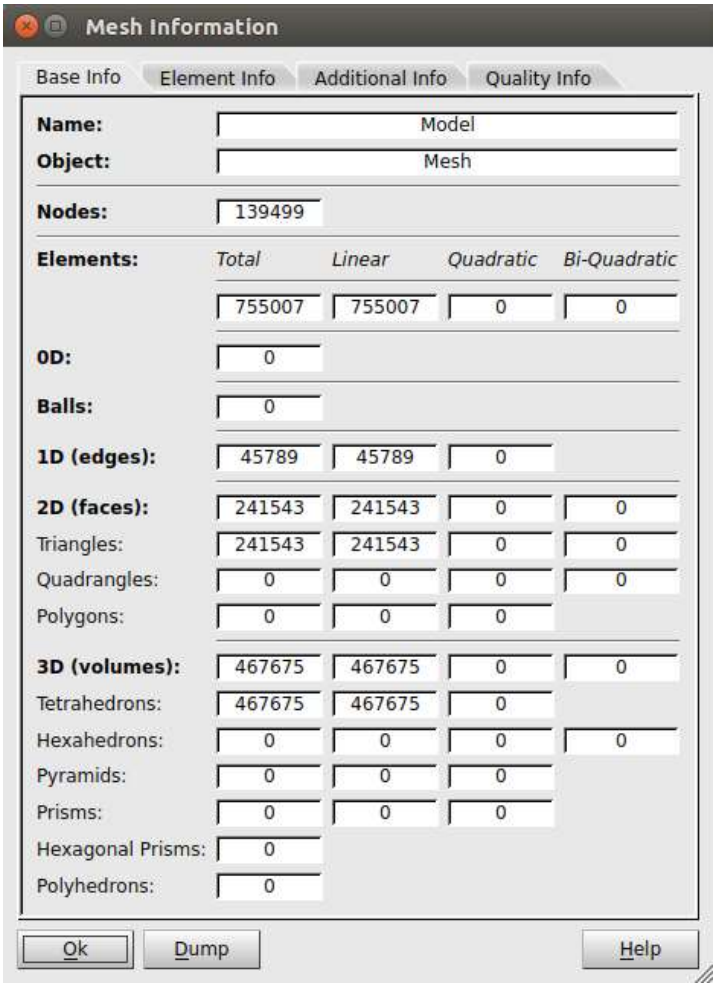


*Figure 29. Summary of the mesh computing of the model B.*

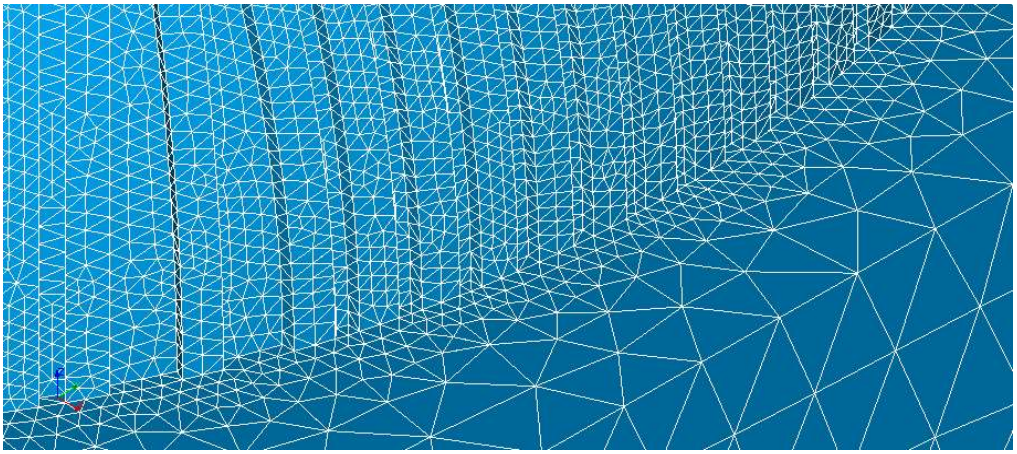

*Figure 30. Detail of the mesh of the nerves in model B*

# 5. Analysis

## 5.1 Introduction

To compare the effect of the nerves on the dome, three analyses have been carried out.

The first analysis has been a linear analysis where the equations do not take into account previous deformations in the analysis.

The second analysis has been a modal analysis to get the natural frequencies of the structure.

And the third analysis carried out is a non-linear analysis, where, on the contrary to the linear analysis, we take into account previous deformations in the analysis.

At the end of the document, in the Annexes there are all the Code-Aster files used for this study.

## 5.2 Linear Analysis

### 5.2.1 Description of the Analysis

The linear analysis is a structural analysis where all the loads are applied to the model at the same time and the forces are calculated without taking into consideration second order effects.

In this analysis the loads applied are the own weight and the weight of the construction elements that are not the structural resistant ones.

### 5.2.2 Reactions

As a first analysis, it is necessary to analyse the results obtained for the reactions at the base of the models.

The main reactions are the vertical reactions due to they are all the loads we have applied to the model. For model A and B, the reactions are:

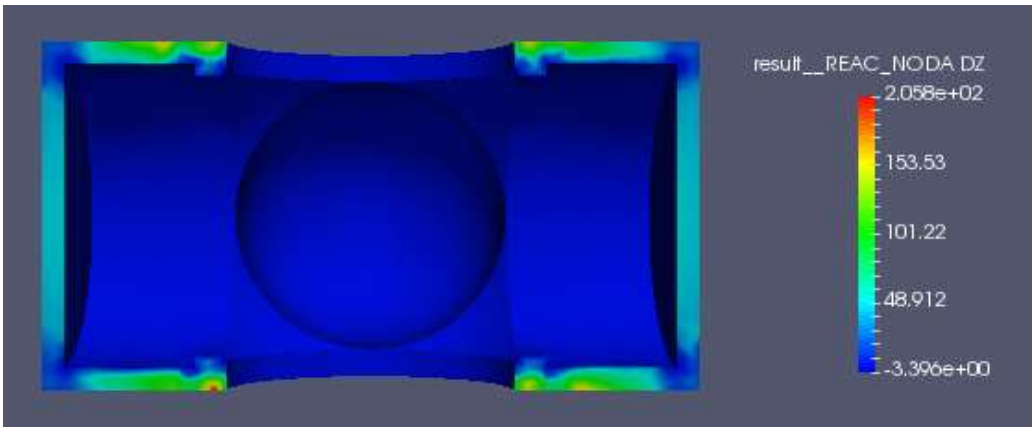


*Figure 31. Vertical reactions in model A*

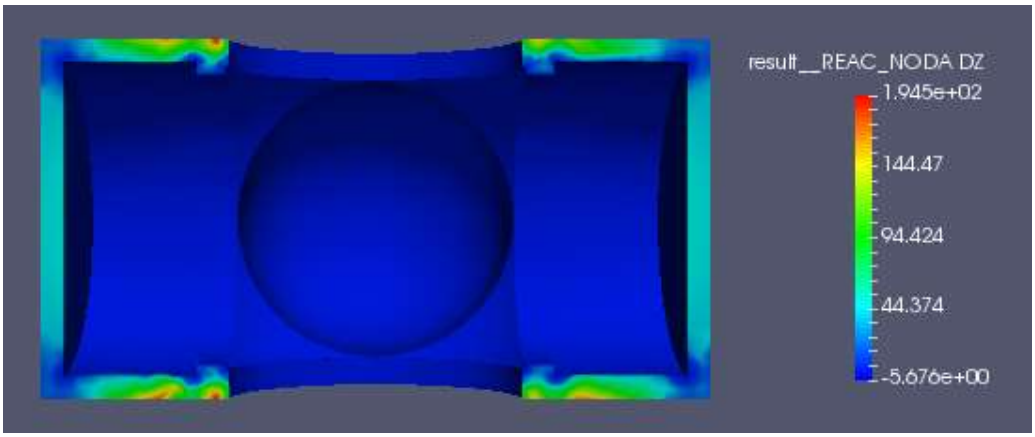


*Figure 32. Vertical reactions in model B*

As it can be seen in the Figure 31 and Figure 32, the biggest reactions are under the four arches that support the drum and the dome and at the longitudinal walls due to they have to support all the weight that the roofs transmit to them (these roofs do not lean on the transversal walls or the arches under the dome). Positive values tell us that the reactions under the structure are Z+, which means that the structure is compressing the structure under it.

The horizontal reactions can be following X axis or Y axis. The results for X axis are in the Figure 33 and Figure 34, and the results for Y axis are in Figure 35 and Figure 36.

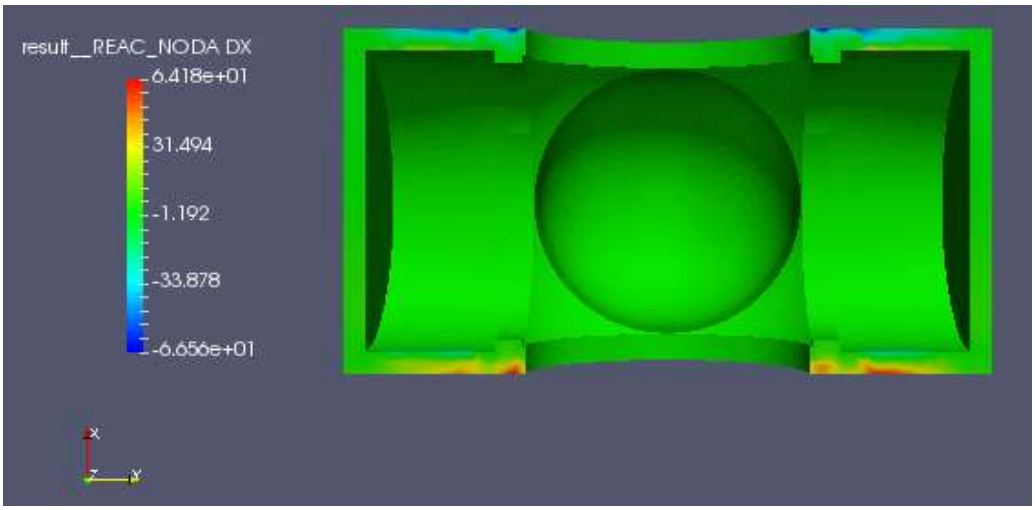


*Figure 33. Horizontal reactions for X axis in model A*

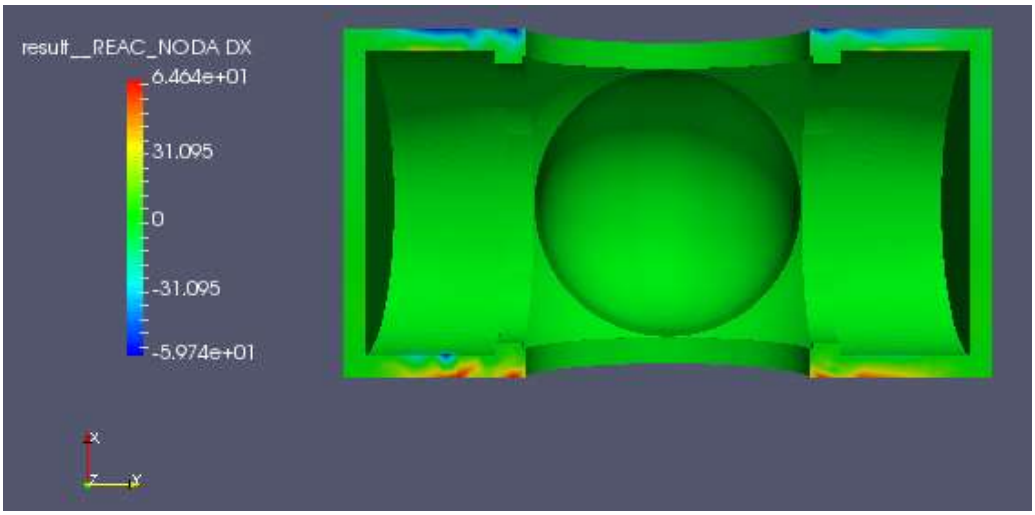


*Figure 34. Horizontal reactions for X axis in model B*

As can be seen on the figures for the reactions for X axis, the positive values (red) are in the longitudinal walls at the bottom part, and the negative values (blue) are in the longitudinal walls at the top part.

This behaviour is the result of the geometry of the roofs that actually are arches that push outwards the walls at the base where they are joined.

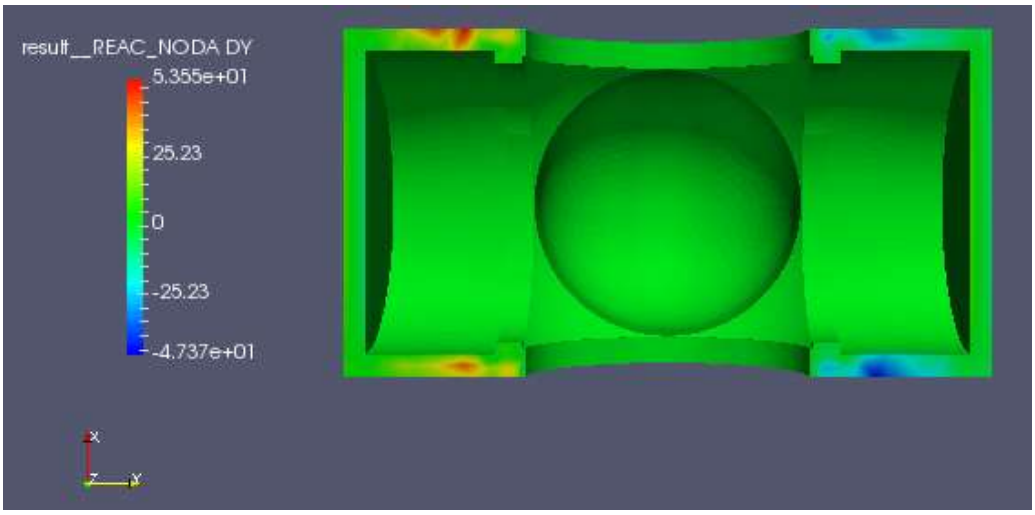


*Figure 35. Horizontal reactions for Y axis in model A*

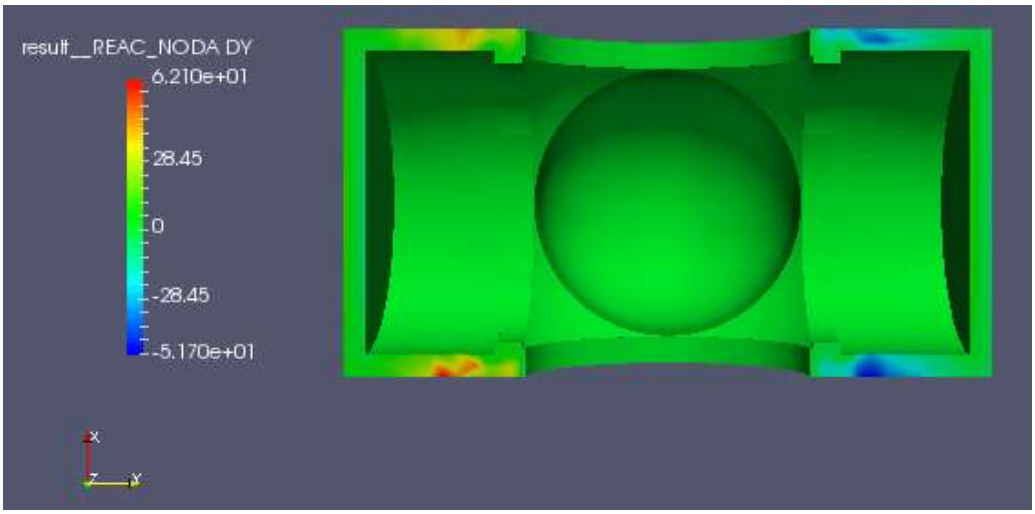


*Figure 36. Horizontal reactions for Y axis in model B*

As can be seen on the figures for the reactions for Y axis, the positive values (red) are on the left and the negative values (blue) are on the right part of the image.

This means that the reactions are avoiding the longitudinal walls to open outwards. These reactions are concentrated near the central arches because the vertical load of the dome and the drum falls directly over the arches and these arches, working by shape, try to widen the bottom part of the arch pushing the closest part of the longitudinal walls.

These horizontal forces produce horizontal shear forces that have to be resisted mainly by the mortar of the stone masonry.

### 5.2.3 Displacements

The max vertical displacement is about 2.3 cm and it is produced on the roofs due to they are the maximum flexible elements. Also can be seen that the roofs have a slightly movement upwards on their sides that correspond to the typical deformation of an arch structure under symmetrical vertical loads.

On model B, the increase of weight because of the nerves of the dome makes to the centre part to descend a bit more than in the model without nerves. The results of vertical deflections are in Figure 37 and Figure 38.

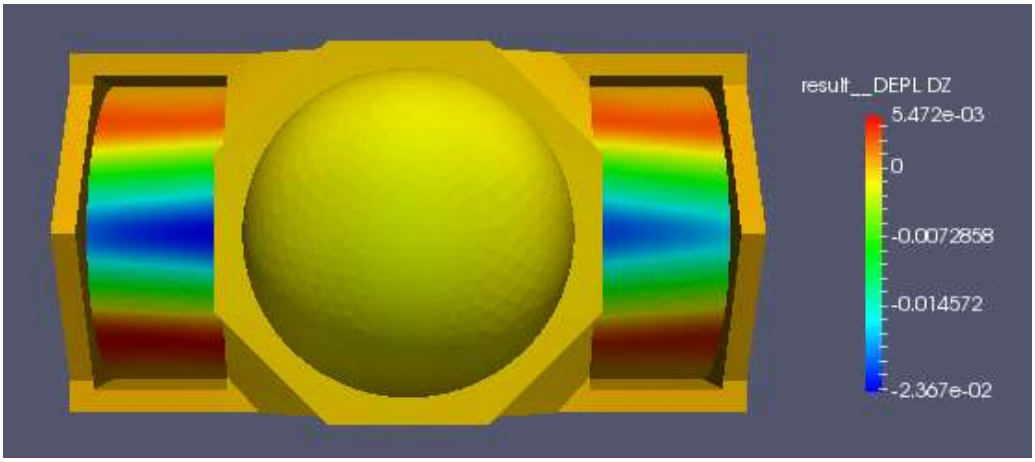


*Figure 37. Vertical displacements of the model A*

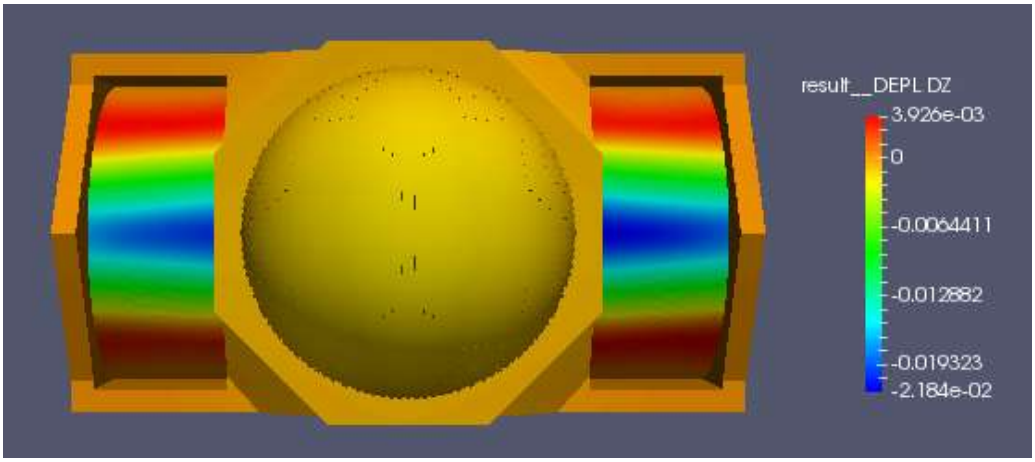


*Figure 38. Vertical displacements of the model B*

The horizontal movement of the roofs perpendicular to the walls is shown on Figure 39 and Figure 40. The zones where the arches move horizontally outwards coincide with the zones with vertical positive displacement as expected.

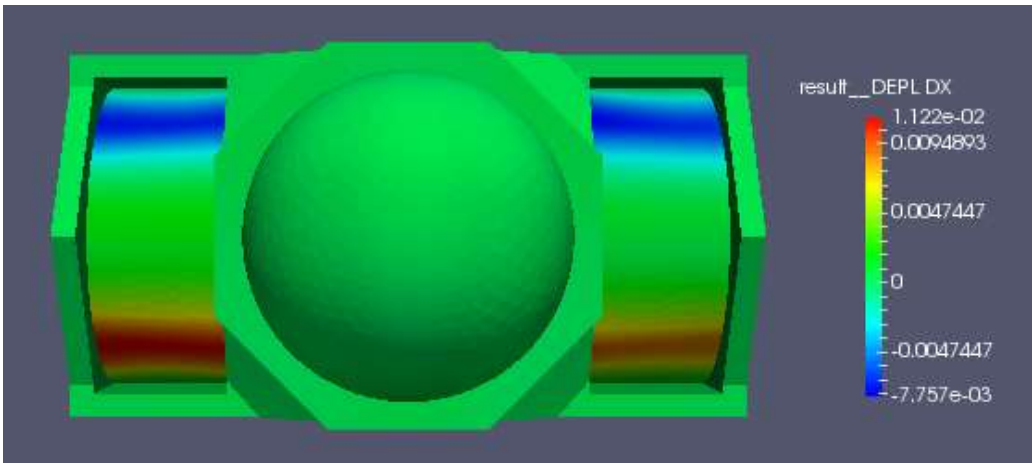


*Figure 39. Horizontal displacement (X axis) of the model A*

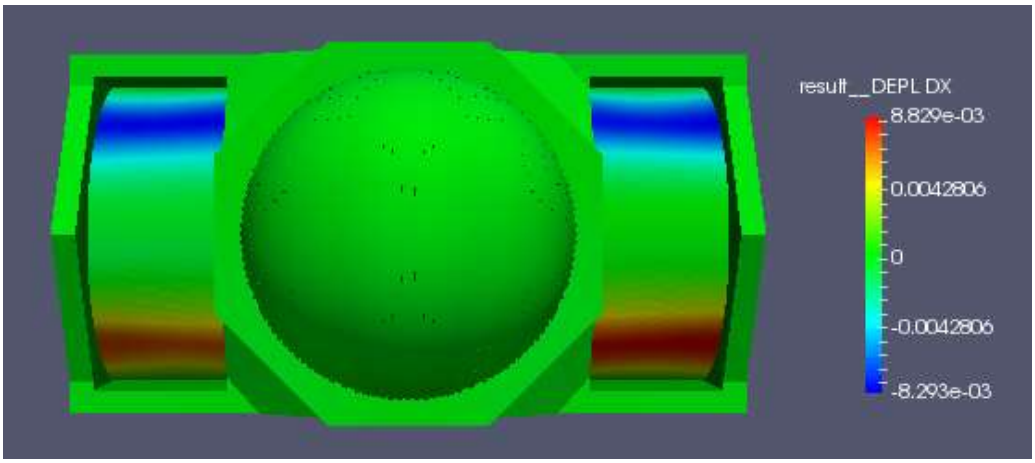


*Figure 40. Horizontal displacement (X axis) of the model B*

### 5.2.4 Stresses

The materials of this structure are materials that have a different resistance against compression stresses and tension stresses. Their value is indicated at chapter 4.3 Materials.

In this analysis we will try to identify the possible points where the structure could fail or be susceptible to crack according to the results of a linear analysis.

In the following figures the stresses according to the axes X, Y and Z are shown for the model without nerves in the dome and for the model with nerves in the dome. Compressions are negative values and tensions are positive values.

The results are for several critical sections where the normal tensions to cross sections are analyzed.

### 5.2.4.1 Normal Stresses

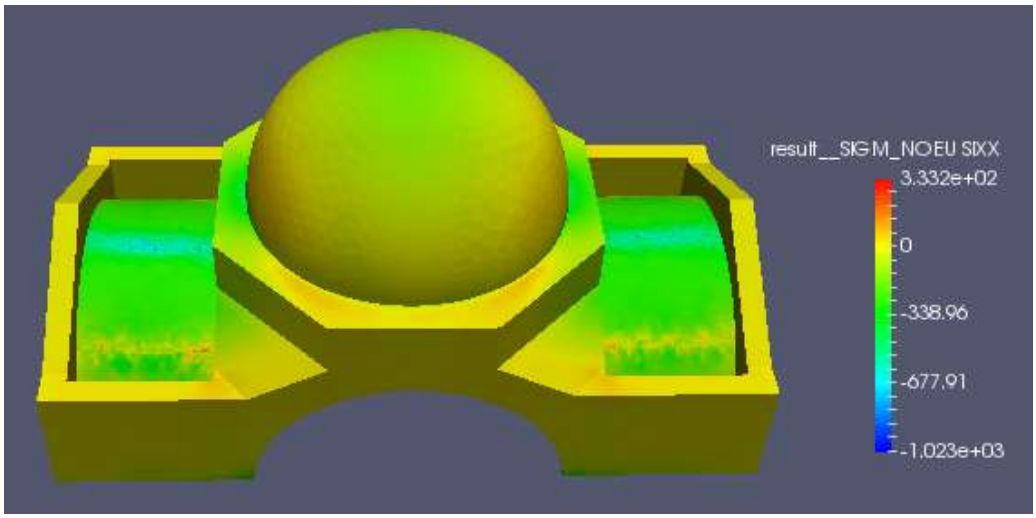


*Figure 41. Result of $\sigma_{xx}$ stresses on top surface in the model A*

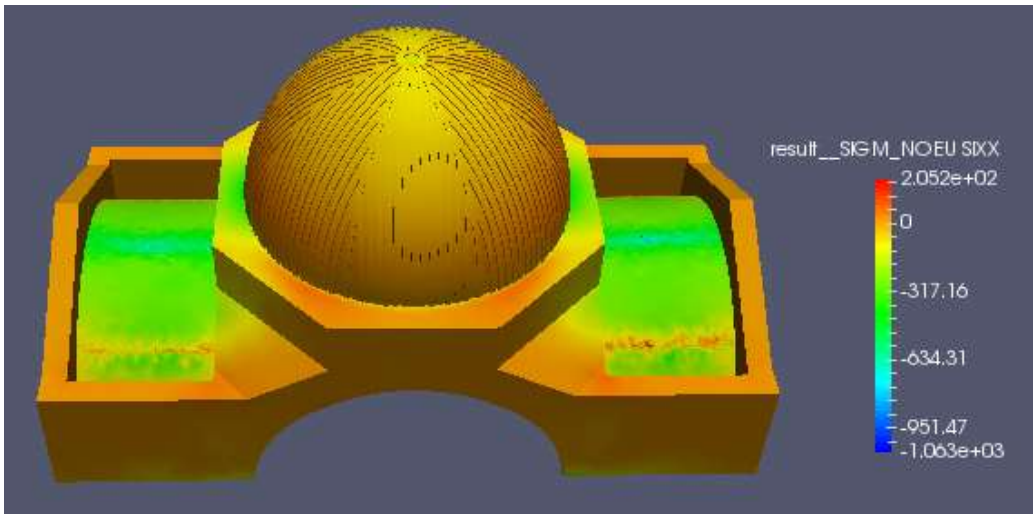


*Figure 42. Result of $\sigma_{xx}$ stresses on top surface in the model B*

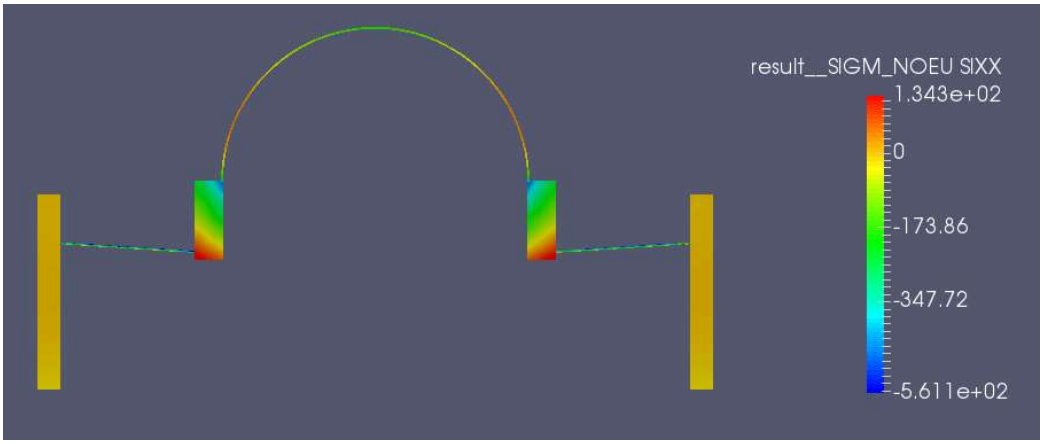


*Figure 43. Model A longitudinal section of $\sigma_{xx}$ stresses*

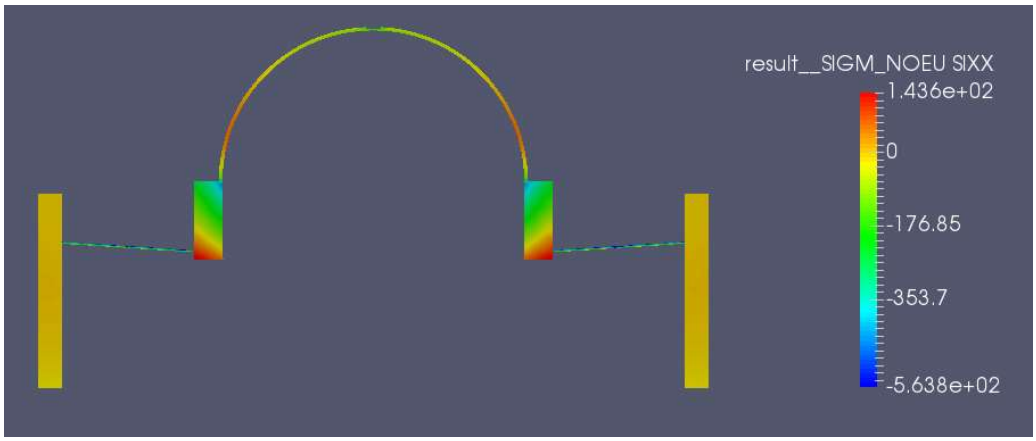


*Figure 44. Model B longitudinal section of $\sigma_{xx}$ stresses*

According to the results obtained in the analysis, the $\sigma_{xx}$ stresses in the ring increase in the model B due to the increase of the own weight. In both models the compression stresses are on the top of the ring and the tension stresses are on the bottom, showing a typical behaviour of the key of an arch under a vertical force over it. The effect of the bending produced by the weight is increased by the torsion due to the eccentricity of the weight of the dome It is necessary to remind that the lateral roofs are not connected to the ring, so they can not balance the eccentricity of the dome weight.

The worst points of the drum are that where tensions are over 70 kN/m$^2$, in this case the bottom of the arches where tensions can arrive up to double the allowable tensions.

In the dome, we can observe that the biggest stresses are concentrated under $\pi/4$ of the angle from the bottom to the top of the sphere.

Although there is part of the dome in red colour, the tensions seem not to arrive to the limit of 70 kN/m$^2$ to think about cracking or structural failing. However, the values in these zones are big enough to reach the limit as soon an additional load is applied over the dome (as can be snow).

The transversal walls have homogenous tensions near to 0.00 kN/m$^2$ due to they only receive the effect of the own weight. The push of the arch in the longitudinal walls is subjected by the constraints at the bottom of the longitudinal walls and this force does not affect the perpendicular walls placed on both sides of the model. These walls are not connected to the roofs either.

The lateral roofs show a high value of tensions at the points where the concavity and convexity of the deformed shape is maximum. These points would be the main places where cracking could appear.

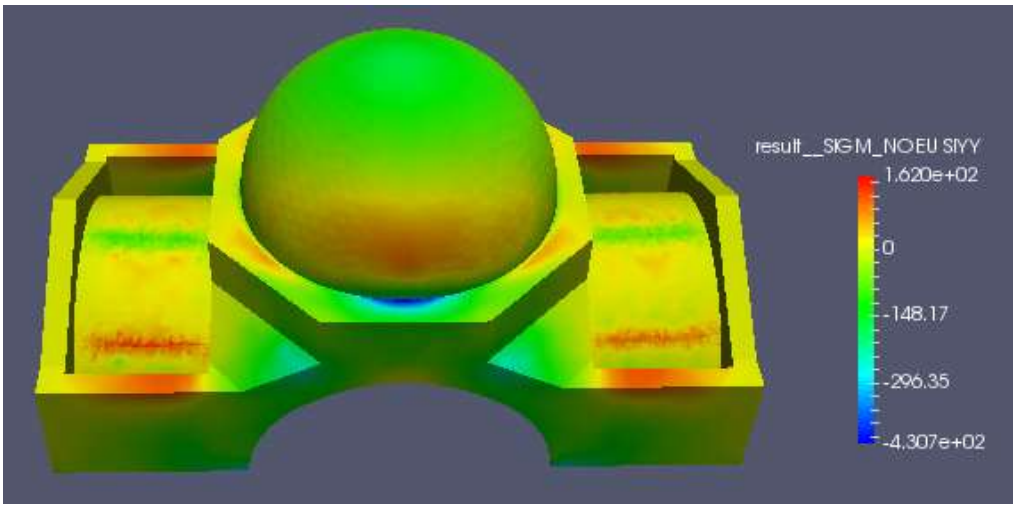


*Figure 45. Result of $\sigma_{yy}$ stresses in the model A*

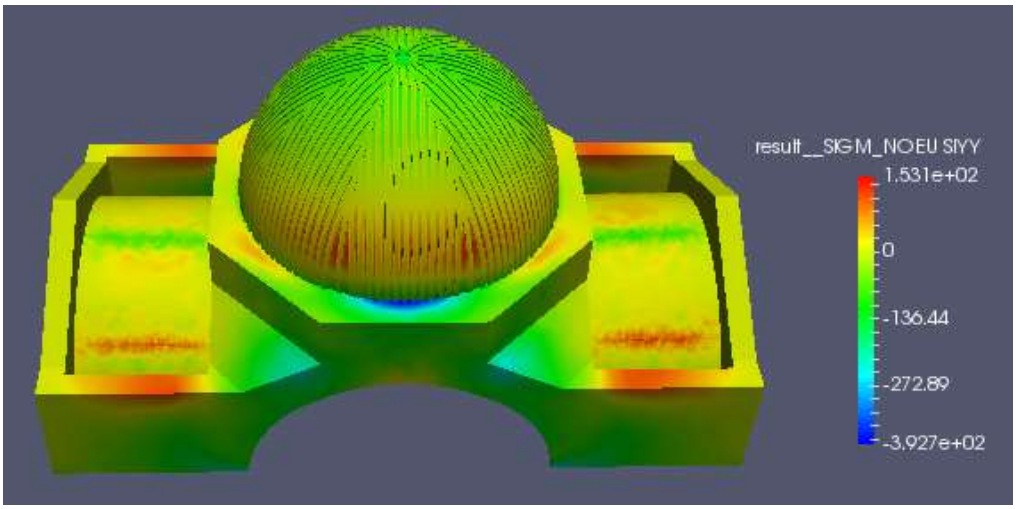


*Figure 46. Result of $\sigma_{yy}$ stresses in the model B*

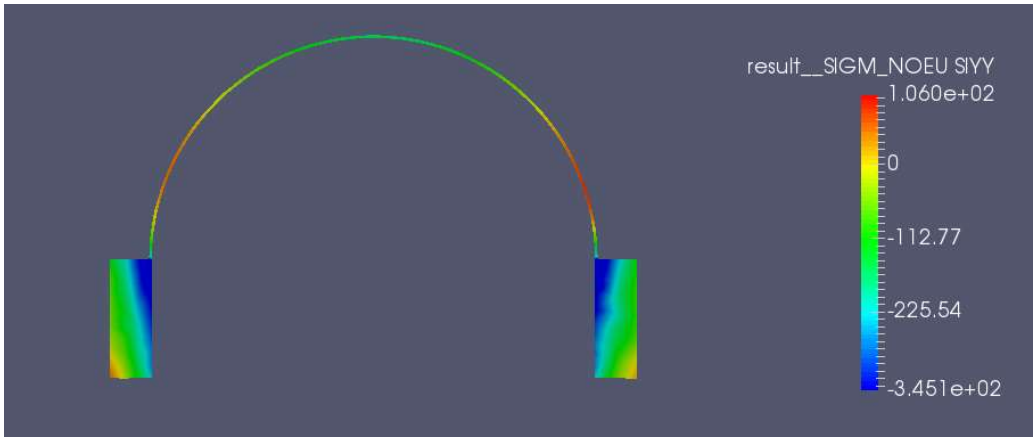


*Figure 47. Model A longitudinal section of $\sigma_{yy}$ stresses*

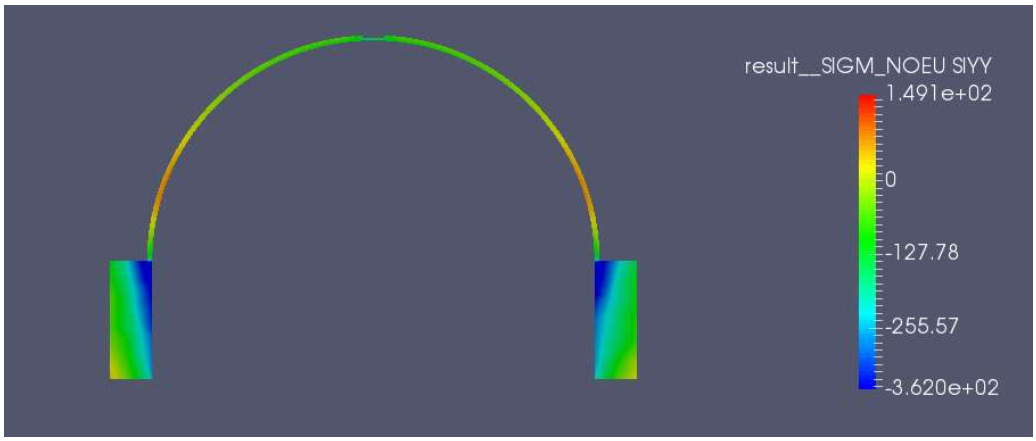


*Figure 48. Model B longitudinal section of $\sigma_{yy}$ stresses*

Analysing the $\sigma_{yy}$ stresses, we can observe that the behaviour is similar to the $\sigma_{xx}$ stresses. The arches concentrate the compressions on the top and the tensions at the bottom, but in this case, as the arches are completely restrained by the longitudinal walls, compressions are bigger than compressions in the perpendicular arches, that avoid the arches to open.

The maximum tensions in this case are below the limit of 70 kN/m$^2$ due to this additional compression that lateral walls produced in the arch restraining the movements and allowing it to work as a compressed element.

Stresses in the dome are concentrated on the same place than in the $\sigma_{xx}$ stresses. Values are similar in both stresses due to the symmetry of the sphere. The difference is caused because the arches under the drum do not have the same degree of restraint in direction X and Y.

The effect of the nerves can be seen clearly in the results of the stresses $\sigma_{xx}$ and $\sigma_{yy}$. In the dome where there are not nerves, the tensions are spread in a big zone, while in the dome with nerves the tensions are concentrated in the space between nerves showing that the nerves are working together with the dome reducing the stresses in those sections.

The longitudinal walls work mainly in this direction YY resisting the forces that they receive from the longitudinal arches. These walls tend to move outwards following the + Y or – Y axis but they are restrained at the bottom resulting a bending effect over their transversal section that produces tensions on the top and compressions at the bottom.

The lateral roofs concentrate the tensions at the points where the bigger bending forces are, causing tensions and compressions on one side or another depending on the sign of the moment.

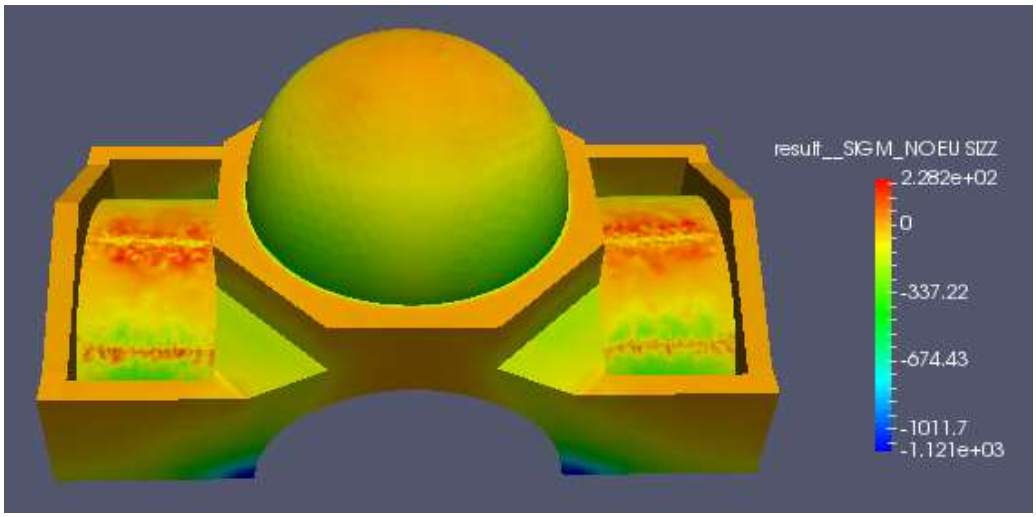


*Figure 49. Result of $\sigma_{zz}$ stresses in the model A*

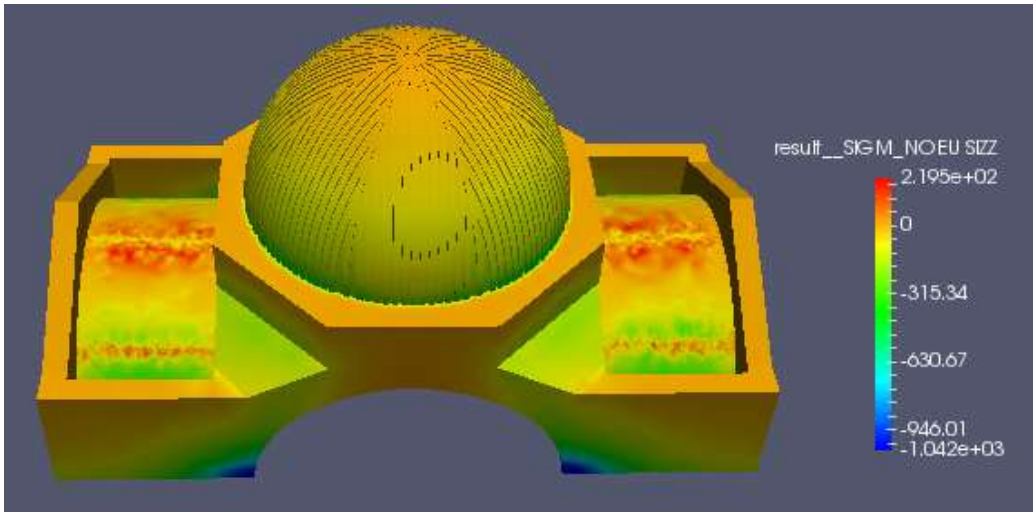


*Figure 50. Result of $\sigma_{zz}$ stresses in the model B*

In Z direction the differences between the two models are basically due to the different weight of the dome. The $\sigma_{zz}$ stresses map on the ring are almost the same and the stiffening of the nerves allows distributing the load over a greater transversal section that permits to reduce the tension.

The biggest compression is concentrated under the start of the arches, due they are the closest points that the loads can find to arrive to the ground. These compressions can cause the failing of the wall by excessive compression due to the stresses are near the limit of 1000 kN/m$^2$.

In the roofs, the maximum tensions are concentrated at the places where bending is maximum, being these places the first for cracking to appear.

### 5.2.4.2 Shear Stresses

Another cause of failing in a structure is because the shear tensions are greater than a limit. In this case, as a first approximation due to lack of information about the materials, the limit tension could be $0.18 \cdot f_c$, obtaining a value with a limit of 180 kN/m$^2$.

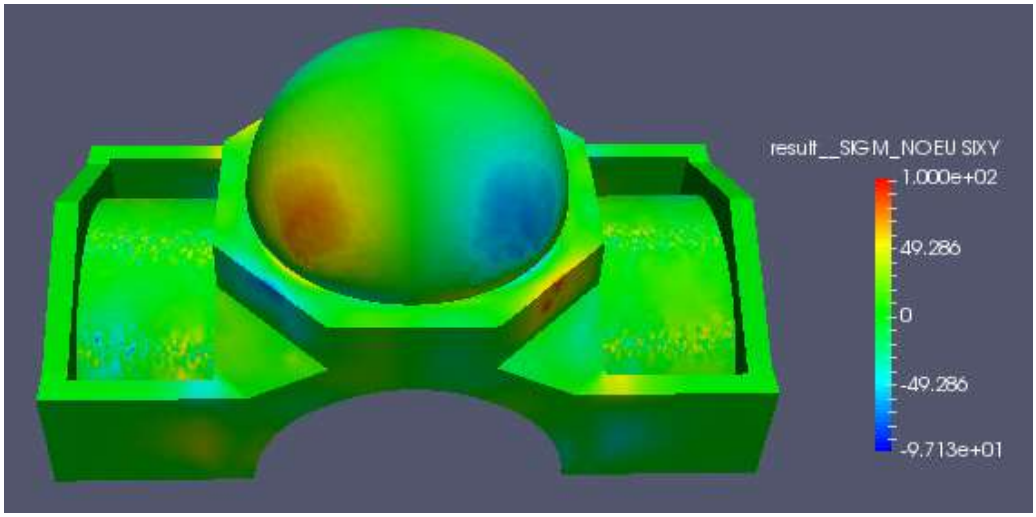


*Figure 51. Result of $\tau_{xy}$ stresses in the model A*

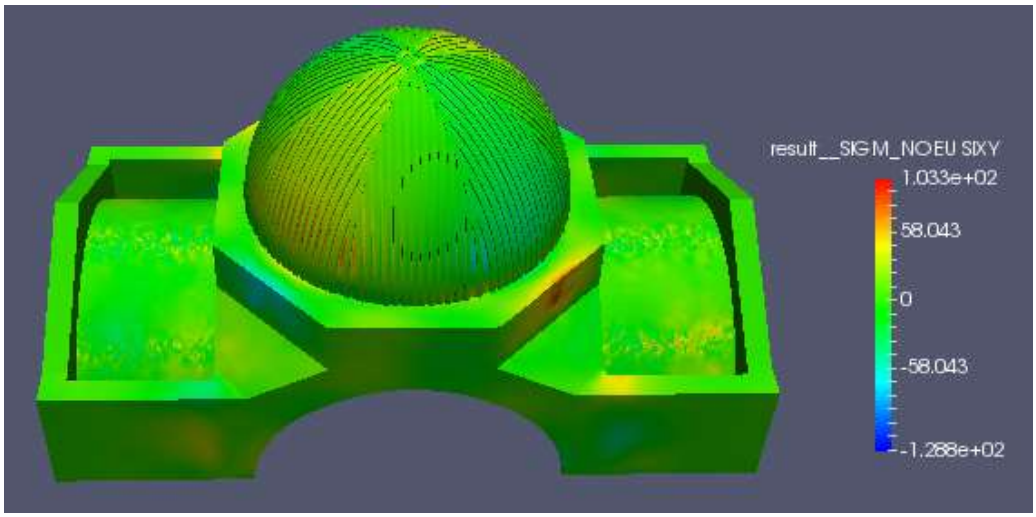


*Figure 52. Result of $\tau_{xy}$ stresses in the model B*

As can be seen on the figures, the values of $\tau_{xy}$ are less than the threshold of 180 kN/m$^2$. This means that cracking for horizontal shear is not expected.

On the dome there are the maximum values of forces in the places where $\sigma_{xx}$ and $\sigma_{yy}$ did not reach the maximum values. The effect of the nerves in the dome is again reflected in the fact that the maximum values are placed among them but not in the nerves.

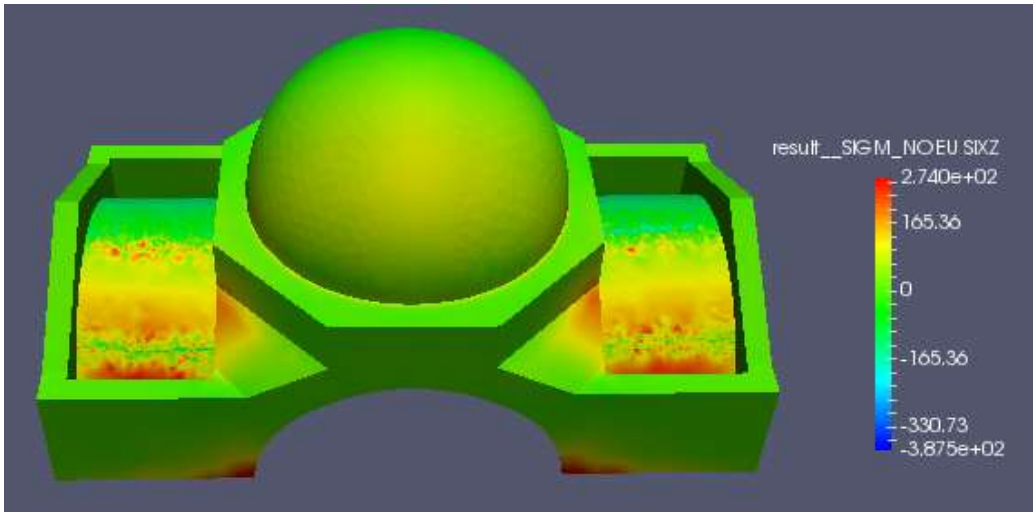


*Figure 53. Result of $\tau_{xz}$ stresses in the model A*

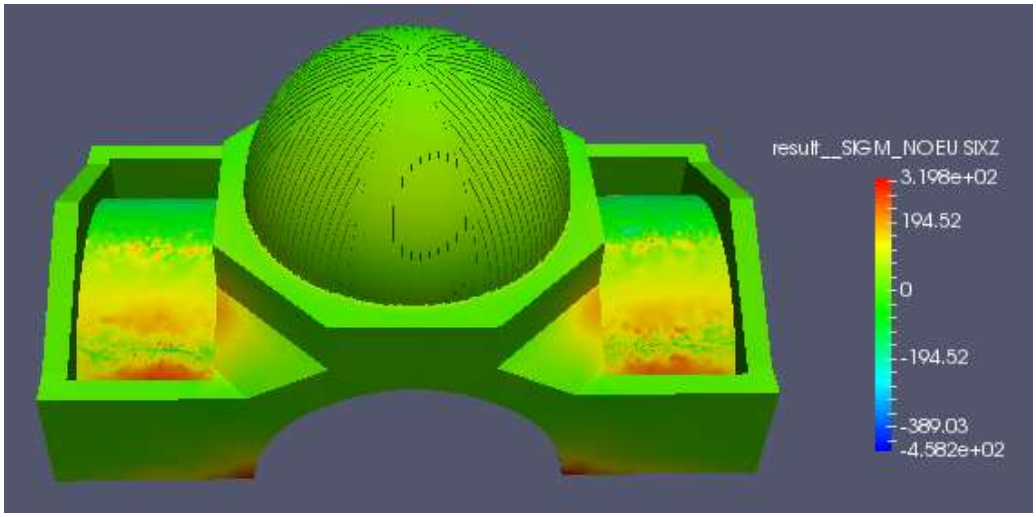


*Figure 54. Result of $\tau_{xz}$ stresses in the model B*

The results of $\tau_{xz}$ show the places where we can have problems of tangential stresses and appear cracking due to these stresses. The first places where stresses are too high are the pendentives at the union between the drum and the transversal arches. The values at these places are near the threshold.

The second place where we can expect cracking is the zone of the roofs in contact with the longitudinal walls. In this place is where the maximum shear force is reached due to this contact is the support of the roofs.

Finally, the longitudinal walls have a concentration of shear forces where the arches discharge the load they transmit from the dome and the drum to the ground. The value of these stresses is big enough to crack the stone masonry and create structural problems in the walls.

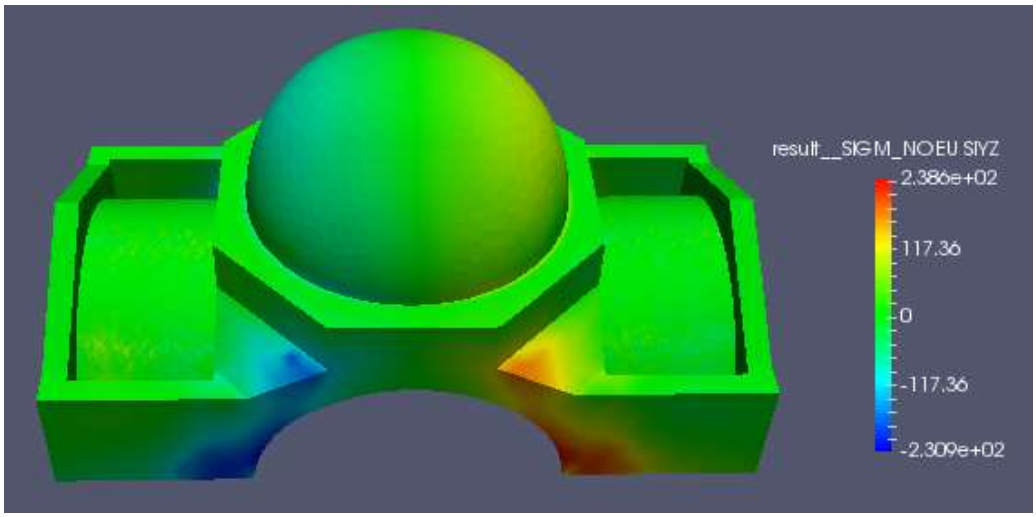


*Figure 55. Result of $\tau_{yz}$ stresses in the model A*

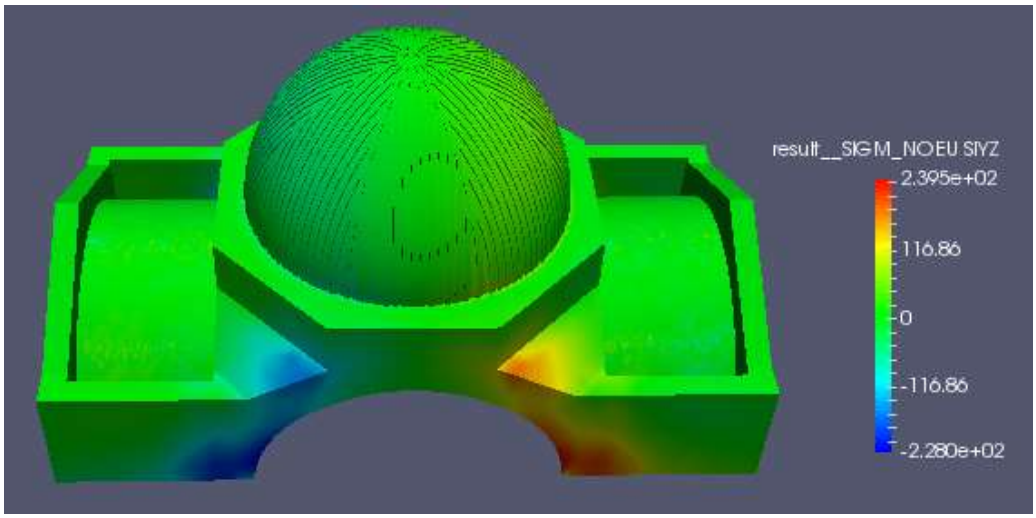


*Figure 56. Result of $\tau_{yz}$ stresses in the model B*

The results of $\tau_{yz}$ as well show the places where we can have problems of tangential stresses and appear cracking due to these stresses. In this case, the pendentives have high values of stresses on the other side of the union between the drum and the transversal arches, comparing to $\tau_{xz}$.

Roofs do not have problems in this case with these tangential stresses, but the longitudinal walls have a bigger concentration of shear forces than in the previous stress at the same place and following the way of the loads through the arches up to the supports.

## 5.3 Modal Analysis

### 5.3.1 Description of the Analysis

In structural engineering, modal analysis uses the overall mass and stiffness of a structure to find the various periods at which it will naturally resonate. These periods of vibration are very important to note in earthquake engineering, as it is imperative that a building's natural frequency does not match the frequency of expected earthquakes in the region in which the building is to be constructed.

If a structure's natural frequency matches an earthquake's frequency, the structure may continue to resonate and experience structural damage.

A modal analysis has been carried out to understand the possible damage that can be produced by different frequencies over the church. In this analysis the first 5 eigenmodes of vibration have been calculated.

### 5.3.2 Results from Model A

The eigenmodes obtained for the model A are the following:

| Eigenmode | Frequency (Hz) | Error |
|---|---|---|
| 1 | 1.22081 Hz | 2.78392e-10 |
| 2 | 1.33229 Hz | 2.39587e-10 |
| 3 | 1.56787 Hz | 2.04520e-10 |
| 4 | 1.64890 Hz | 1.90089e-10 |
| 5 | 2.37836 Hz | 2.21022e-11 |

*Table 2. Eigenmodes from Model A*

As it is shown in the following figures, the 4 first eigenmodes are related to the roofs. This is due to the fact that the roofs are the part of the structure with minor elastic modulus and small thickness than the walls and the central part.

The dome although is a thin structure compared with the masonry part of the structure, its shape allows it to resist by shape and have different vibration mode than the roofs.

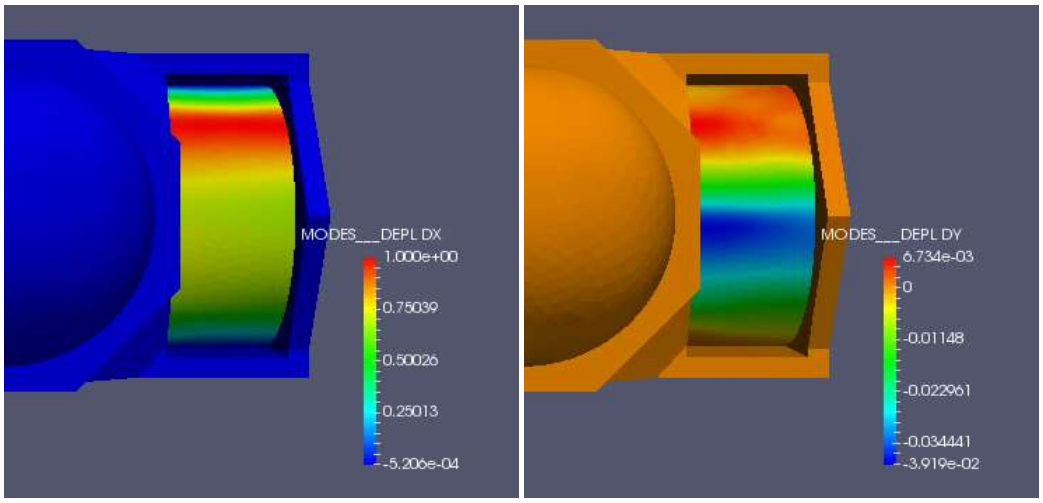


*Figure 57. Displacements X and Y for the first eigenmode in model A*

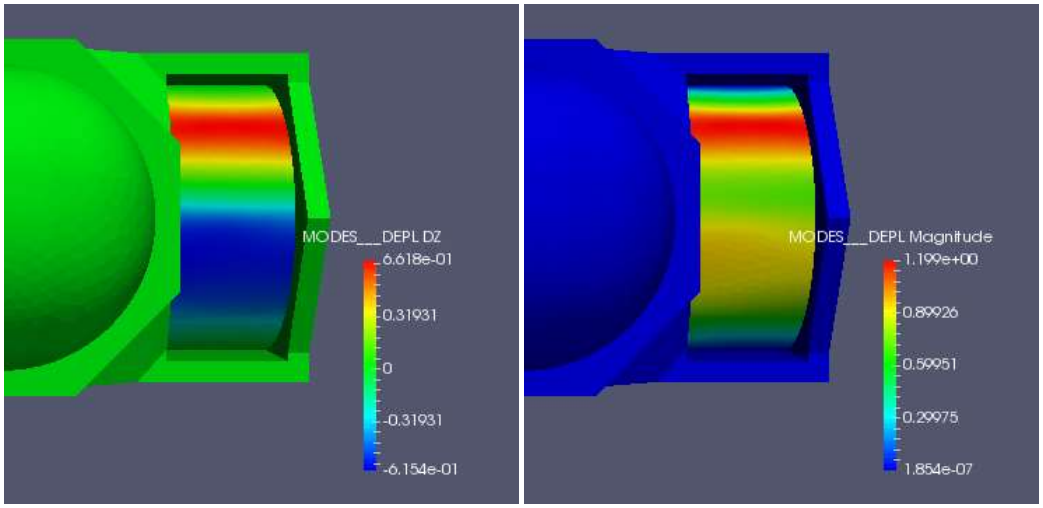


*Figure 58. Displacements Z and total for the first eigenmode in model A*

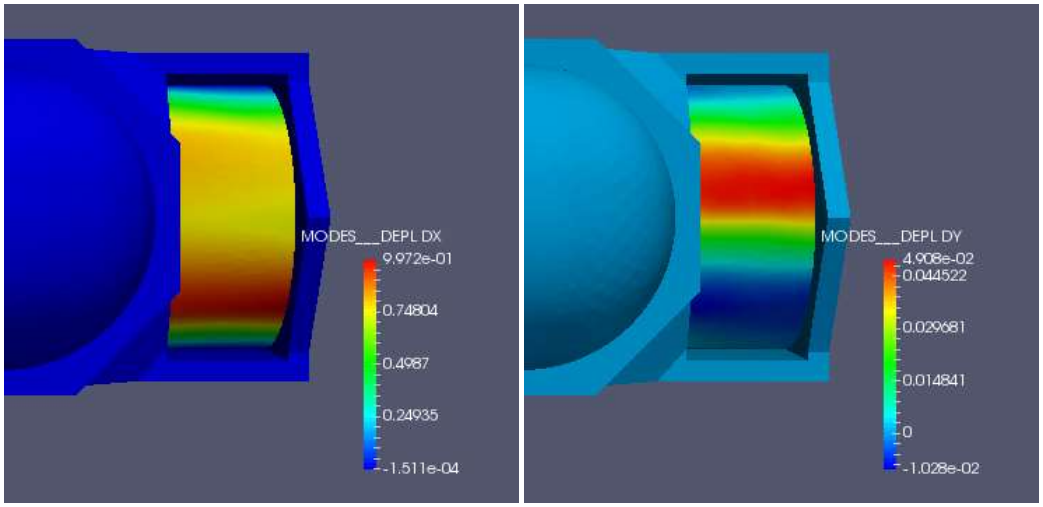


*Figure 59. Displacements X and Y for the second eigenmode in model A*

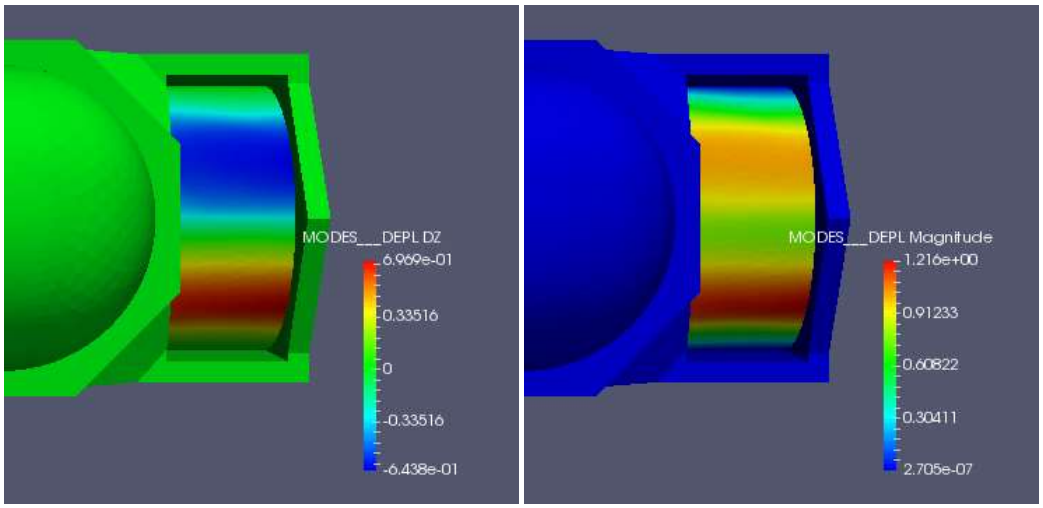


*Figure 60. Displacements Z and total for the second eigenmode in model A*

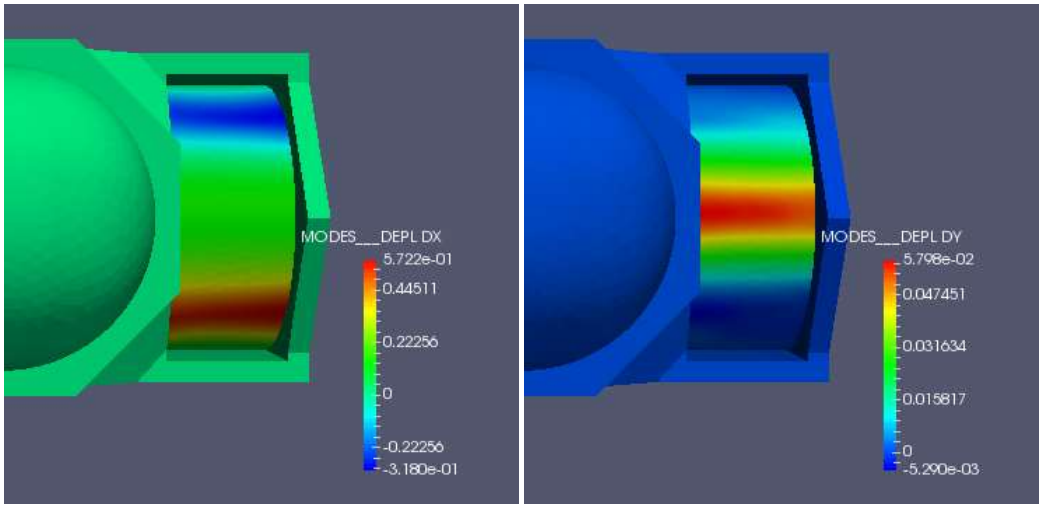


*Figure 61. Displacements X and Y for the third eigenmode in model A*

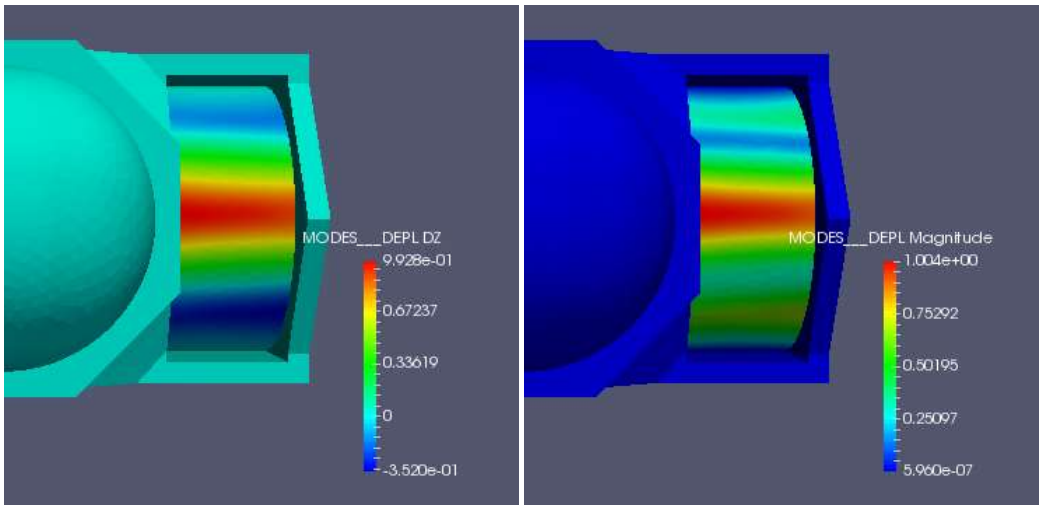


*Figure 62. Displacements Z and total for the third eigenmode in model A*

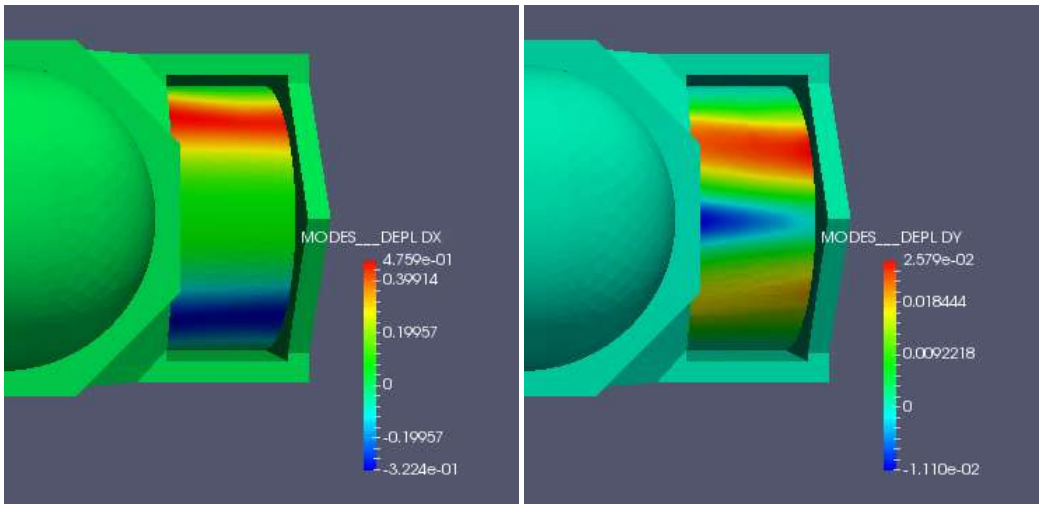


*Figure 63. Displacements X and Y for the fourth eigenmode in model A*

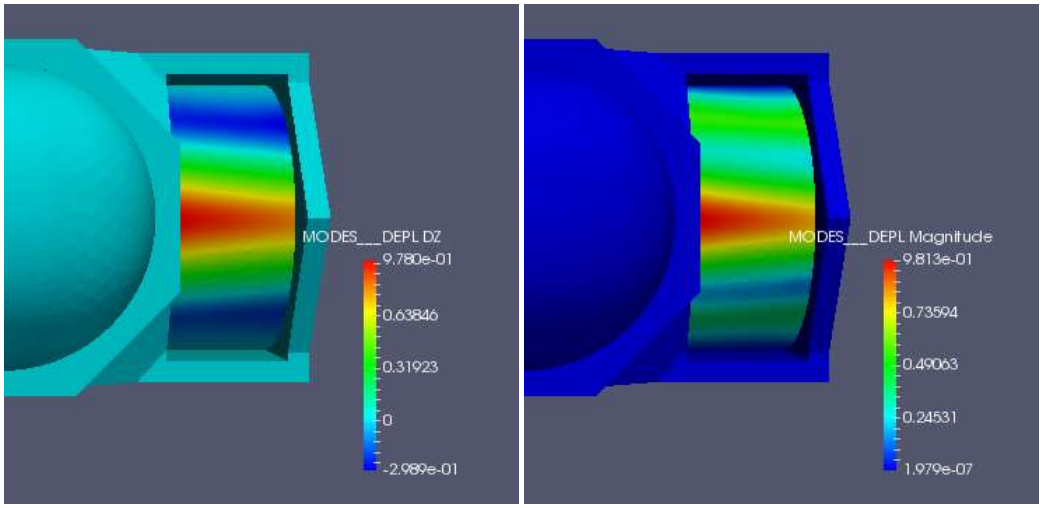


*Figure 64. Displacements Z and total for the fourth eigenmode in model A*

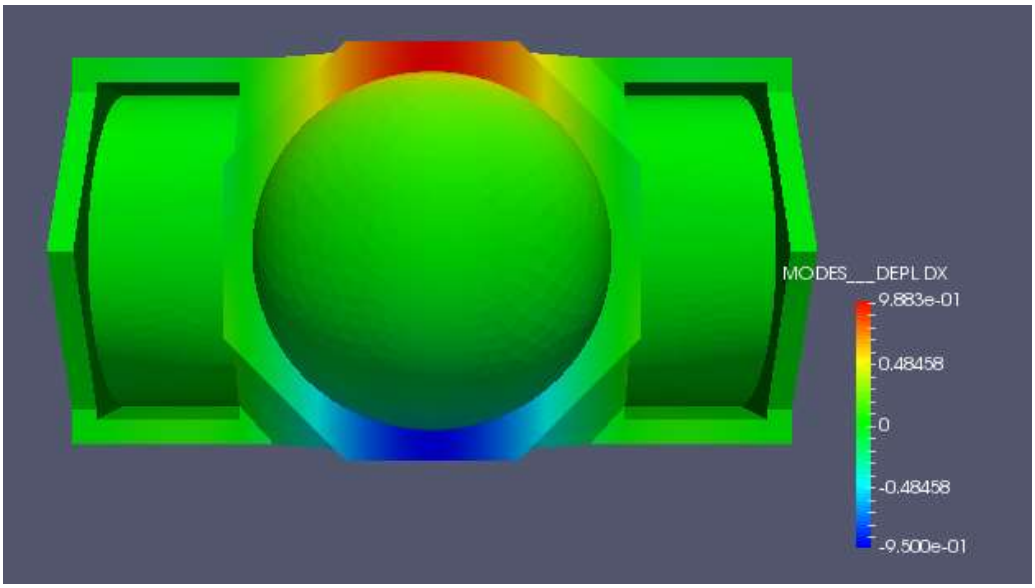


*Figure 65. Top view of X displacement for the fifth eigenmode in model A*

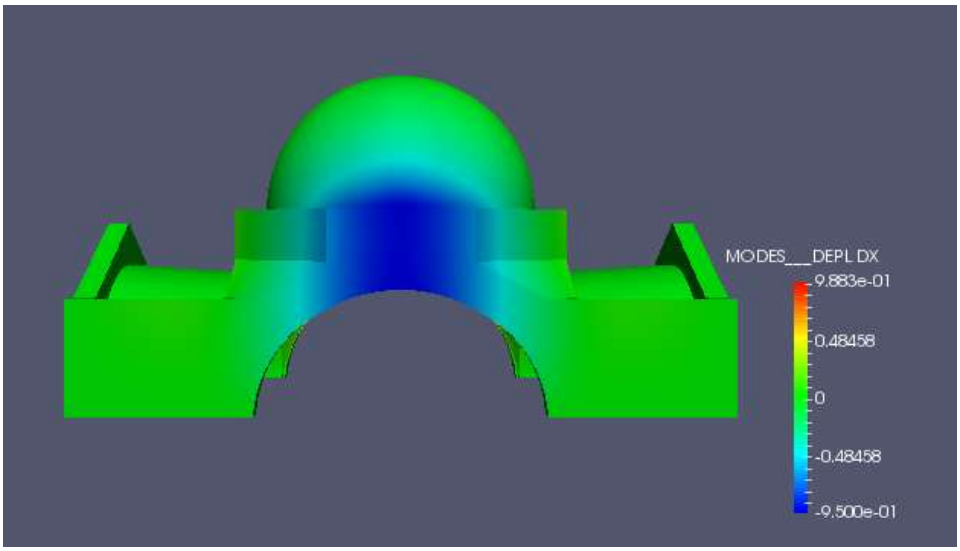


*Figure 66. Front view of X displacement for the fifth eigenmode in model A*

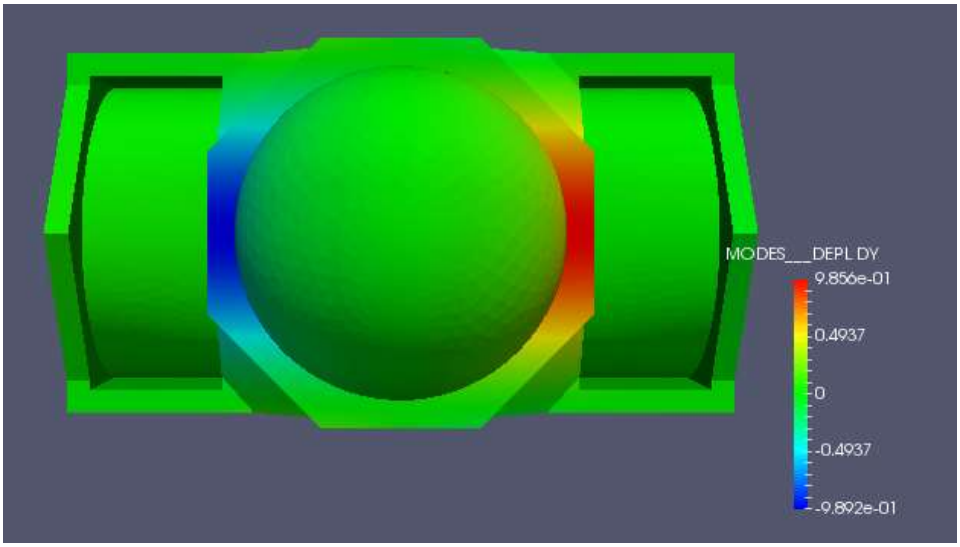


*Figure 67. Top view of Y displacement for the fifth eigenmode in model A*

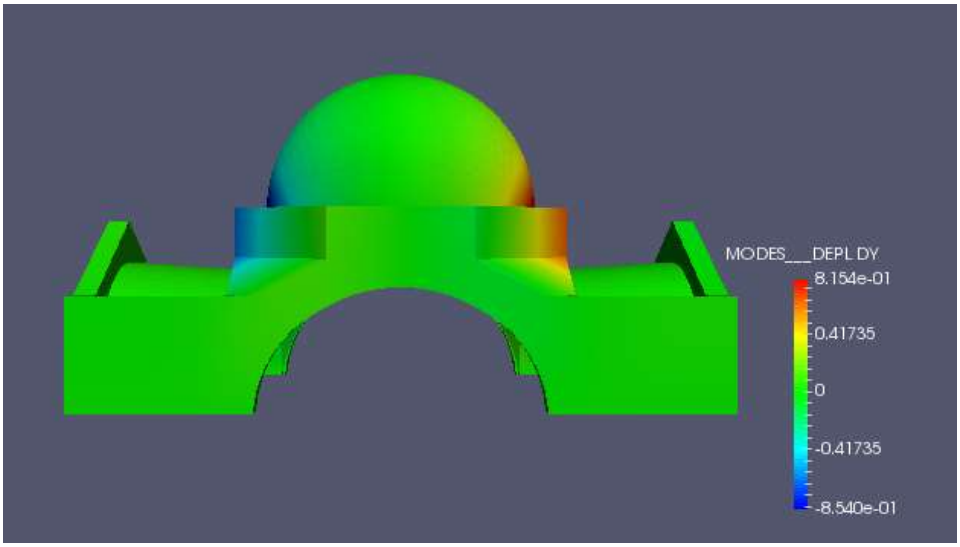


*Figure 68. Front view of Y displacement for the fifth eigenmode in model A*

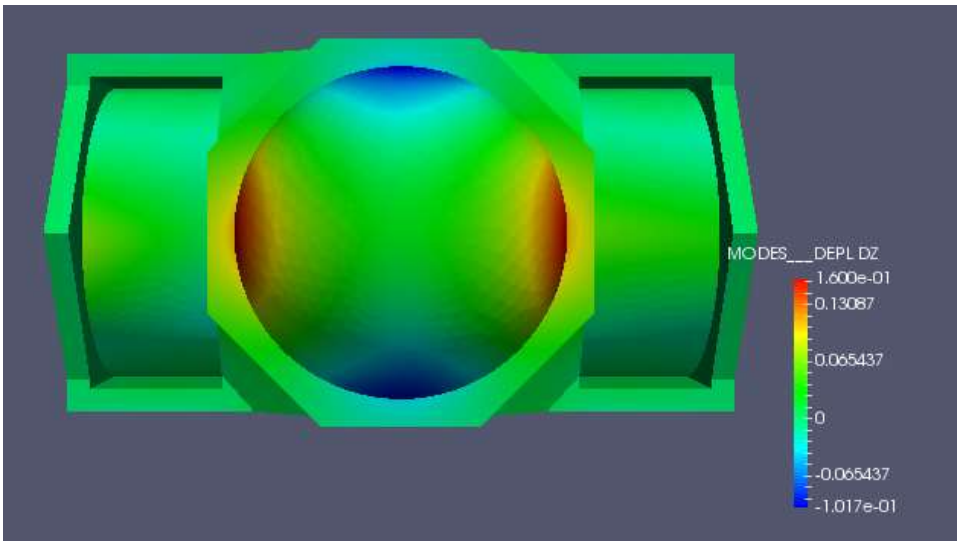


*Figure 69. Top view of Z displacement for the fifth eigenmode in model A*

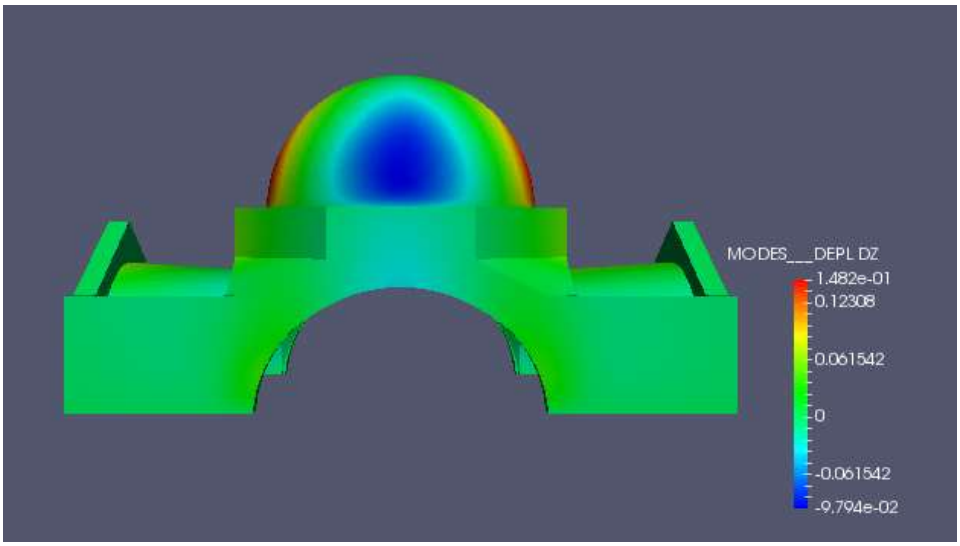


*Figure 70. Front view of Z displacement for the fifth eigenmode in model A*

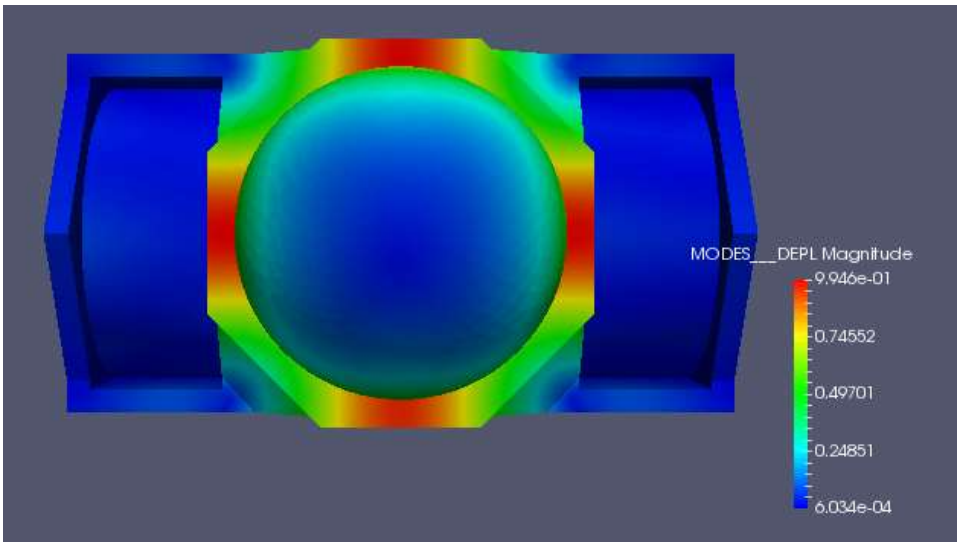


*Figure 71. Top view of total displacement for the fifth eigenmode in model A*

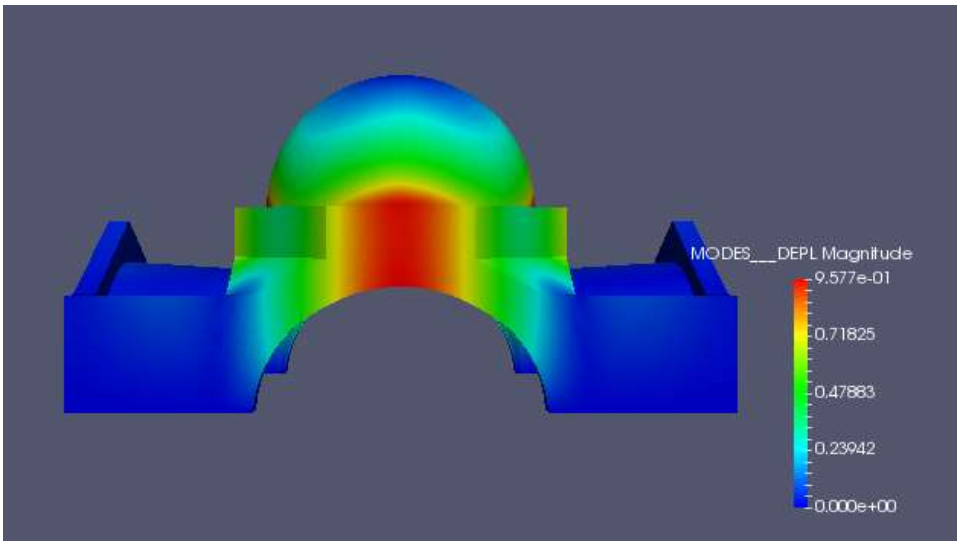


*Figure 72. Front view of Total displacement for the fifth eigenmode. Model A*

### 5.3.3 Results from Model B

The eigenmodes obtained for the model B are the following:

| Eigenmode | Frequency (Hz) | Error |
|---|---|---|
| 1 | 1.34274 Hz | 2.14688e-10 |
| 2 | 1.37363 Hz | 2.18853e-10 |
| 3 | 1.61050 Hz | 1.90321e-10 |
| 4 | 1.67209 Hz | 1.72509e-10 |
| 5 | 2.38842 Hz | 1.30028e-11 |

*Table 3. Eigenmodes from Model B*

As it is shown in the following figures, the 4 first eigenmodes are related to the roofs. This is due to the fact that the roofs are the part of the structure with minor elastic modulus and small thickness than the walls and the central part.

The dome although is a thin structure compared with the masonry part of the structure, its shape allows it to resist by shape and have different vibration mode than the roofs.

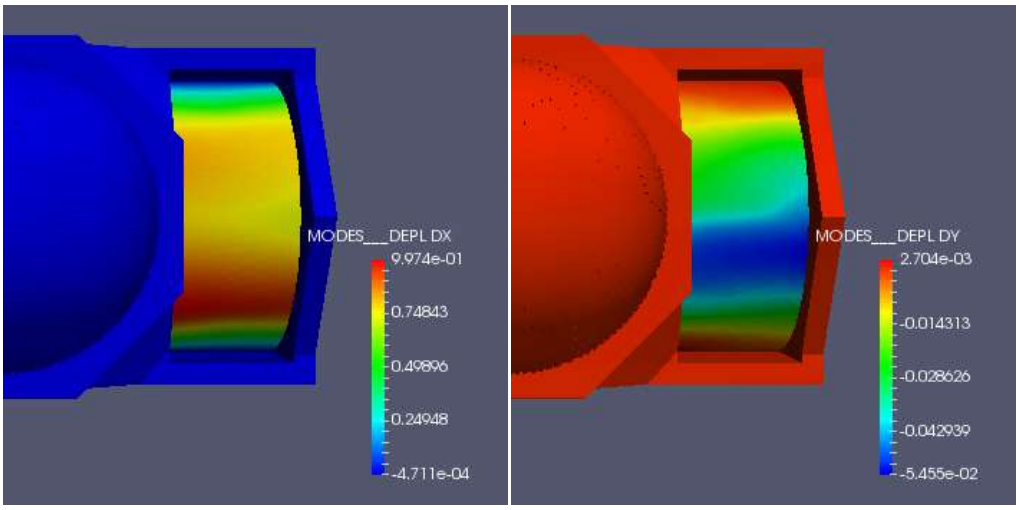


*Figure 73. Displacements X and Y for the first eigenmode in model B*

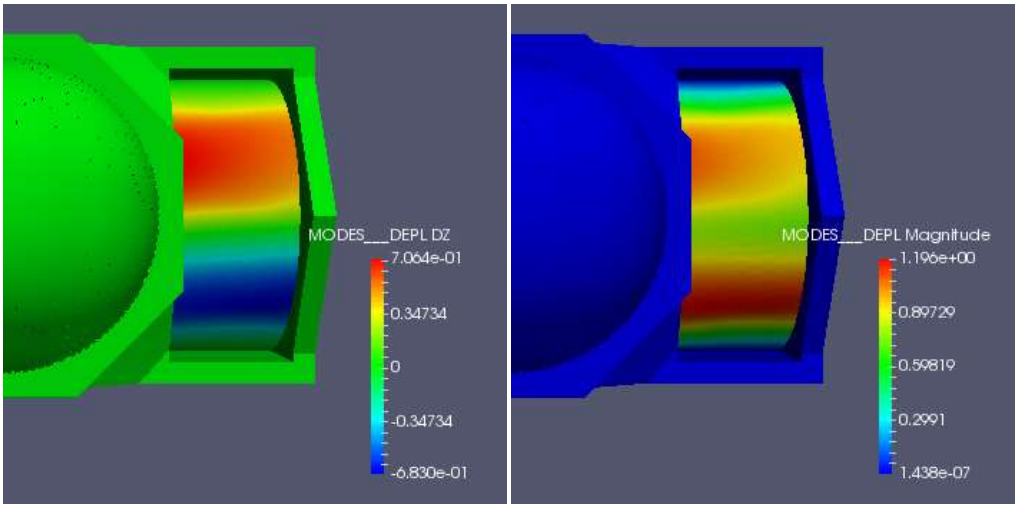


*Figure 74. Displacements Z and total for the first eigenmode in model B*

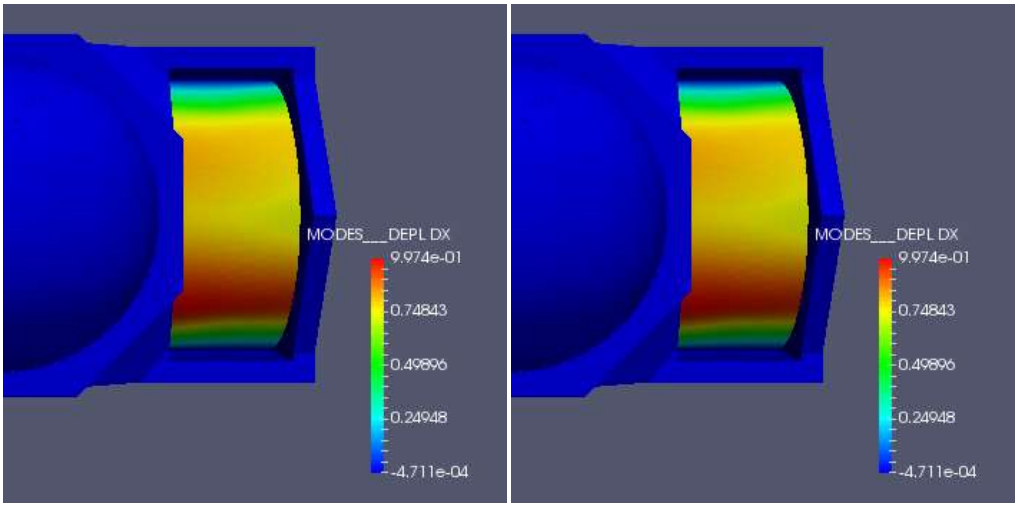


*Figure 75. Displacements X and Y for the second eigenmode in model B*

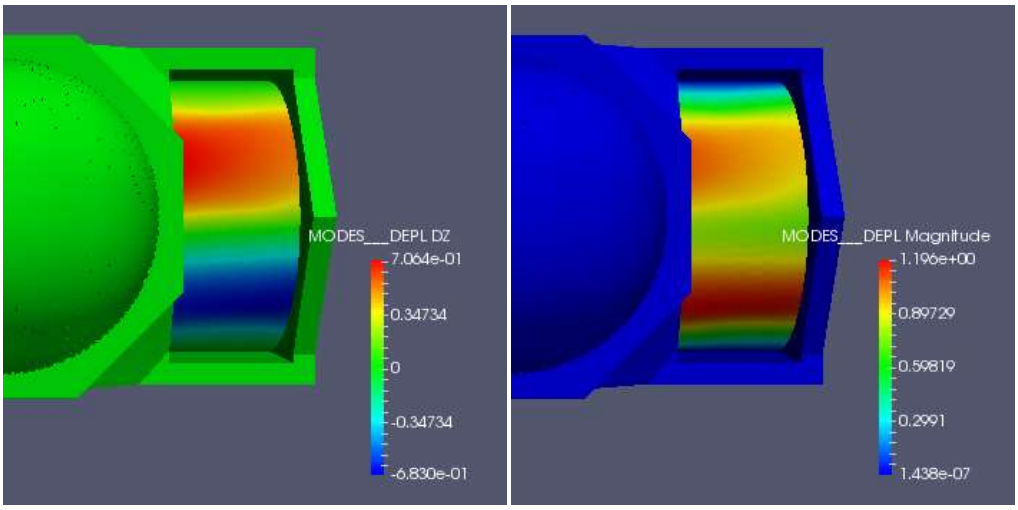


*Figure 76. Displacements Z and total for the second eigenmode in model B*

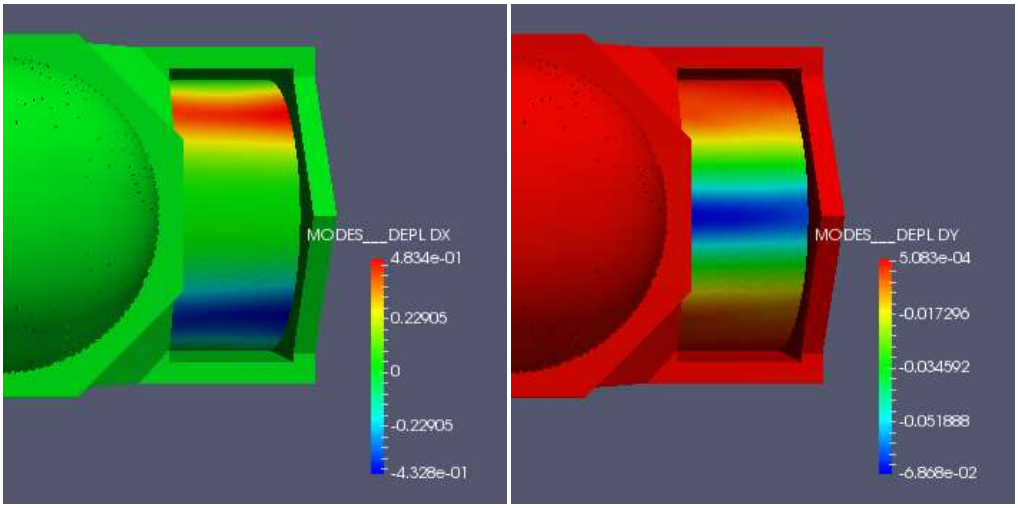


*Figure 77. Displacements X and Y for the third eigenmode in model B*

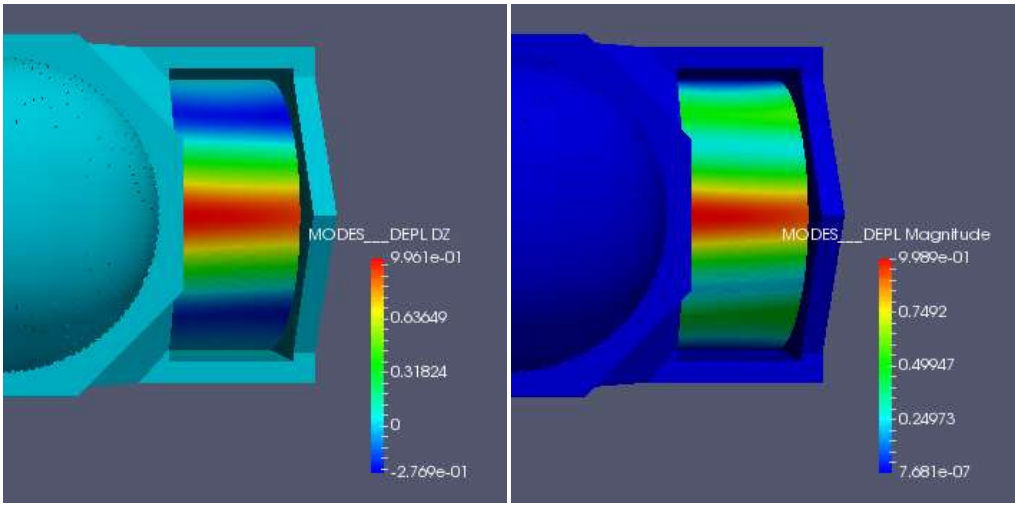


*Figure 78. Displacements Z and total for the third eigenmode in model B*

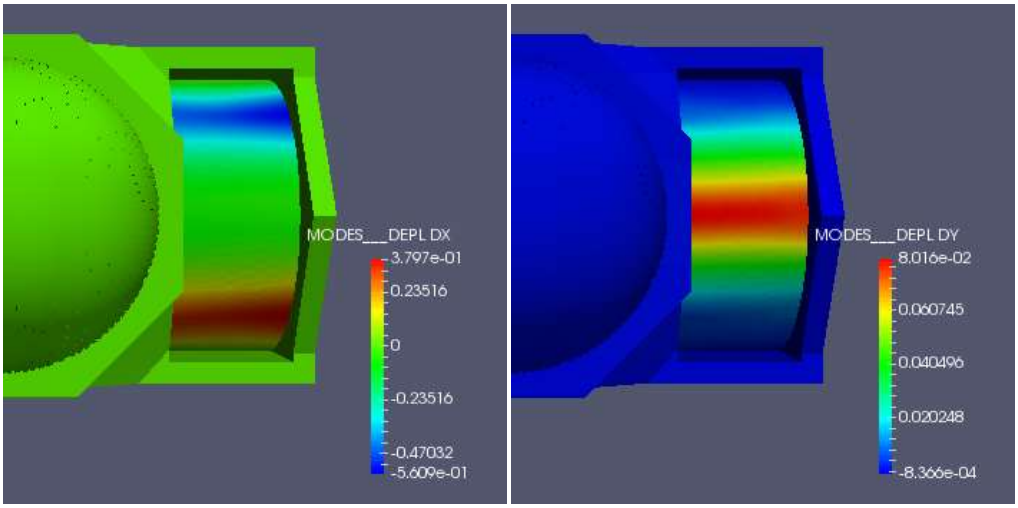


*Figure 79. Displacements X and Y for the fourth eigenmode in model B*

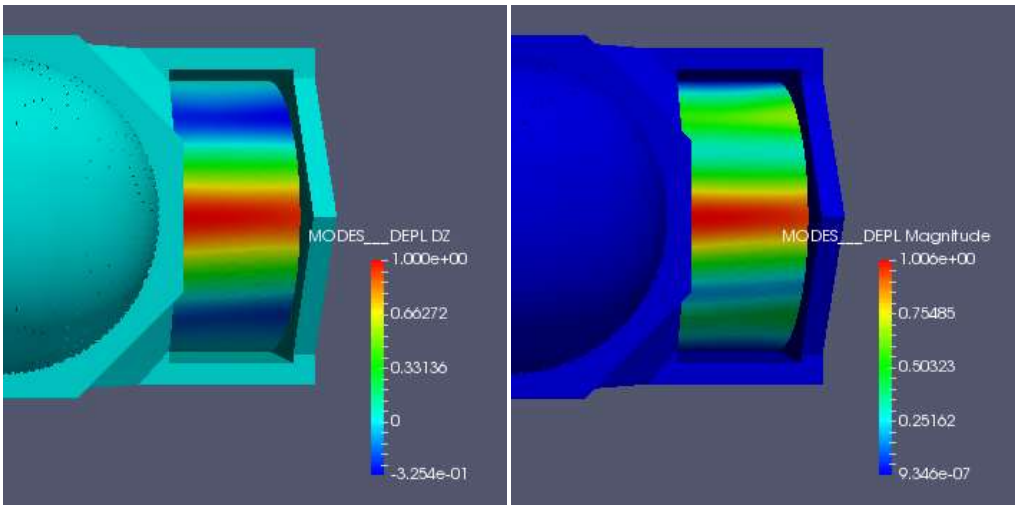


*Figure 80. Displacements Z and total for the fourth eigenmode in model B*

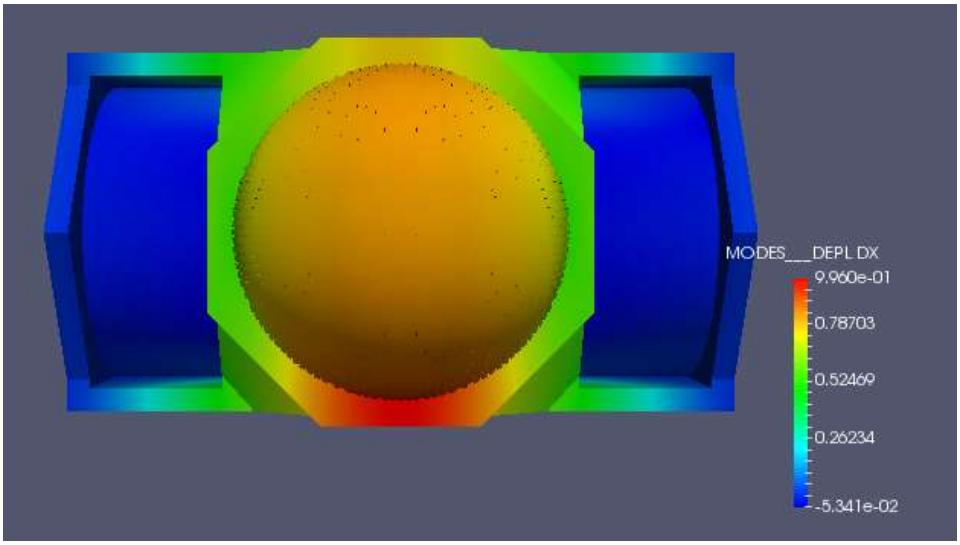


*Figure 81. Top view of X displacement for the fifth eigenmode in model B*

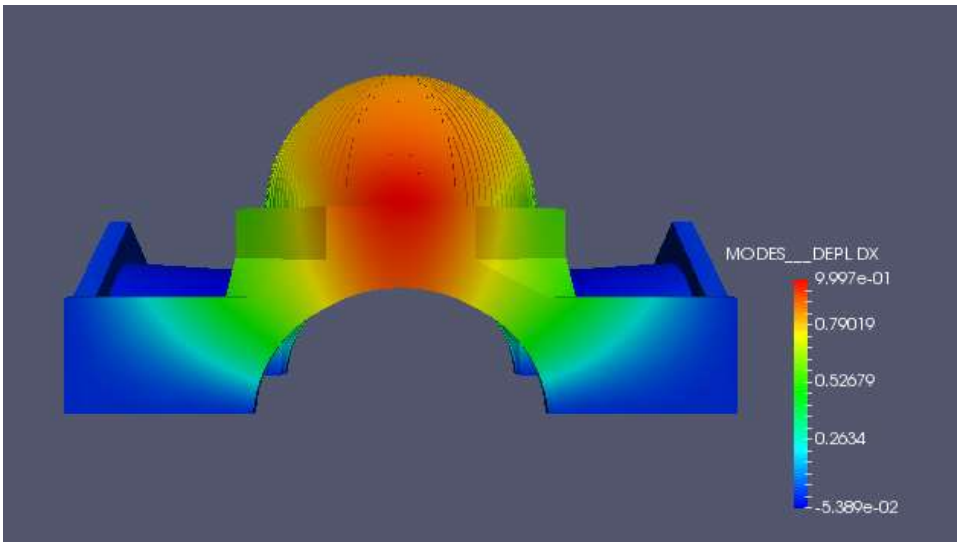


*Figure 82. Front view of X displacement for the fifth eigenmode in model B*

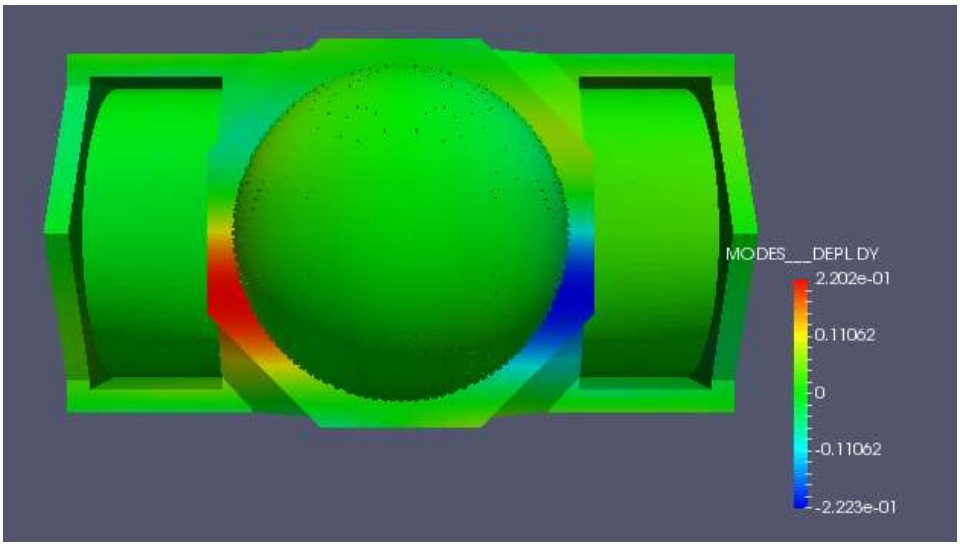


*Figure 83. Top view of Y displacement for the fifth eigenmode in model B*

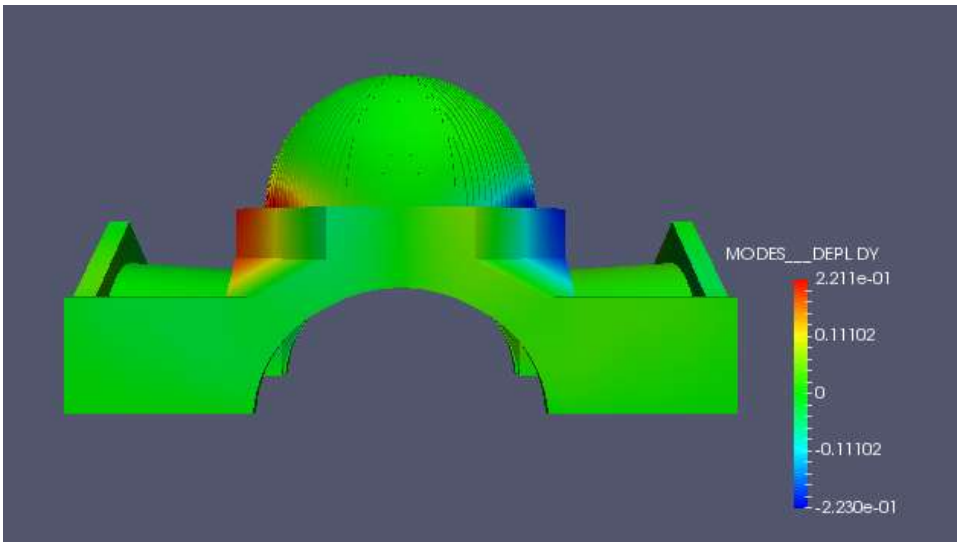


*Figure 84. Front view of Y displacement for the fifth eigenmode in model B*

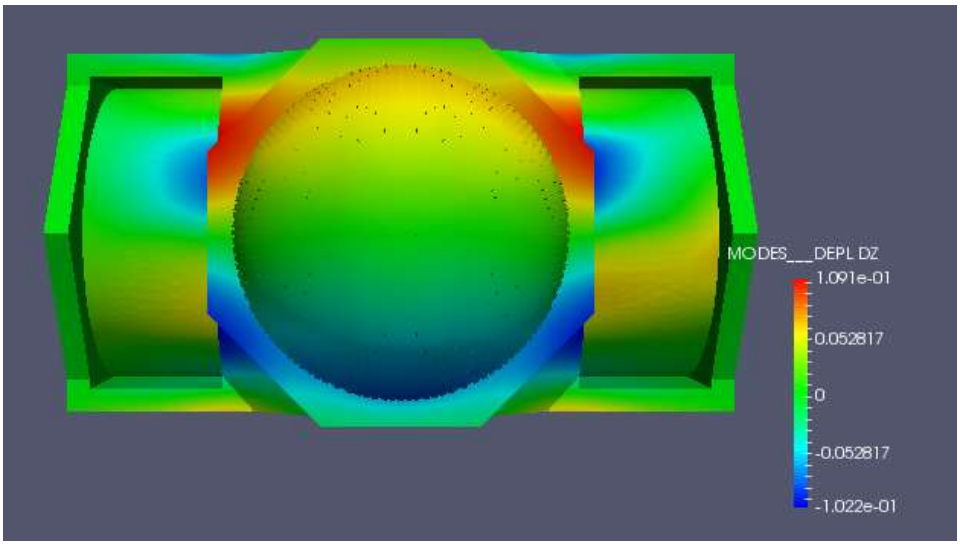


*Figure 85. Top view of Z displacement for the fifth eigenmode in model B*

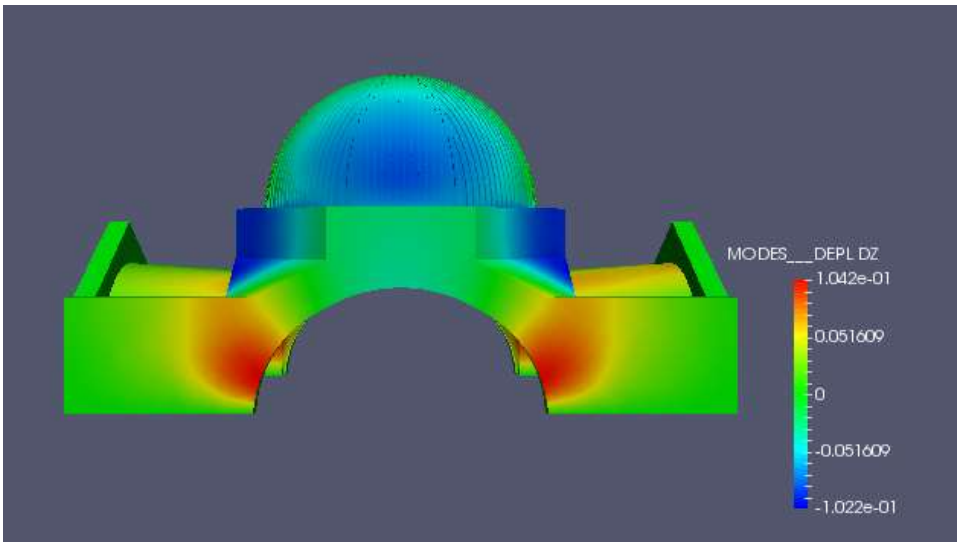


*Figure 86. Front view of Z displacement for the fifth eigenmode in model B*

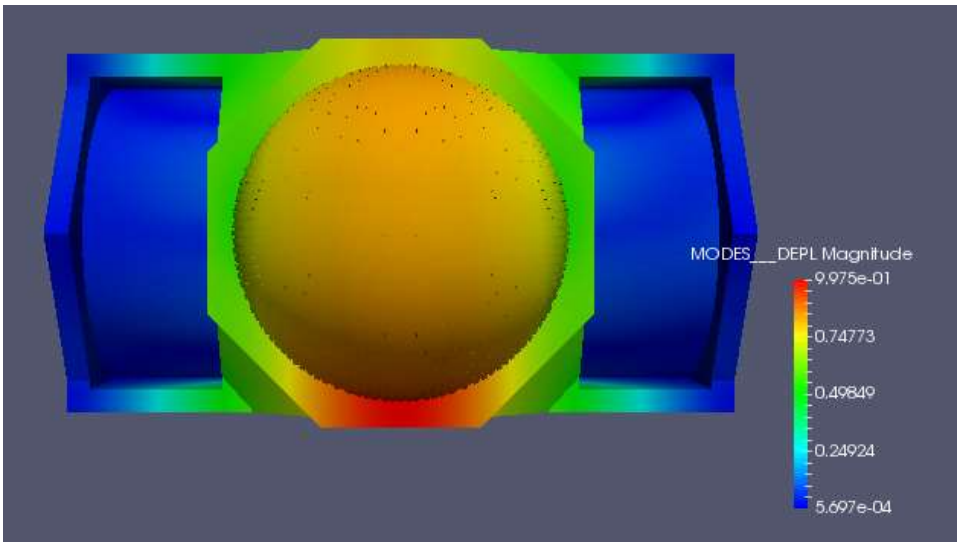


*Figure 87. Top view of total displacement for the fifth eigenmode in model B*

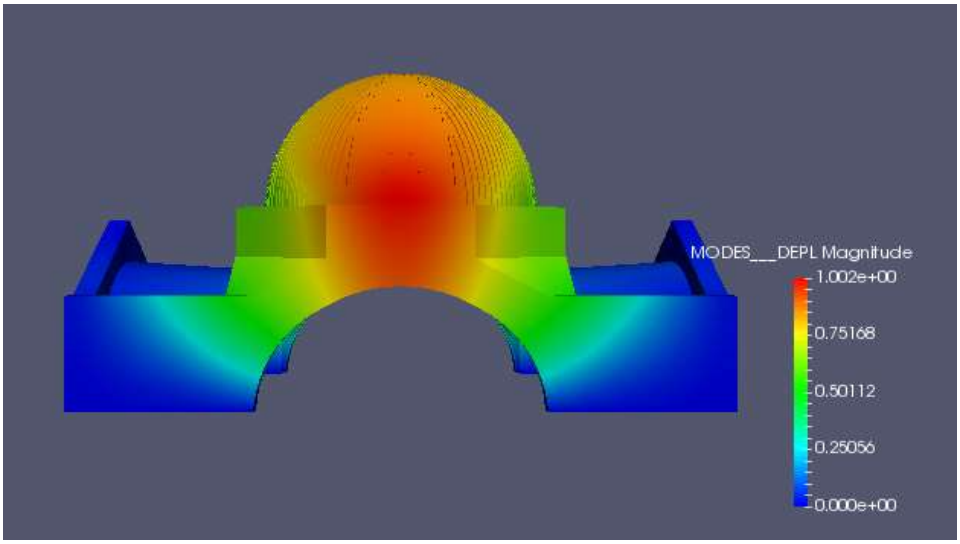


*Figure 88. Front view of total displacement for the fifth eigenmode. Model B*

Doing a comparison between the two models, we see that the fact that when the dome is a nerved structure, the firsts eigenmodes vary slightly but they tend to equal as the frequencies increase. In the Figure 89 the eigenmodes of both structures are compared.

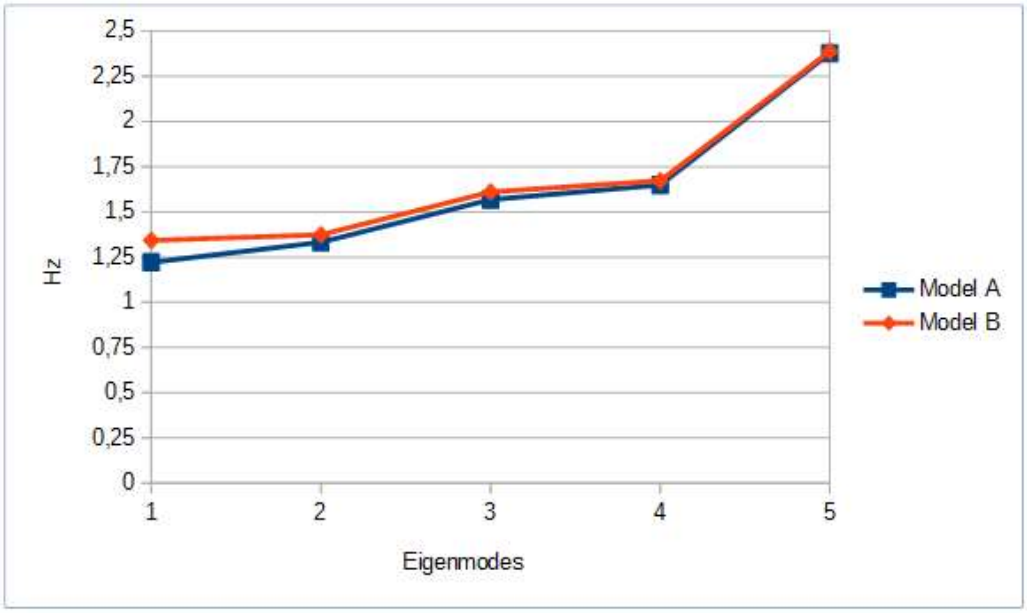


*Figure 89. Eigenmodes of the models*

5.4 Non-Linear Analysis

### 5.4.1 Description of the Analysis

The non-linear analysis takes into account the time where each load is applied to the model and calculates the stresses each time starting at the position obtained at the end of the previous step of calculation.

To take into account these stages of loading the time has been divided into two stages and each stage in five steps for each load applied. This discretization of the time has been applied to both models A and B.

Doing this, the second order effects can be considered into the stresses of the models. This will let us to compare the results between the linear analysis and the non-linear analysis.

In the first stage only the own weight of the structure is applied, in the second stage, the own weight of the structure is maintained and the superimposed load is applied.

At first stage, we have not applied any load over the structure, so there is not any stress in the structure. The different stages and steps are the following:

- Stage 0 – Step 0: 0.00 % of own weight load applied.
- Stage 0 – Step 1: 20.00 % of own weight load applied.
- Stage 0 – Step 2: 40.00 % of own weight load applied.
- Stage 0 – Step 3: 60.00 % of own weight load applied.
- Stage 0 – Step 4: 80.00 % of own weight load applied.
- Stage 0 – Step 5: 100.00 % of own weight load applied.
- Stage 1 – Step 1: 100.00 % of own weight
  + 20.00 % of superimposed load applied.
- Stage 1 – Step 2: 100.00 % of own weight
  + 40.00 % of superimposed load applied.
- Stage 1 – Step 3: 100.00 % of own weight
  + 60.00 % of superimposed load applied.
- Stage 1 – Step 4: 100.00 % of own weight
  + 80.00 % of superimposed load applied.
- Stage 1 – Step 5: 100.00 % of own weight
  + 100.00 % of superimposed load applied.

### 5.2.2 Displacements

The displacements obtained in the non-linear analysis are the same than in the non-linear analysis, with a maximum displacement of the roofs of 2,3 cm.

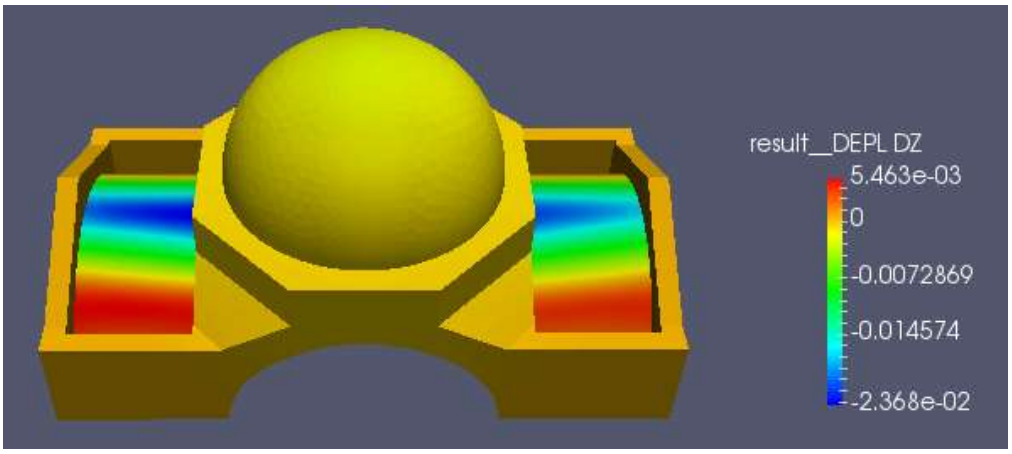


*Figure 90. Vertical displacements of the model A at final step*

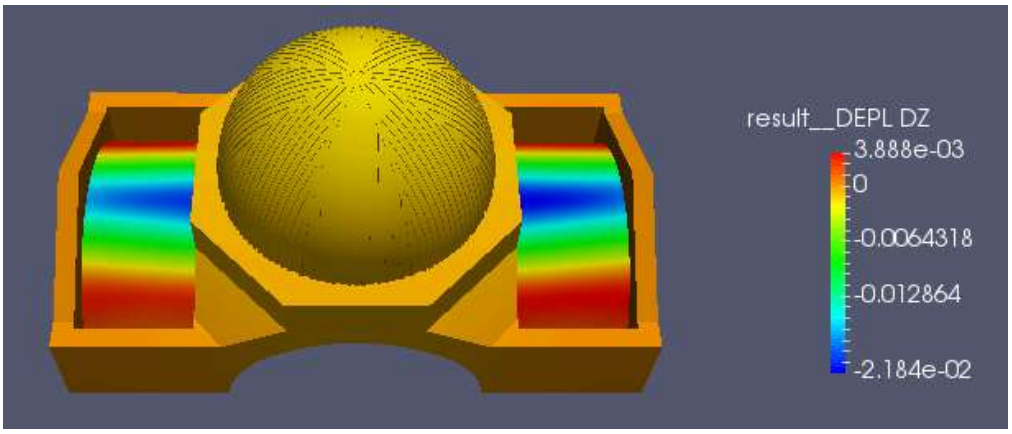


*Figure 91. Vertical displacements of the model B at final step*

### 5.2.3 Stresses

#### *5.2.3.1 Normal Stresses*

The results obtained in the non-linear analysis for $\sigma_{xx}$, show that in the roofs the compressions and tractions increase their values but there is not a significant change in the stresses in the dome and the walls.

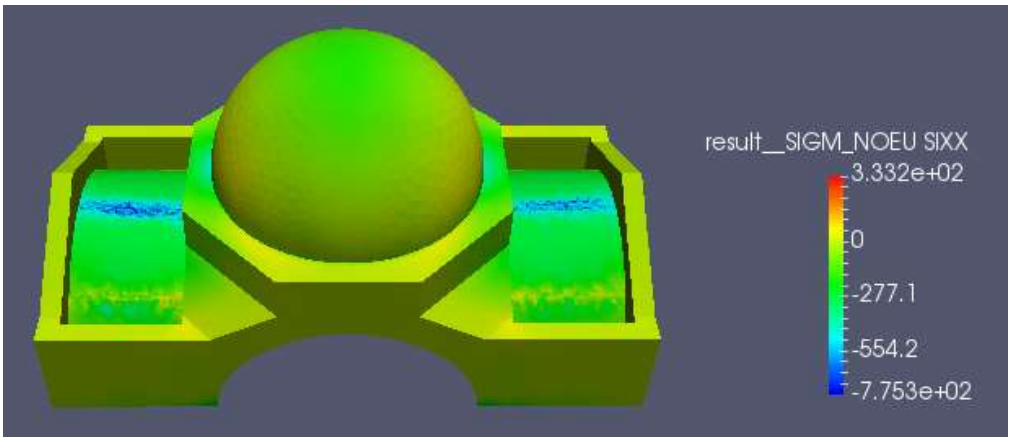


*Figure 92. Result of $\sigma_{xx}$ stresses in the model A at final step*

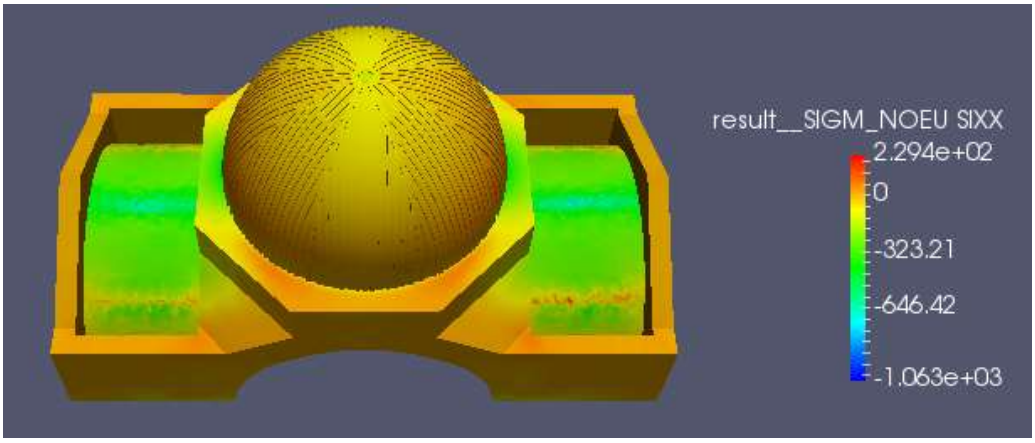


*Figure 93. Result of $\sigma_{xx}$ stresses in the model B at final step*

For $\sigma_{yy}$, the results obtained show that there is not any change in the values of the stresses in the model A and a slightly increase of the compression stresses in model B that seems not to be significant. This is caused by big stiffness of the longitudinal walls working along the y axis. The small deformation of the lateral walls along the y axis avoids the amplification of the forces in a second order analysis.

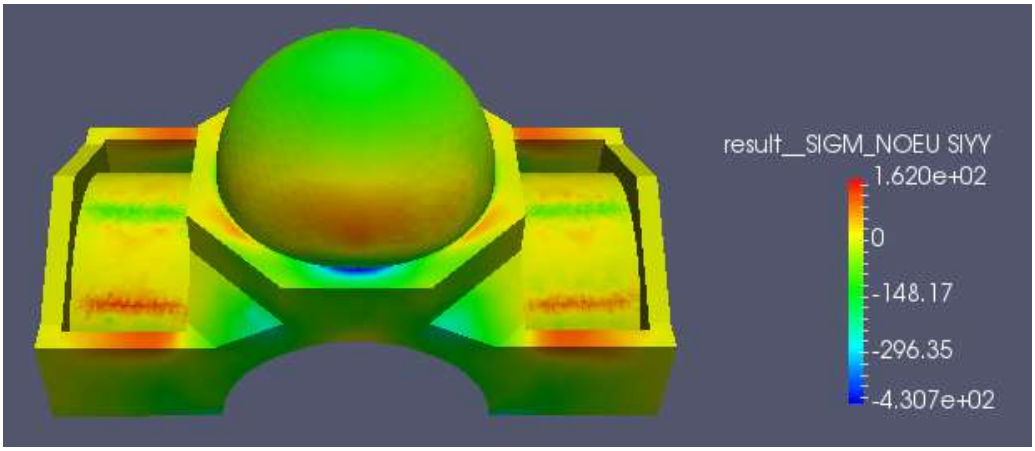


*Figure 94. Result of $\sigma_{yy}$ stresses in the model A at final step*

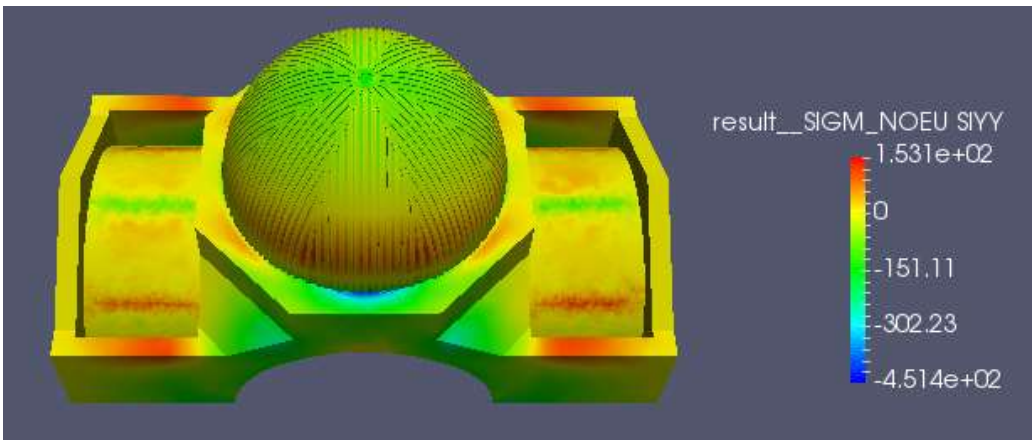


*Figure 95. Result of $\sigma_{yy}$ stresses in the model B at final step*

The results for $\sigma_{zz}$ are the same than in the linear analysis. Vertical loads are the same than the other analysis and they are not affected by second order effects.

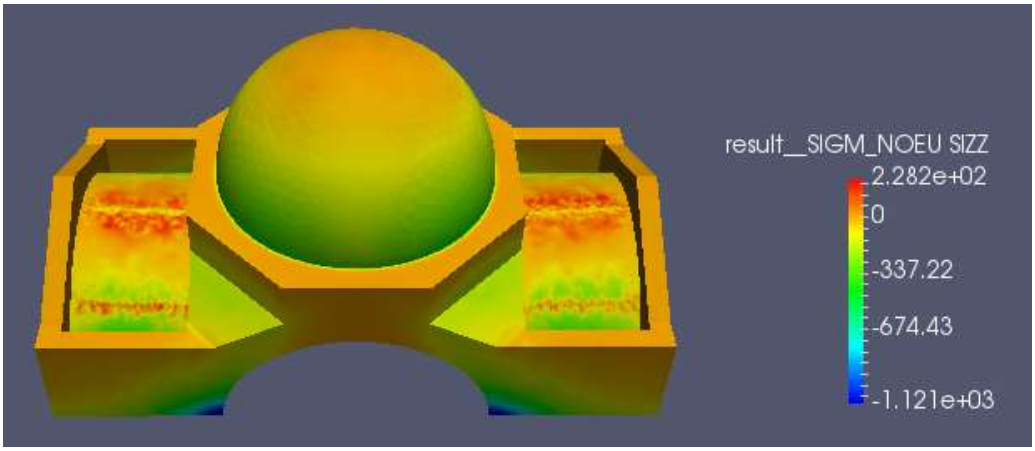


*Figure 96. Result of $\sigma_{zz}$ stresses in the model A at final step*

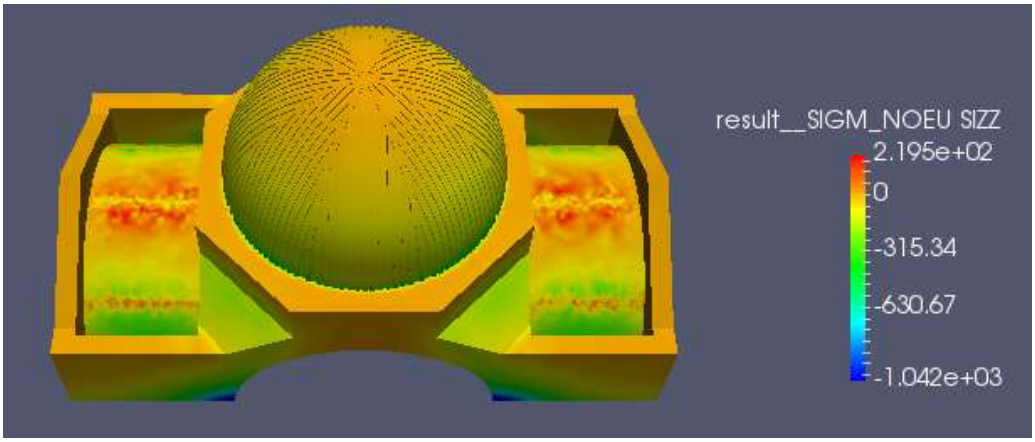


*Figure 97. Result of $\sigma_{zz}$ stresses in the model B at final step*

### *5.2.3.2 Shear Stresses*

The results for $\tau_{xy}$ are the same than in the linear analysis. These stresses have not been increased by the second order effects producing more points of failure or cracking.

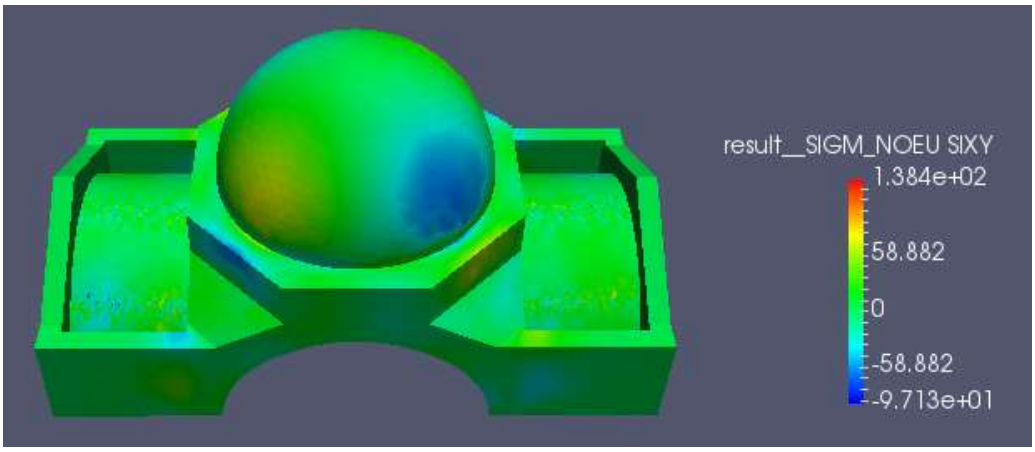


*Figure 98. Result of $\tau_{xy}$ stresses in the model A at final step*

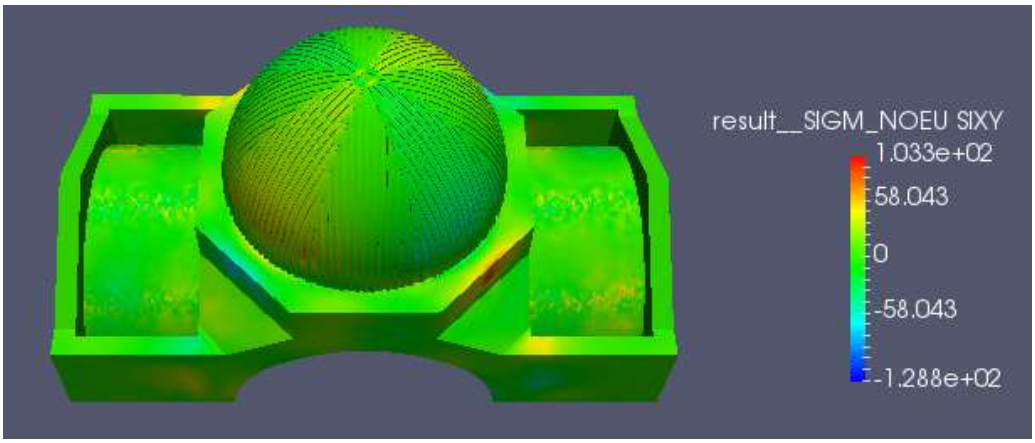


*Figure 99. Result of $\tau_{xy}$ stresses in the model B at final step*

The results for $\tau_{xz}$ are a bit different than the results in the linear analysis. The maximum positive values have experienced a decrease in their values and the negative values have increased. This variation is bigger in the model B than in model A. In model A, the values obtained have varied at about an 8 % while in the model B, the values have varied almost a 30 %, creating new potential points of failure.

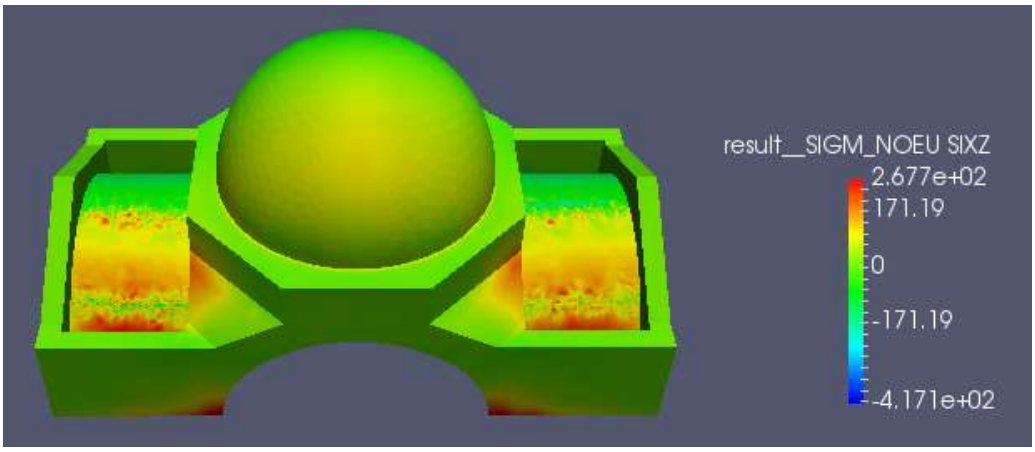


*Figure 100. Result of $\tau_{xz}$ stresses in the model A at final step*

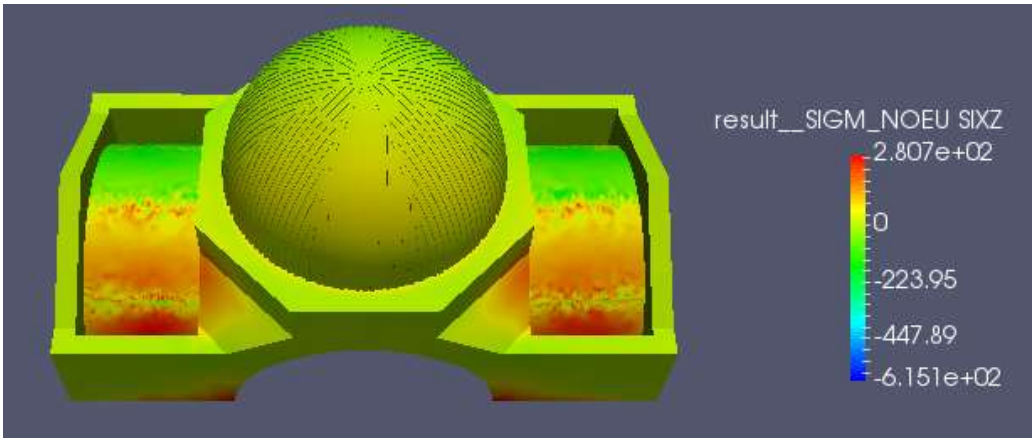


*Figure 101. Result of $\tau_{xz}$ stresses in the model B at final step*

The results for $\tau_{yz}$ are the same than in the linear analysis. These stresses have not been increased by the second order effects producing more points of failure or cracking.

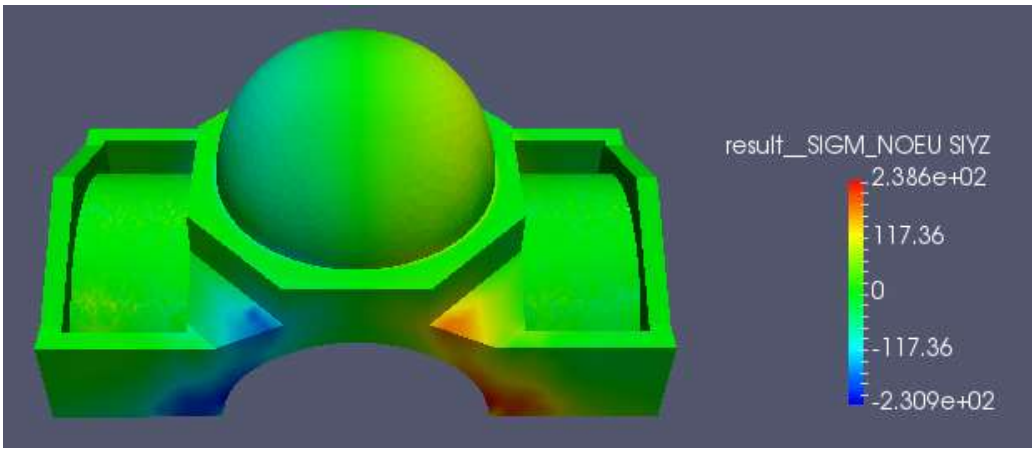


*Figure 102. Result of $\tau_{yz}$ stresses in the model A at final step*

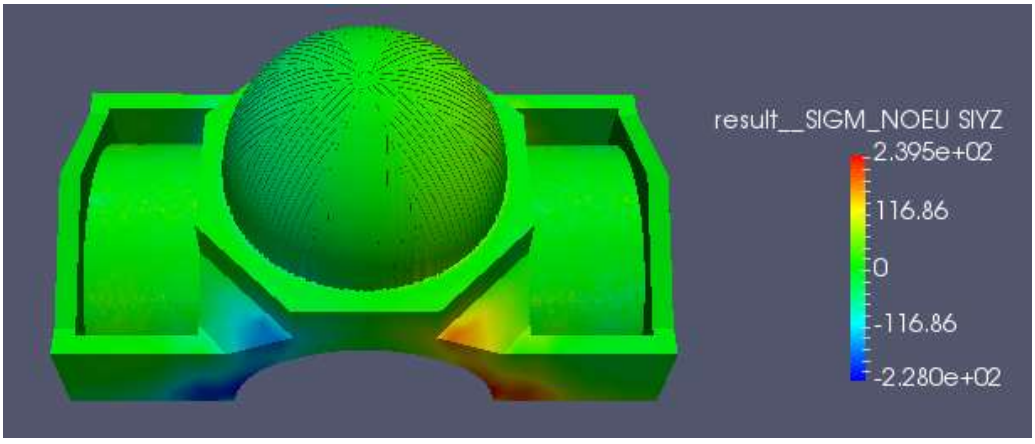


*Figure 103. Result of $\tau_{xz}$ stresses in the model B at final step*

# 3. Conclusions

## 3.1. Description of the conclusions of the work

This work was focused on the structural analysis of an historical church. One of the targets was to compare the behaviour of a dome with nerves with a dome without nerves. According to this the main conclusions that arise from the study are:

- The dome with nerves allow to control the stresses due to its increase of cross section and inertia.
- The stresses are controlled among the nerves, while in the dome without nerves, the stresses spread in big areas.
- The drum allows to control the deformation of the dome avoiding the dome to open outwards at its base.
- The eigenvalues between the model with the dome with nerves and the model with the dome without nerves are different in the first modes, but they close as the number of modes increase.
- Shear stresses are concentrated in the walls following the shape of the arches in the longitudinal walls.

## 3.2. Aims initially posed

The aim of this work was to create two models with 3D finite elements and compare them to analyse the differences that appear if the structure is constructed with a dome as a half sphere or a dome with external nerves.

On the other hand, related to the analysis of the dome, it is the analysis of the rest of the structure.

Three analysis have been able to be done thus all the initial aims have been able to carry out in this work.

## 3.3. Analysis of the follow-up of the planning and methodology

The analysis of a structure has a relative simple planning, once the dimensions of the structure are defined and set, the first step is to create the model (2D or 3D).

The second step is to mesh the volume of the structure.

After the mesh has been created, the model needs to be load with the actions that act over the structure (own load, superimposed loads, live loads, etc.).

Finally, when all the previous steps are finished, the stresses, the displacements and the reactions are calculated and the results analysed.

All these steps are linked in an only way, so it is not possible to change the order.

According to this the planning has been very simple to follow, knowing all the steps to do, the time has been able to be distributed according to the requirements of every step.

## 3.4. Lines of future work

This work has been delimited to a specific part of a structure doing some assumptions to simplify the analysis.

In future works it would be very interesting to be able to model the whole structure. Modelling the structure completely we could approach better to the real behaviour.

Another important fact is that in this study all the loads are symmetric. It would be interesting to analyse the structure under asymmetrical loads and earthquake loads.

Another possible study is to do a non-linear analysis with finite elements with the capacity of allow relative movements among elements when the maximum stresses are reached. This will allow to follow the grow of cracks.

# 4. Glossary

## B.

Bending moment: It is the reaction induced in a structural element when an external force or moment is applied to the element causing the element to bend.

Brickwork: Brick construction, as contrasted with that using other materials.

## D.

Dome: A roof or ceiling that is rounded or in the form of a part of a sphere.

Drum: A cylindrical or faceted construction supporting a dome.

## F.

Finite Elements Method: General numerical method for the approximation of solutions of very complex partial differential equations used in diverse problems of engineering and physics.

## M.

Mason: one whose trade is building with stones or bricks.

Masonry: Work constructed by a mason, esp. stonework.

Moment: The product of a physical quantity and its directed distance from an axis.

## P.

Pendentive: Any of several spandrels, in the form of spherical triangles, forming a transition between the circular plan of a dome and the polygonal plan of the supporting masonry.

## S.

Shear forces: They are unaligned forces pushing one part of a body in one direction, and another part of the body in the opposite direction.

# 5. Bibliography


ARTICLES:

- **[a1]** Bacigalupo etal, A simplified assessment of the dome and drum of the Basilica of S. Maria Assunta in Carignano in Genoa, Engineering Structures, pages 749-760, Number 56, 2013.

BOOKS:

- **[b1]** Elena Galve Martín,La iglesia de San Bartolomé, un hito para Benicarló. Análisis e intervención, Escola Tècnica Superior d'Arquitectura, Universitat Politècnica de València, 2014.

SOFTWARE:

- **[s1] Ubuntu Operative System:** https://www.ubuntu.com/, November 2016.
- **[s2] Salome-Meca:** http://www.salome-platform.org/, November 2016
- **[s3] Code-Aster:** http://www.code-aster.org/spip.php?rubrique2, November 2016
- **[s4] Efficient:** http://engineering.moonish.biz/efficient/, November 2016

WEBS:

- **[w1] Benicarló Council:** https://www.ajuntamentdebenicarlo.org/mon/pmon-santbertomeu.php3, April 2017.
- **[w2] Wikipedia:** https://ca.wikipedia.org/wiki/Esgl%C3%A9sia_de_Sant_Bartomeu_de_Benicarl%C3%B3, April 2017.

# 6. Annexes

## 6.1. Code-Aster files

### 6.1.1. Model A – Linear Analysis .comm file

```
DEBUT();

mesh=LIRE_MAILLAGE(FORMAT='MED',);

model=AFFE_MODELE(MAILLAGE=mesh,
      AFFE=_F(TOUT='OUI',PHENOMENE='MECANIQUE',
              MODELISATION='3D',),);

SM=DEFI_MATERIAU(ELAS=_F(E=5000000, NU=0.2, RHO=22,),);

BW=DEFI_MATERIAU(ELAS=_F(E=2000000, NU=0.2, RHO=17,),);

material=AFFE_MATERIAU(MAILLAGE=mesh,
                       AFFE=(_F(GROUP_MA='Drum',MATER=SM,),
                             _F(GROUP_MA='Dome',MATER=BW,),
                             _F(GROUP_MA='Roof_1',MATER=BW,),
                             _F(GROUP_MA='Roof_2',MATER=BW,),
                       ),);

Support=AFFE_CHAR_MECA(MODELE=model,
                       DDL_IMPO=_F(GROUP_MA='Base',
                       DX=0,DY=0,DZ=0,),);

Density=AFFE_CHAR_MECA(MODELE=model,PESANTEUR=_F(GRAVITE=-1,
                       DIRECTION=(0.0,0.0,1.0,),),);

Dm_Load=AFFE_CHAR_MECA(MODELE=model,
                       FORCE_FACE=(_F(GROUP_MA='Dm_Fc',
                                  FZ = -3,),),);

R1_Load=AFFE_CHAR_MECA(MODELE=model,
                       FORCE_FACE=(_F(GROUP_MA='R1_Fc',
                                  FZ = -3,),),);

R2_Load=AFFE_CHAR_MECA(MODELE=model,
                       FORCE_FACE=(_F(GROUP_MA='R2_Fc',
                                  FZ = -3,),),);

result=MECA_STATIQUE(MODELE=model,CHAM_MATER=material,
                     EXCIT=(_F(CHARGE=Support,),
                            _F(CHARGE=Density,),
                            _F(CHARGE=Dm_Load,),
                            _F(CHARGE=R1_Load,),
                            _F(CHARGE=R2_Load,),),);

result=CALC_CHAMP(reuse=result,RESULTAT=result,
                  CONTRAINTE=('SIGM_ELNO','SIGM_NOEU',),
                  CRITERES=('SIEQ_ELNO','SIEQ_NOEU',),
                  FORCE=('REAC_NODA',),);
                  IMPR_RESU(FORMAT='MED',UNITE=80,
                  RESU=_F(MAILLAGE=mesh,RESULTAT=result,
```

```
                    NOM_CHAM=('DEPL','SIGM_ELNO','SIGM_NOEU',
                              'SIEQ_ELNO','SIEQ_NOEU','REAC_NODA',
                    ),),);

FIN();
```

### 6.1.2. Model A – Modal Analysis .comm file

```
DEBUT(IGNORE_ALARM='UTILITAI4_2');

MAIL=LIRE_MAILLAGE(UNITE=20,
                   FORMAT='MED',);

MODELE=AFFE_MODELE(MAILLAGE=MAIL,
                   AFFE=_F(TOUT='OUI',
                           PHENOMENE='MECANIQUE',
                           MODELISATION='3D',),);

SM=DEFI_MATERIAU(ELAS=_F(E=5000000, NU=0.2, RHO=22,),);

BW=DEFI_MATERIAU(ELAS=_F(E=2000000, NU=0.2, RHO=17,),);

CHMAT=AFFE_MATERIAU(MAILLAGE=MAIL,      AFFE=(_F(GROUP_MA='Drum',
MATER=SM,),_F(GROUP_MA='Dome',   MATER=BW,),_F(GROUP_MA='Roof_1',
MATER=BW,),_F(GROUP_MA='Roof_2', MATER=BW,),),);

BLOCAGE=AFFE_CHAR_MECA(MODELE=MODELE,
                       DDL_IMPO=(
                           _F(GROUP_MA='Base',
                              DX=0.0,
                              DY=0.0,
                              DZ=0.0,),),);

ASSEMBLAGE(MODELE=MODELE,
           CHAM_MATER=CHMAT,
           CHARGE=BLOCAGE,
           NUME_DDL=CO('NUMEDDL'),
           MATR_ASSE=(_F(MATRICE=CO('RIGIDITE'),
                         OPTION='RIGI_MECA',),
                      _F(MATRICE=CO('MASSE'),
                         OPTION='MASS_MECA',),),);

MODES=CALC_MODES(MATR_RIGI=RIGIDITE,
                 MATR_MASS=MASSE,
                 OPTION='PLUS_PETITE',
                 CALC_FREQ=_F(NMAX_FREQ=5,));

MODES=CALC_CHAMP(reuse=MODES,
                 RESULTAT=MODES,
                 CONTRAINTE=('SIEF_ELGA'),);

IMPR_RESU(FORMAT='MED',
          RESU=_F(RESULTAT=MODES,),);

FIN();
```

### 6.1.3. Model A – Non Linear Analysis .comm file

```
DEBUT();

mesh=LIRE_MAILLAGE(FORMAT='MED',);

model=AFFE_MODELE(MAILLAGE=mesh,AFFE=_F(TOUT='OUI',
                  PHENOMENE='MECANIQUE', MODELISATION='3D',),);

SM=DEFI_MATERIAU(ELAS=_F(E=5000000, NU=0.2, RHO=22,),);

BW=DEFI_MATERIAU(ELAS=_F(E=2000000, NU=0.2, RHO=17,),);

material=AFFE_MATERIAU(MAILLAGE=mesh,
                       AFFE=(_F(GROUP_MA='Drum', MATER=SM,),
                             _F(GROUP_MA='Dome',MATER=BW,),
                             _F(GROUP_MA='Roof_1',MATER=BW,),
                             _F(GROUP_MA='Roof_2',MATER=BW,),),);

Support=AFFE_CHAR_MECA(MODELE=model,
                       DDL_IMPO=_F(GROUP_MA='Base',DX=0,DY=0,
                                   DZ=0,),);

Density=AFFE_CHAR_MECA(MODELE=model,
                       PESANTEUR=_F(GRAVITE=-1,DIRECTION=(0.0,
                                    0.0,1.0,),),);

Dm_Load=AFFE_CHAR_MECA(MODELE=model,
                       FORCE_FACE=(_F(GROUP_MA='Dm_Fc',
                                   FZ = -3,),),);

R1_Load=AFFE_CHAR_MECA(MODELE=model,
                       FORCE_FACE=(_F(GROUP_MA='R1_Fc',
                                   FZ = -3,),),);

R2_Load=AFFE_CHAR_MECA(MODELE=model,
                       FORCE_FACE=(_F(GROUP_MA='R2_Fc',
                                   FZ = -3,),),);

time=DEFI_LIST_REEL(DEBUT=0,INTERVALLE=(_F(JUSQU_A=1,
                                           NOMBRE=5,),
                                        _F(JUSQU_A=2,
                                        NOMBRE=5,),),);

timeA=DEFI_LIST_INST(DEFI_LIST=_F(METHODE='AUTO',
                                  LIST_INST=time,),
                     ECHEC=_F(EVENEMENT='ERREUR',
                              SUBD_PAS=2,),
                     ADAPTATION=(_F(NB_INCR_SEUIL=1,
                                 CRIT_COMP='LE',VALE_I=100,
                                 PCENT_AUGM=100,),
                                 _F(NB_INCR_SEUIL=1,
                                  CRIT_COMP='GT',
                                 VALE_I=1000,
                                 PCENT_AUGM=50,),),);


ramp1=DEFI_FONCTION(NOM_PARA='INST',VALE=(0,0,1,1,2,1),);

ramp2=DEFI_FONCTION(NOM_PARA='INST', VALE=(0, 0,1,0,2,1),);
```

```
result=STAT_NON_LINE(MODELE=model,
                     CHAM_MATER=material,
                     EXCIT=(_F(CHARGE=Support,),
                            _F(CHARGE=Density,FONC_MULT=ramp1,),
                            _F(CHARGE=Dm_Load,FONC_MULT=ramp2,),
                            _F(CHARGE=R1_Load,FONC_MULT=ramp2,),
                            _F(CHARGE=R2_Load,FONC_MULT=ramp2,),
                            ),
                     INCREMENT=_F(LIST_INST=timeA,INST_FIN=2.0,),
                     NEWTON=_F(REAC_INCR=1,MATRICE='TANGENTE',
                               REAC_ITER=1,),
                      CONVERGENCE=_F(RESI_GLOB_RELA=0.0001,
                                     ITER_GLOB_MAXI=5000,),);

result=CALC_CHAMP(reuse=result,RESULTAT=result,
                  CONTRAINTE=('SIGM_ELNO','SIGM_NOEU',),
                  CRITERES=('SIEQ_ELNO','SIEQ_NOEU',),
                           FORCE=('REAC_NODA',),);

IMPR_RESU(FORMAT='MED',UNITE=80,
          RESU=_F(MAILLAGE=mesh,RESULTAT=result,
                  NOM_CHAM=('DEPL','SIGM_ELNO','SIGM_NOEU',
                            'SIEQ_ELNO','SIEQ_NOEU','REAC_NODA',
                            ),),);

FIN();
```

### 6.1.4. Model B – Linear Analysis .comm file

```
DEBUT();

mesh=LIRE_MAILLAGE(FORMAT='MED',);

model=AFFE_MODELE(MAILLAGE=mesh,
      AFFE=_F(TOUT='OUI',PHENOMENE='MECANIQUE',
              MODELISATION='3D',),);

SM=DEFI_MATERIAU(ELAS=_F(E=5000000, NU=0.2, RHO=22,),);

BW=DEFI_MATERIAU(ELAS=_F(E=2000000, NU=0.2, RHO=17,),);

material=AFFE_MATERIAU(MAILLAGE=mesh,
                       AFFE=(_F(GROUP_MA='Drum',MATER=SM,),
                             _F(GROUP_MA='Dome',MATER=BW,),
                             _F(GROUP_MA='Roof_1',MATER=BW,),
                             _F(GROUP_MA='Roof_2',MATER=BW,),
                       ),);

Support=AFFE_CHAR_MECA(MODELE=model,
                       DDL_IMPO=_F(GROUP_MA='Base',
                       DX=0,DY=0,DZ=0,),);

Density=AFFE_CHAR_MECA(MODELE=model,PESANTEUR=_F(GRAVITE=-1,
                       DIRECTION=(0.0,0.0,1.0,),),);

Dm_Load=AFFE_CHAR_MECA(MODELE=model,
                       FORCE_FACE=(_F(GROUP_MA='Dm_Fc',
                                  FZ = -2,),),);
```

```
R1_Load=AFFE_CHAR_MECA(MODELE=model,
                       FORCE_FACE=(_F(GROUP_MA='R1_Fc',
                                      FZ = -3,),),);

R2_Load=AFFE_CHAR_MECA(MODELE=model,
                       FORCE_FACE=(_F(GROUP_MA='R2_Fc',
                                      FZ = -3,),),);

result=MECA_STATIQUE(MODELE=model,CHAM_MATER=material,
                     EXCIT=(_F(CHARGE=Support,),
                            _F(CHARGE=Density,),
                            _F(CHARGE=Dm_Load,),
                            _F(CHARGE=R1_Load,),
                            _F(CHARGE=R2_Load,),),);

result=CALC_CHAMP(reuse=result,RESULTAT=result,
                  CONTRAINTE=('SIGM_ELNO','SIGM_NOEU',),
                  CRITERES=('SIEQ_ELNO','SIEQ_NOEU',),
                  FORCE=('REAC_NODA',),);
                  IMPR_RESU(FORMAT='MED',UNITE=80,
                  RESU=_F(MAILLAGE=mesh,RESULTAT=result,
                  NOM_CHAM=('DEPL','SIGM_ELNO','SIGM_NOEU',
                            'SIEQ_ELNO','SIEQ_NOEU','REAC_NODA',
                  ),),);

FIN();
```

### 6.1.5. Model B – Modal Analysis .comm file

```
DEBUT(IGNORE_ALARM='UTILITAI4_2');

MAIL=LIRE_MAILLAGE(UNITE=20,
                   FORMAT='MED',);

MODELE=AFFE_MODELE(MAILLAGE=MAIL,
                   AFFE=_F(TOUT='OUI',
                           PHENOMENE='MECANIQUE',
                           MODELISATION='3D',),);

SM=DEFI_MATERIAU(ELAS=_F(E=5000000, NU=0.2, RHO=22,),);

BW=DEFI_MATERIAU(ELAS=_F(E=2000000, NU=0.2, RHO=17,),);

CHMAT=AFFE_MATERIAU(MAILLAGE=MAIL,      AFFE=(_F(GROUP_MA='Drum',
MATER=SM,),_F(GROUP_MA='Dome',   MATER=BW,),_F(GROUP_MA='Roof_1',
MATER=BW,),_F(GROUP_MA='Roof_2', MATER=BW,),),);

BLOCAGE=AFFE_CHAR_MECA(MODELE=MODELE,
                       DDL_IMPO=(
                           _F(GROUP_MA='Base',
                              DX=0.0,
                              DY=0.0,
                              DZ=0.0,),),);

ASSEMBLAGE(MODELE=MODELE,
           CHAM_MATER=CHMAT,
           CHARGE=BLOCAGE,
           NUME_DDL=CO('NUMEDDL'),
           MATR_ASSE=(_F(MATRICE=CO('RIGIDITE'),
```

```
                          OPTION='RIGI_MECA',),
                        _F(MATRICE=CO('MASSE'),
                          OPTION='MASS_MECA',),),);

MODES=CALC_MODES(MATR_RIGI=RIGIDITE,
                 MATR_MASS=MASSE,
                 OPTION='PLUS_PETITE',
                 CALC_FREQ=_F(NMAX_FREQ=5,));

MODES=CALC_CHAMP(reuse=MODES,
                 RESULTAT=MODES,
                 CONTRAINTE=('SIEF_ELGA'),);

IMPR_RESU(FORMAT='MED',
          RESU=_F(RESULTAT=MODES,),);

FIN();
```

### 6.1.6. Model B – Non Linear Analysis .comm file

```
DEBUT();

mesh=LIRE_MAILLAGE(FORMAT='MED',);

model=AFFE_MODELE(MAILLAGE=mesh,AFFE=_F(TOUT='OUI',
                  PHENOMENE='MECANIQUE', MODELISATION='3D',),);

SM=DEFI_MATERIAU(ELAS=_F(E=5000000, NU=0.2, RHO=22,),);

BW=DEFI_MATERIAU(ELAS=_F(E=2000000, NU=0.2, RHO=17,),);

material=AFFE_MATERIAU(MAILLAGE=mesh,
                       AFFE=(_F(GROUP_MA='Drum', MATER=SM,),
                             _F(GROUP_MA='Dome',MATER=BW,),
                             _F(GROUP_MA='Roof_1',MATER=BW,),
                             _F(GROUP_MA='Roof_2',MATER=BW,),),);

Support=AFFE_CHAR_MECA(MODELE=model,
                       DDL_IMPO=_F(GROUP_MA='Base',DX=0,DY=0,
                                   DZ=0,),);

Density=AFFE_CHAR_MECA(MODELE=model,
                       PESANTEUR=_F(GRAVITE=-1,DIRECTION=(0.0,
                                    0.0,1.0,),),);

Dm_Load=AFFE_CHAR_MECA(MODELE=model,
                       FORCE_FACE=(_F(GROUP_MA='Dm_Fc',
                                   FZ = -2,),),);

R1_Load=AFFE_CHAR_MECA(MODELE=model,
                       FORCE_FACE=(_F(GROUP_MA='R1_Fc',
                                   FZ = -3,),),);

R2_Load=AFFE_CHAR_MECA(MODELE=model,
                       FORCE_FACE=(_F(GROUP_MA='R2_Fc',
                                   FZ = -3,),),);

time=DEFI_LIST_REEL(DEBUT=0,INTERVALLE=(_F(JUSQU_A=1,
                                           NOMBRE=5,),
```

```
                                        _F(JUSQU_A=2,
                                        NOMBRE=5,),),);

timeA=DEFI_LIST_INST(DEFI_LIST=_F(METHODE='AUTO',
                                  LIST_INST=time,),
                     ECHEC=_F(EVENEMENT='ERREUR',
                              SUBD_PAS=2,),
                     ADAPTATION=(_F(NB_INCR_SEUIL=1,
                                    CRIT_COMP='LE',VALE_I=100,
                                    PCENT_AUGM=100,),
                                    _F(NB_INCR_SEUIL=1,
                                     CRIT_COMP='GT',
                                    VALE_I=1000,
                                    PCENT_AUGM=50,),),);


ramp1=DEFI_FONCTION(NOM_PARA='INST',VALE=(0,0,1,1,2,1),);

ramp2=DEFI_FONCTION(NOM_PARA='INST', VALE=(0, 0,1,0,2,1),);

result=STAT_NON_LINE(MODELE=model,
                     CHAM_MATER=material,
                     EXCIT=(_F(CHARGE=Support,),
                            _F(CHARGE=Density,FONC_MULT=ramp1,),
                            _F(CHARGE=Dm_Load,FONC_MULT=ramp2,),
                            _F(CHARGE=R1_Load,FONC_MULT=ramp2,),
                            _F(CHARGE=R2_Load,FONC_MULT=ramp2,),
                            ),
                     INCREMENT=_F(LIST_INST=timeA,INST_FIN=2.0,),
                     NEWTON=_F(REAC_INCR=1,MATRICE='TANGENTE',
                               REAC_ITER=1,),
                      CONVERGENCE=_F(RESI_GLOB_RELA=0.0001,
                                     ITER_GLOB_MAXI=5000,),);

result=CALC_CHAMP(reuse=result,RESULTAT=result,
                  CONTRAINTE=('SIGM_ELNO','SIGM_NOEU',),
                  CRITERES=('SIEQ_ELNO','SIEQ_NOEU',),
                           FORCE=('REAC_NODA',),);

IMPR_RESU(FORMAT='MED',UNITE=80,
          RESU=_F(MAILLAGE=mesh,RESULTAT=result,
                  NOM_CHAM=('DEPL','SIGM_ELNO','SIGM_NOEU',
                           'SIEQ_ELNO','SIEQ_NOEU','REAC_NODA',
                           ),),);

FIN();
```

## 6.2. Non-linear Analysis Results

### 6.2.1. Introduction

The non-linear analysis has been divided into 2 stages and each stage into 5 steps. At each step the load applied is added to the previous deformed model. In this Annex the results of the intermediate steps are shown.

The results of the following stages and steps are gathered in this annex to show the evolution of the results:

- Stage 0 – Step 3.
- Stage 0 – Step 5.
- Stage 1 – Step 3.

### 6.2.2. Model A Results

#### *6.2.2.1. Stage 0 – Step 3*

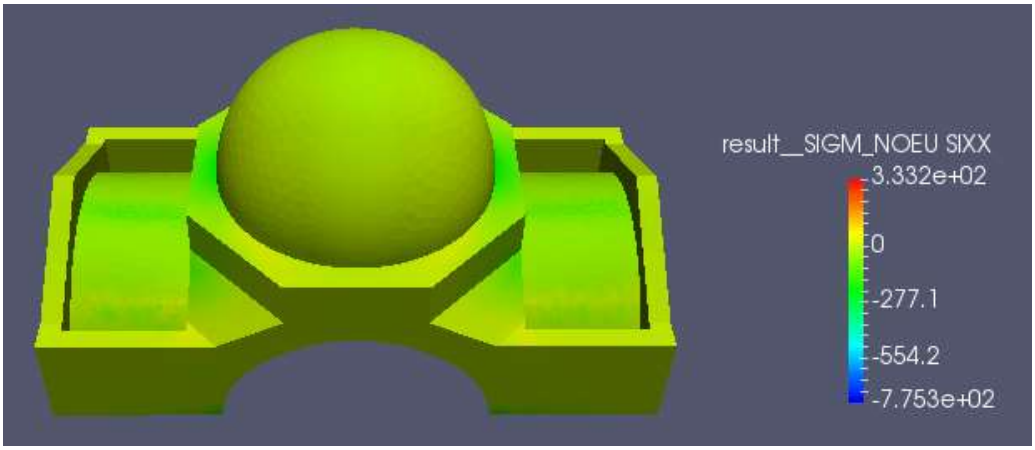


*Figure 104. Result of $\sigma_{xx}$ stresses in the model A. Stage 0 – Step 3*

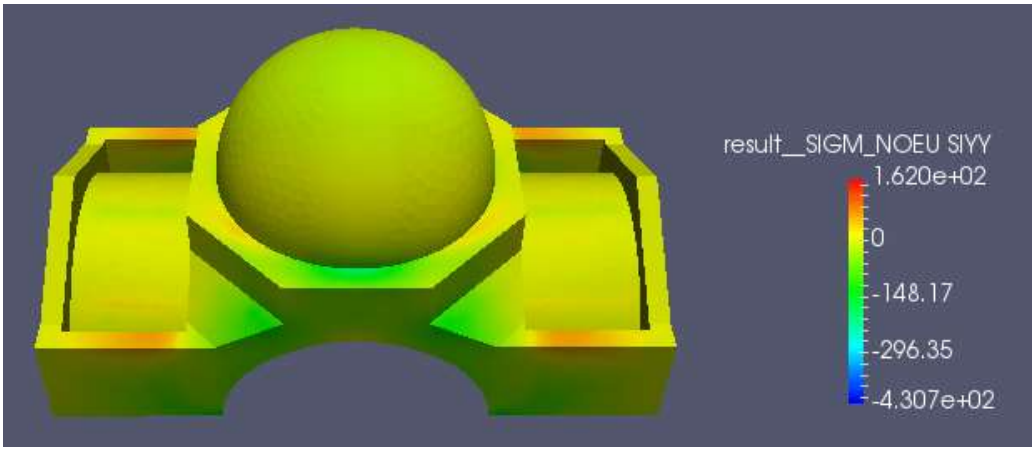


*Figure 105. Result of $\sigma_{yy}$ stresses in the model A. Stage 0 – Step 3*

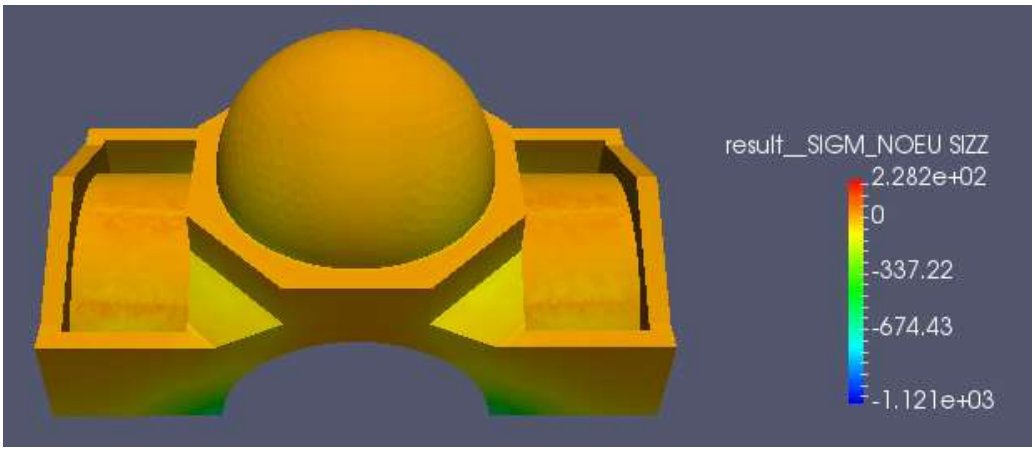


*Figure 106. Result of $\sigma_{zz}$ stresses in the model A. Stage 0 – Step 3*

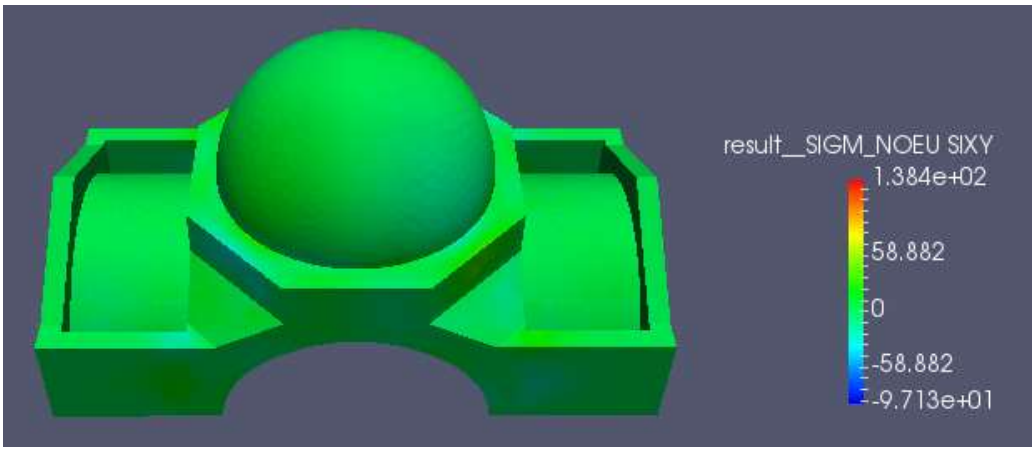


*Figure 107. Result of $\tau_{xy}$ stresses in the model A. Stage 0 – Step 3*

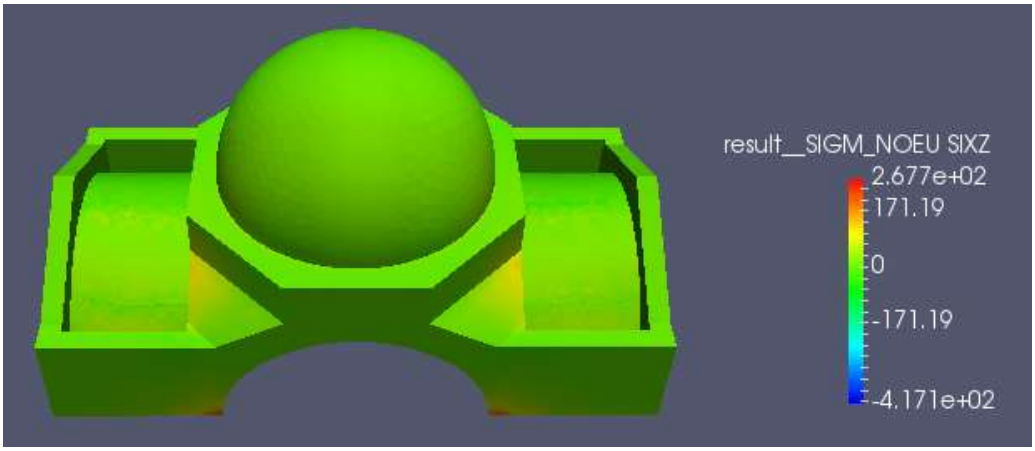


*Figure 108. Result of $\tau_{xz}$ stresses in the model A. Stage 0 – Step 3*

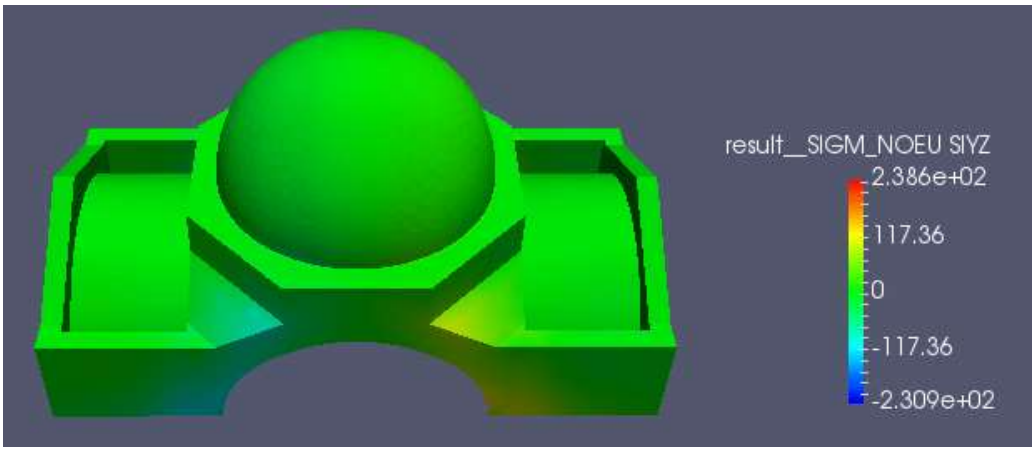


*Figure 109. Result of $\tau_{yz}$ stresses in the model A. Stage 0 – Step 3*

### 6.2.2.2. Stage 0 – Step 5

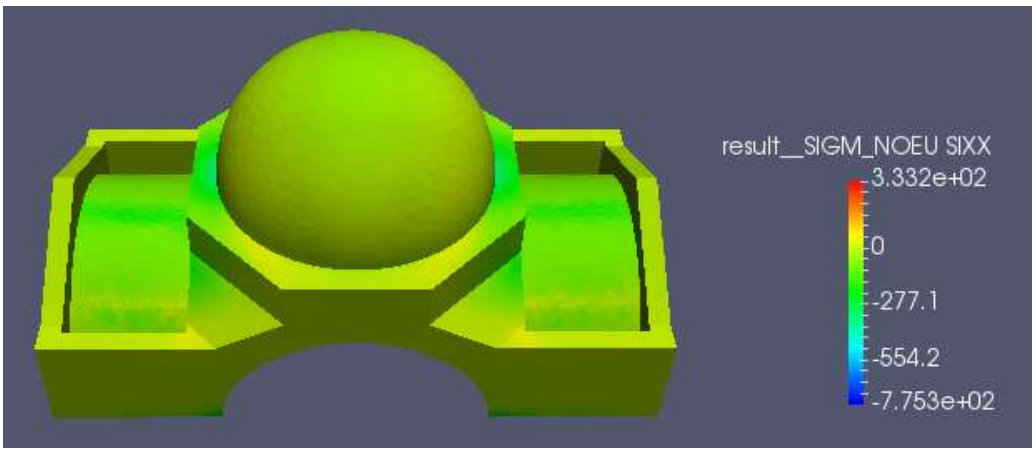


*Figure 110. Result of $\sigma_{xx}$ stresses in the model A. Stage 0 – Step 5*

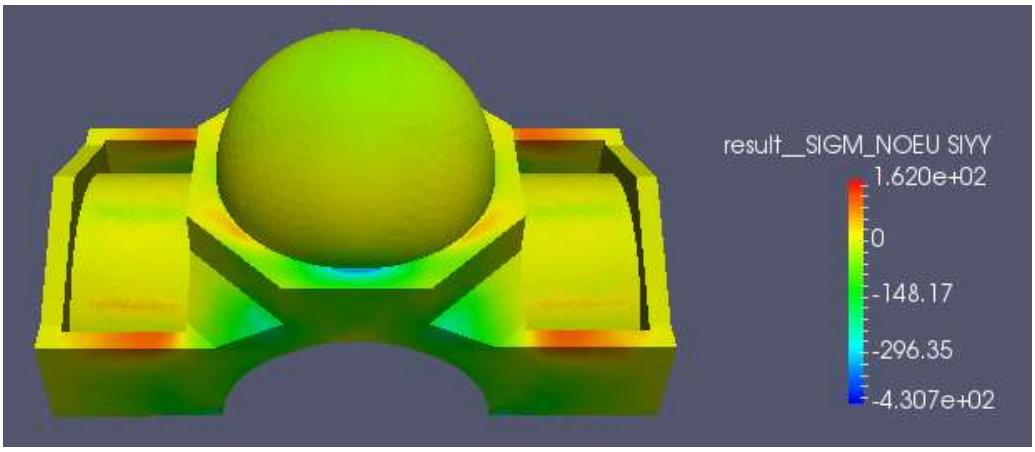


*Figure 111. Result of $\sigma_{yy}$ stresses in the model A. Stage 0 – Step 5*

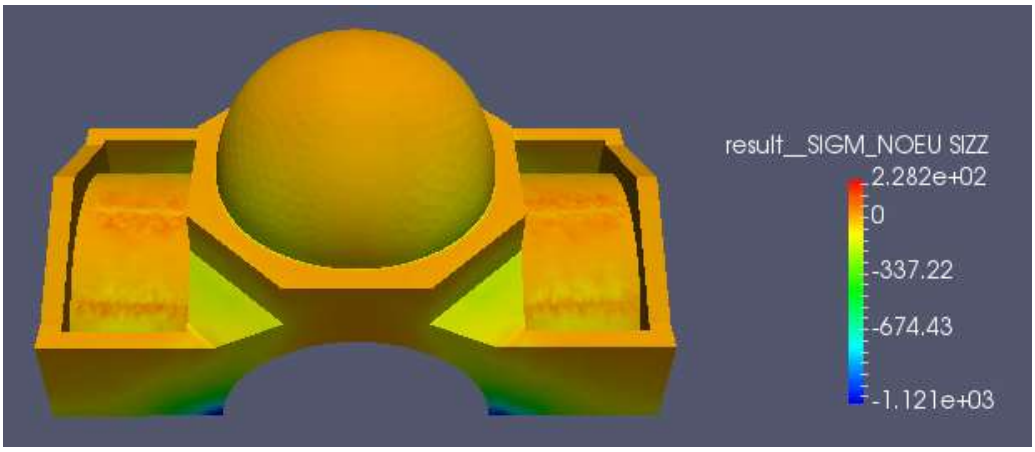


*Figure 112. Result of $\sigma_{zz}$ stresses in the model A. Stage 0 – Step 5*

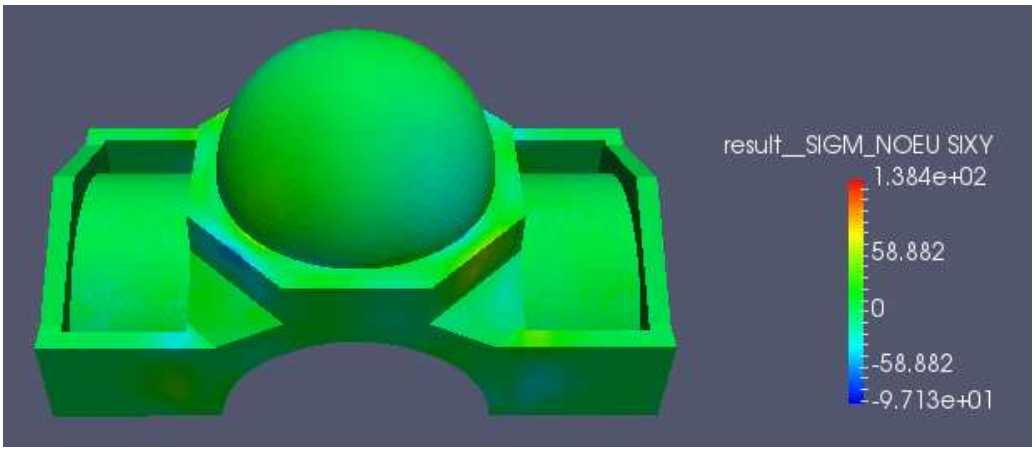


*Figure 113. Result of $\tau_{xy}$ stresses in the model A. Stage 0 – Step 5*

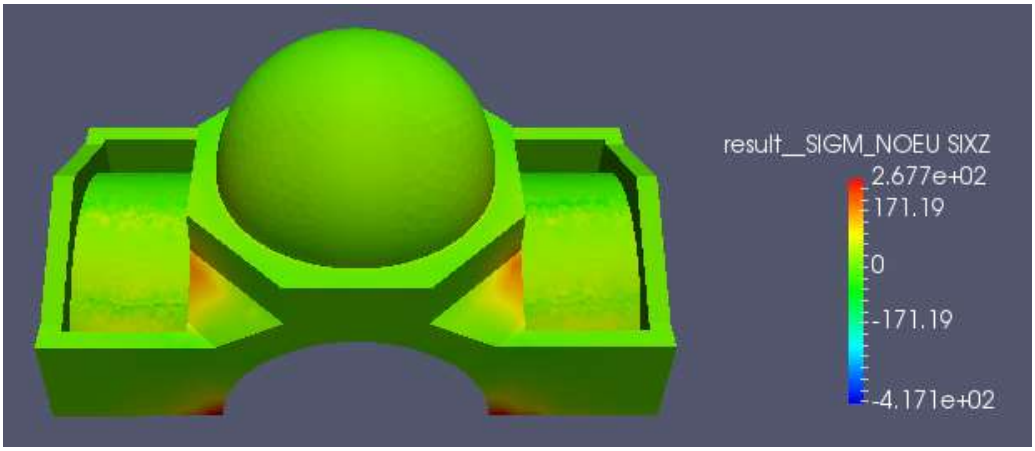


*Figure 114. Result of $\tau_{xz}$ stresses in the model A. Stage 0 – Step 5*

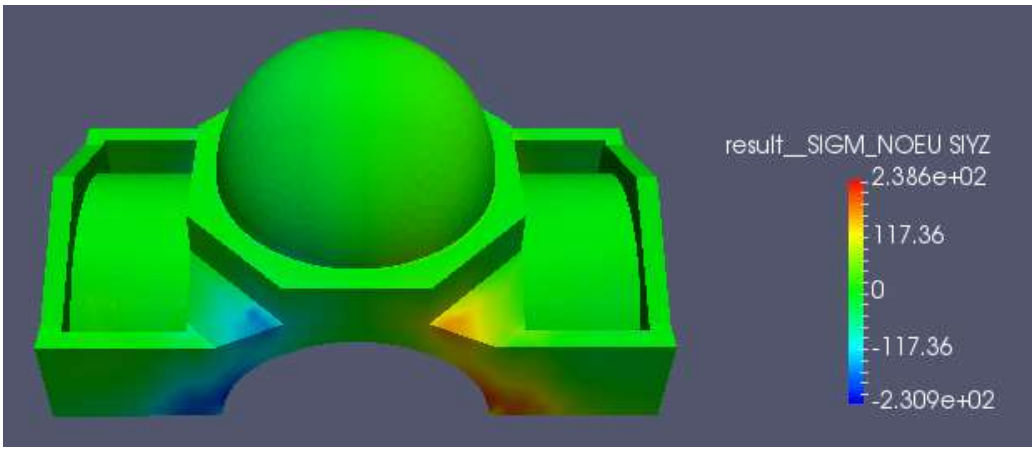


*Figure 115. Result of $\tau_{yz}$ stresses in the model A. Stage 0 – Step 5*

### 6.2.2.3. Stage 1 – Step 3

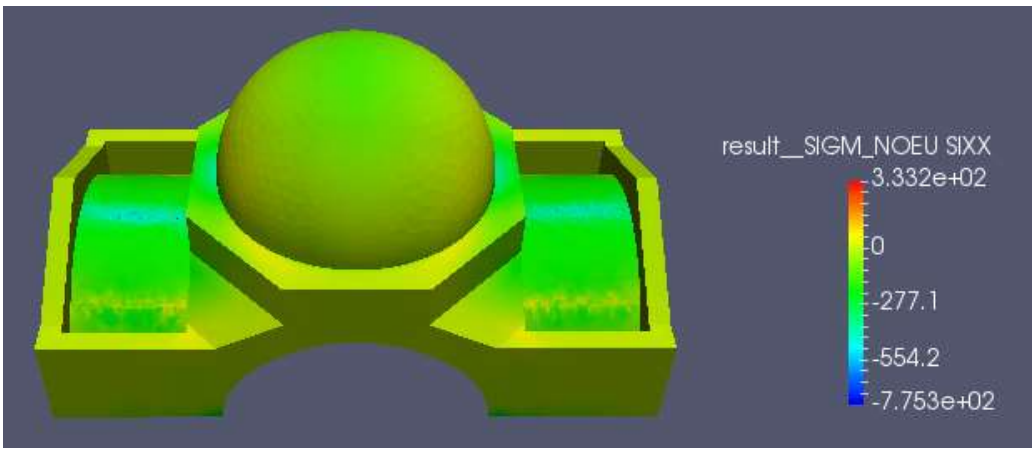


*Figure 116. Result of $\sigma_{xx}$ stresses in the model A. Stage 1 – Step 3*

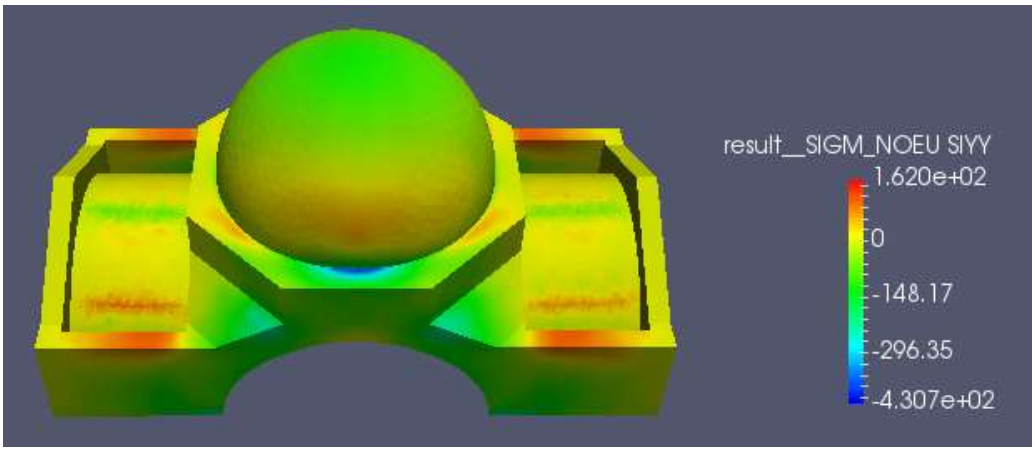


*Figure 117. Result of $\sigma_{yy}$ stresses in the model A. Stage 1 – Step 3*

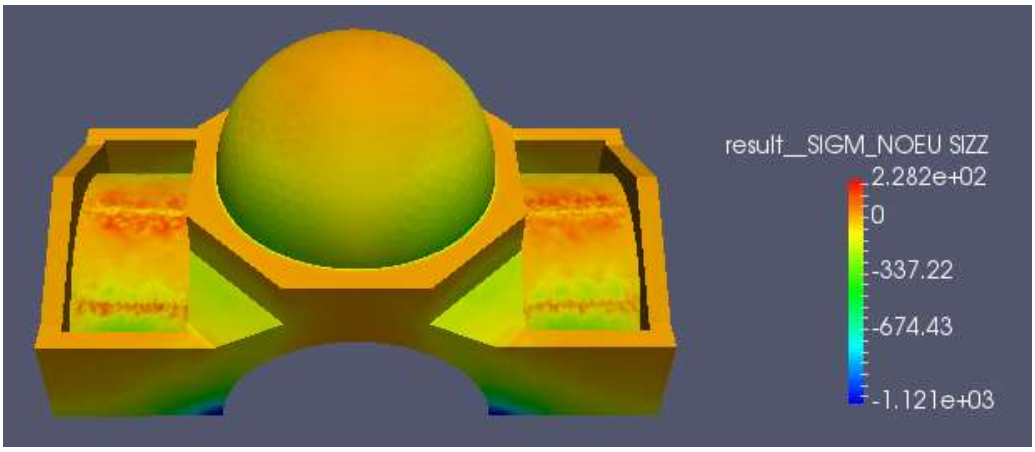


*Figure 118. Result of $\sigma_{zz}$ stresses in the model A. Stage 1 – Step 3*

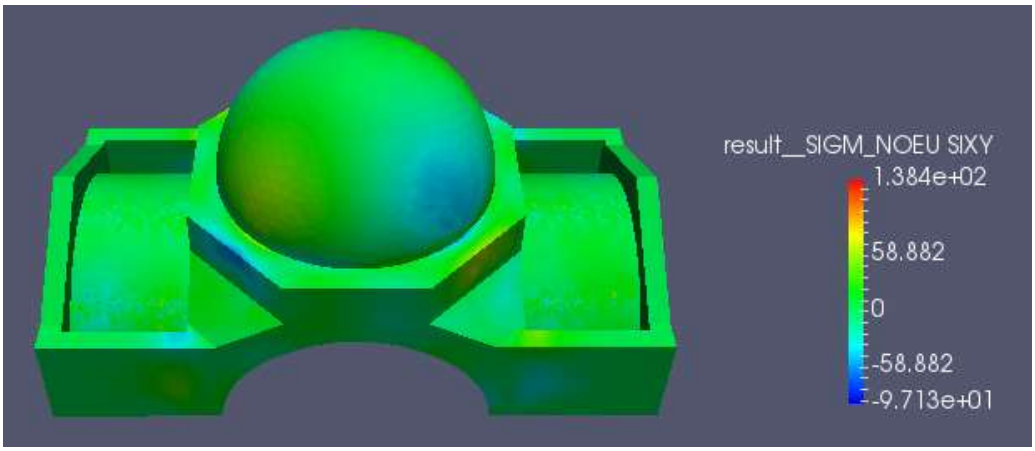


*Figure 119. Result of $\tau_{xy}$ stresses in the model A. Stage 1 – Step 3*

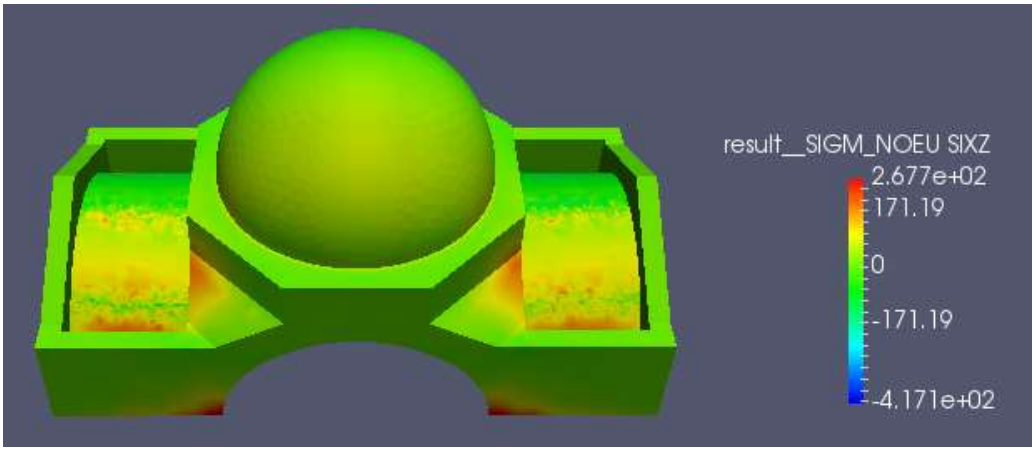


*Figure 120. Result of $\tau_{xz}$ stresses in the model A. Stage 1 – Step 3*

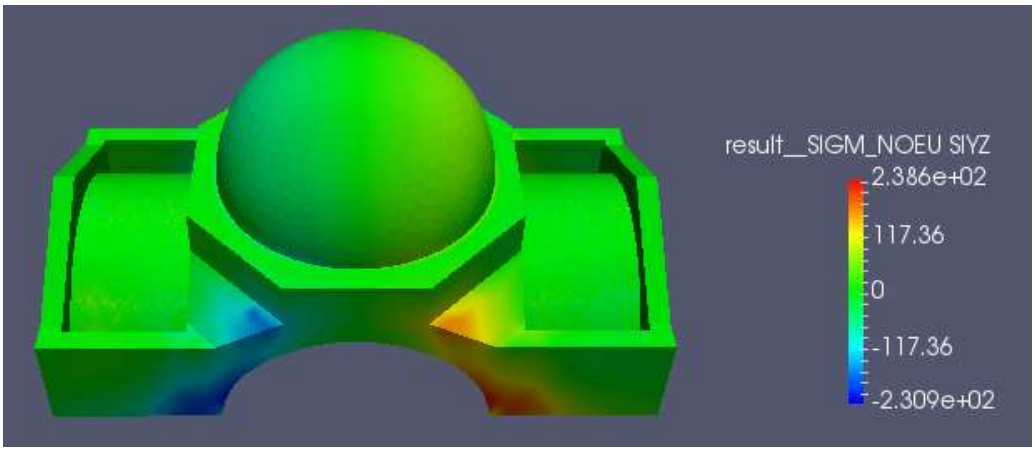


*Figure 121. Result of $\tau_{yz}$ stresses in the model A. Stage 1 – Step 3*

### 6.2.3. Model B Results

#### *6.2.3.1. Stage 0 – Step 3*

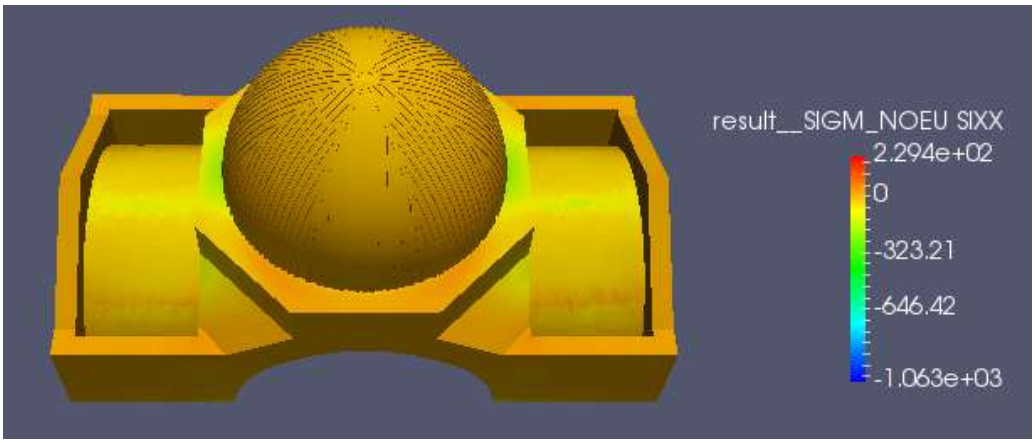


*Figure 122. Result of $\sigma_{xx}$ stresses in the model B. Stage 0 – Step 3*

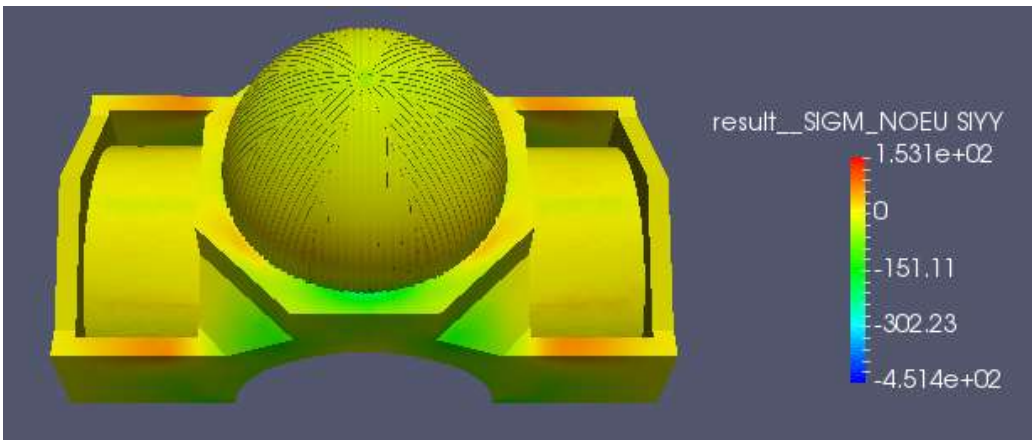


*Figure 123. Result of $\sigma_{yy}$ stresses in the model B. Stage 0 – Step 3*

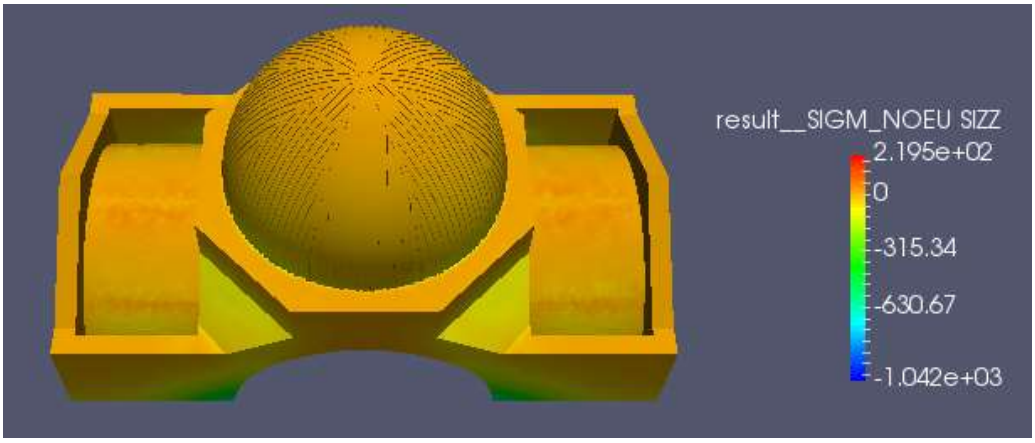


*Figure 124. Result of $\sigma_{zz}$ stresses in the model B. Stage 0 – Step 3*

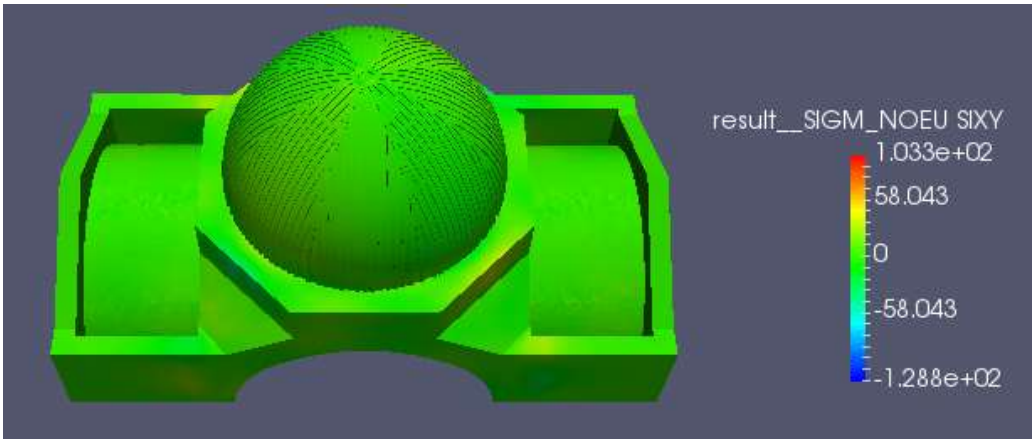


*Figure 125. Result of $\tau_{xy}$ stresses in the model B. Stage 0 – Step 3*

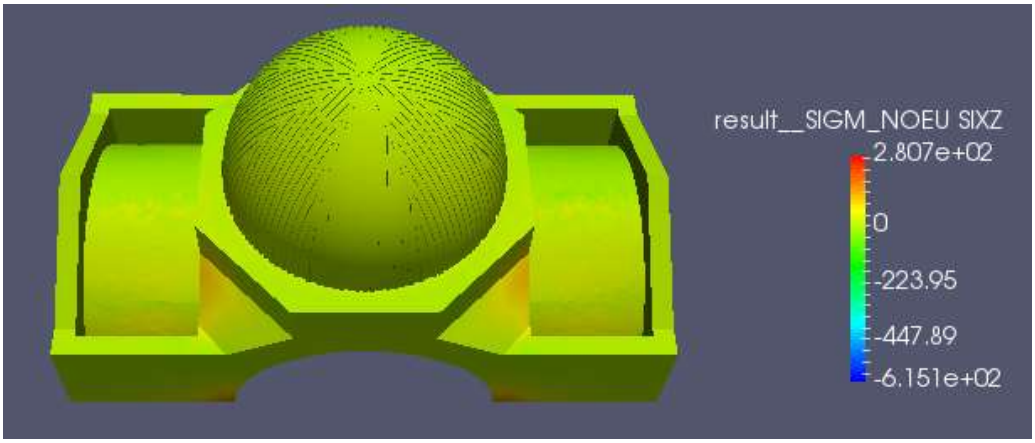


*Figure 126. Result of $\tau_{xz}$ stresses in the model B. Stage 0 – Step 3*

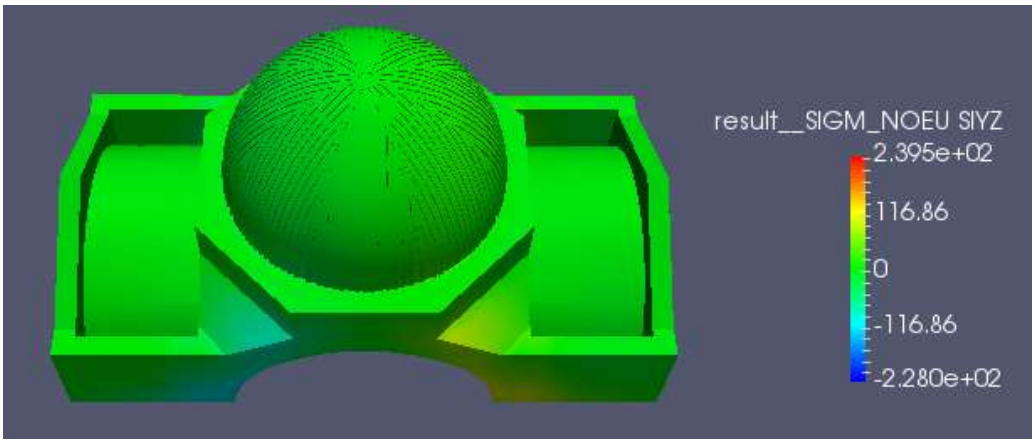


*Figure 127. Result of $\tau_{yz}$ stresses in the model B. Stage 0 – Step 3*

### *6.2.3.2. Stage 0 – Step 5*

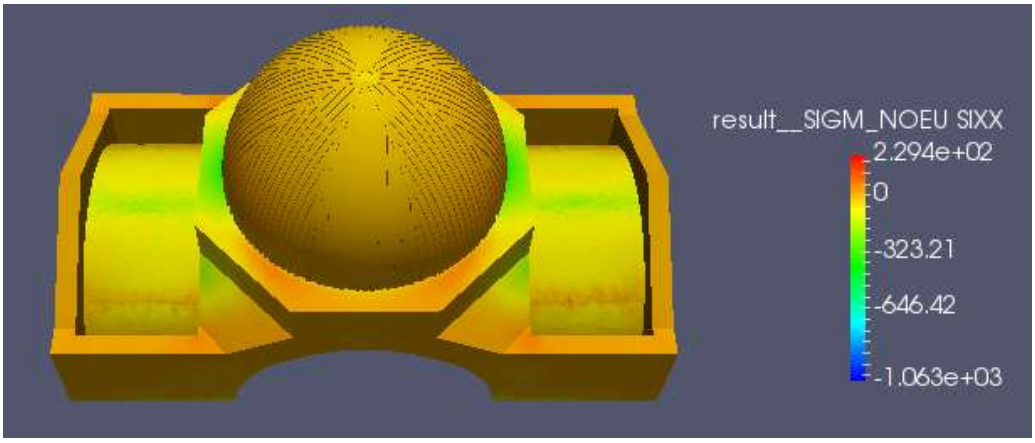


*Figure 128. Result of $\sigma_{xx}$ stresses in the model B. Stage 0 – Step 5*

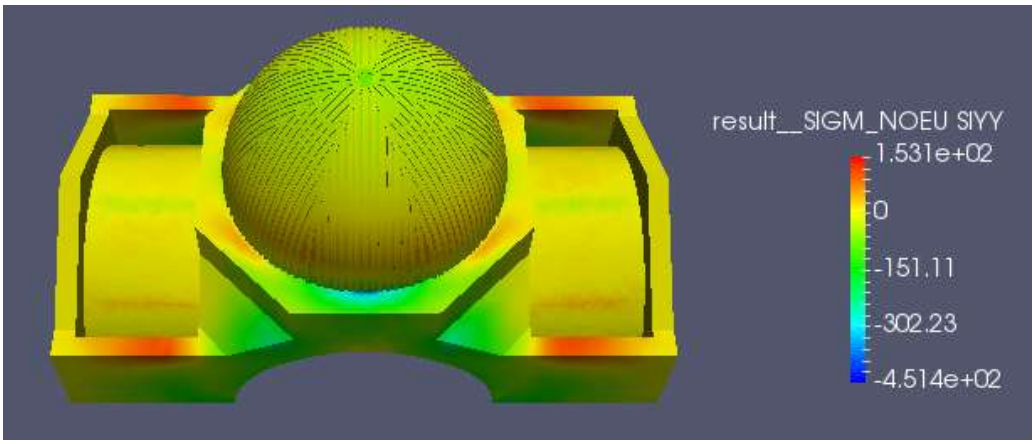


*Figure 129. Result of $\sigma_{yy}$ stresses in the model B. Stage 0 – Step 5*

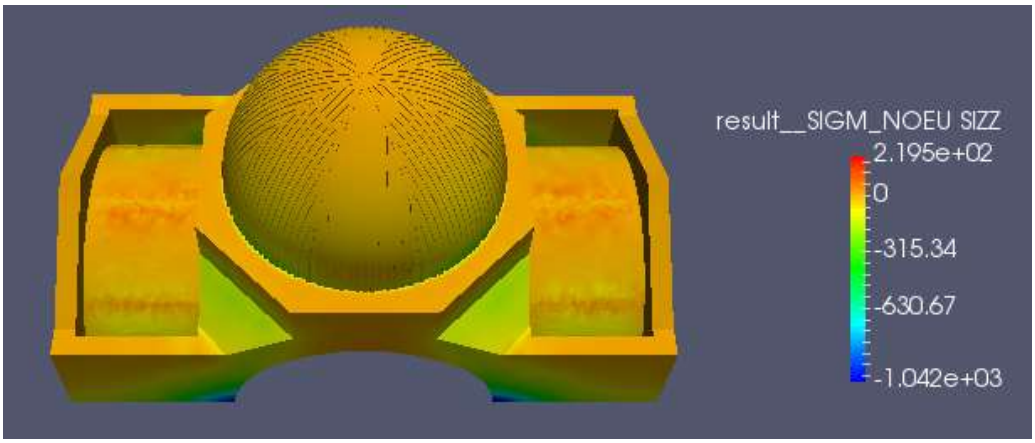


*Figure 130. Result of $\sigma_{zz}$ stresses in the model B. Stage 0 – Step 5*

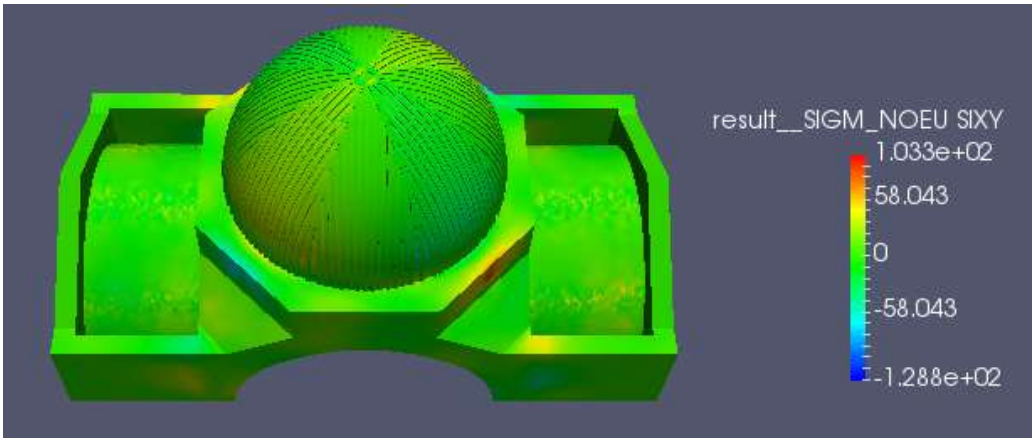


*Figure 131. Result of $\tau_{xy}$ stresses in the model B. Stage 0 – Step 5*

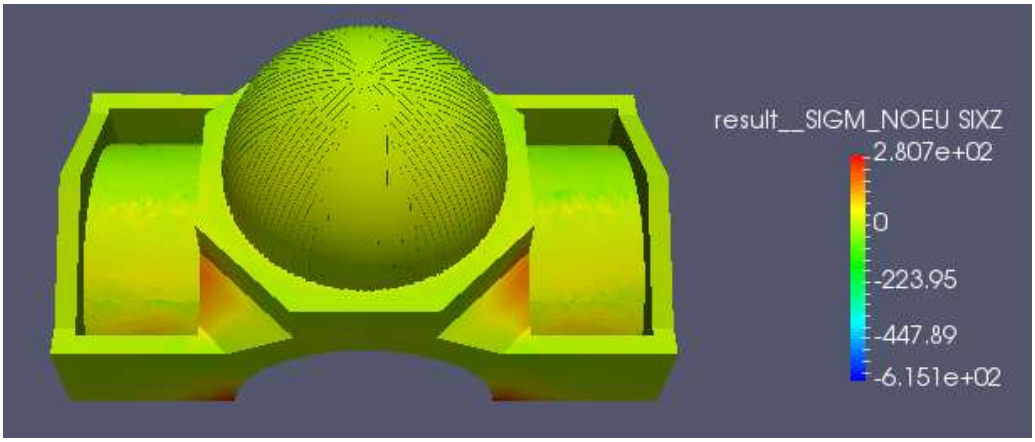


*Figure 132. Result of $\tau_{xz}$ stresses in the model B. Stage 0 – Step 5*

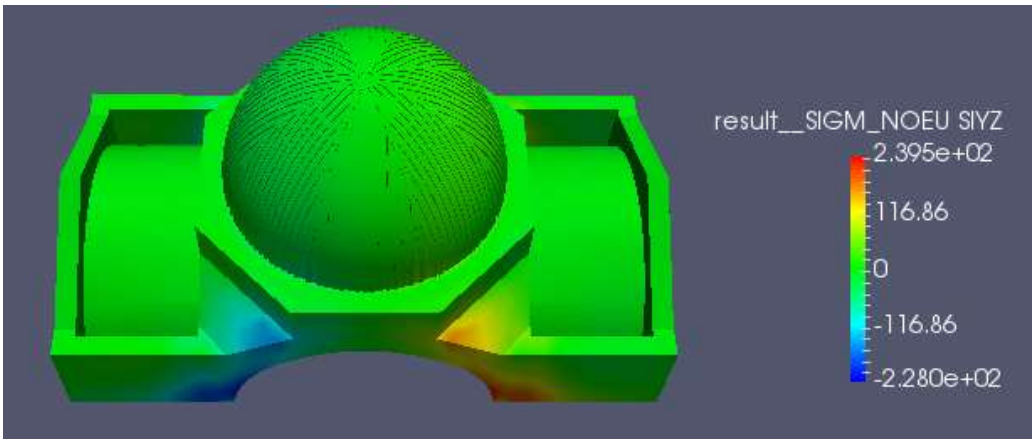


*Figure 133. Result of $\tau_{yz}$ stresses in the model B. Stage 0 – Step 5*

### *6.2.3.3. Stage 1 -Step 3*

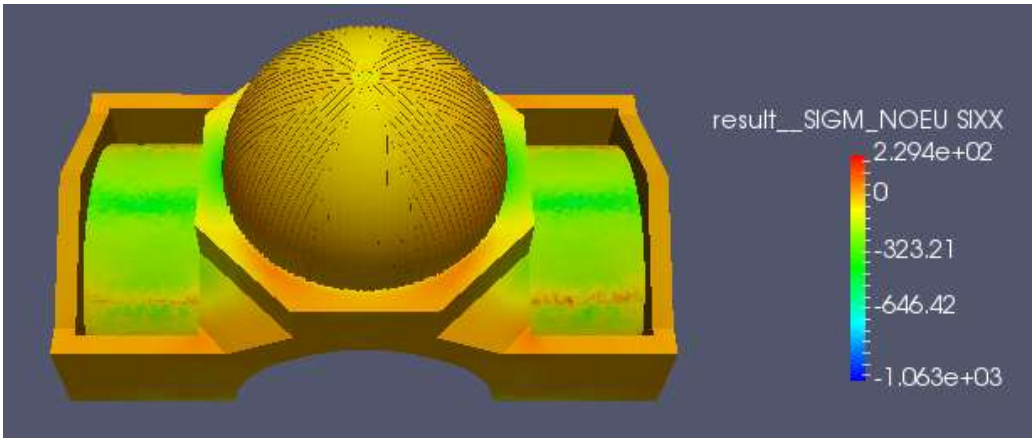


*Figure 134. Result of $\sigma_{xx}$ stresses in the model B. Stage 1 – Step 3*

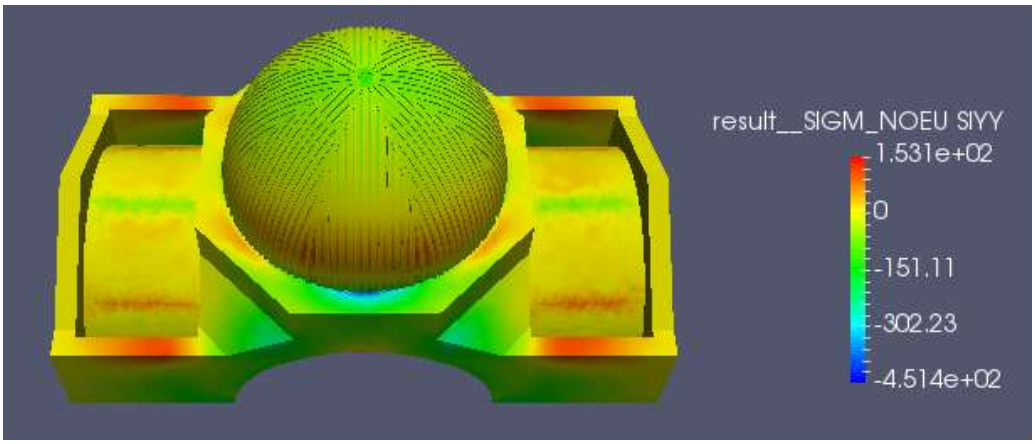


*Figure 135. Result of $\sigma_{yy}$ stresses in the model B. Stage 1 – Step 3*

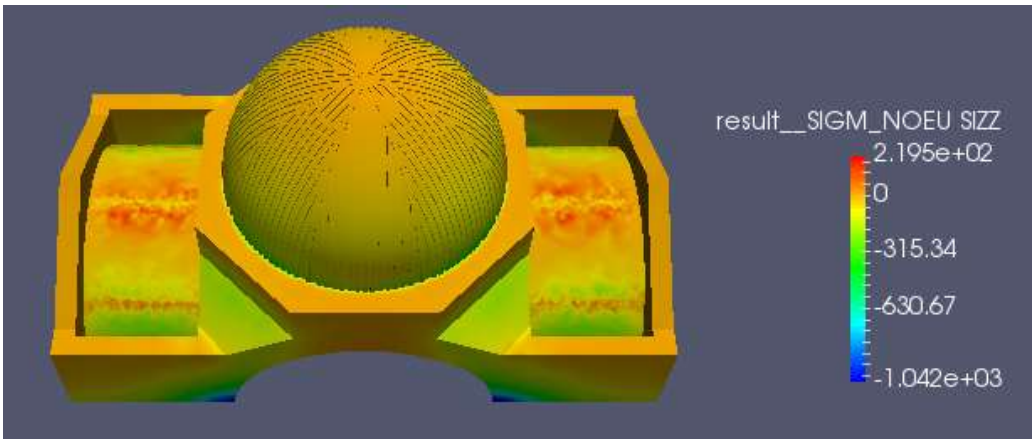


*Figure 136. Result of $\sigma_{zz}$ stresses in the model B. Stage 1 – Step 3*

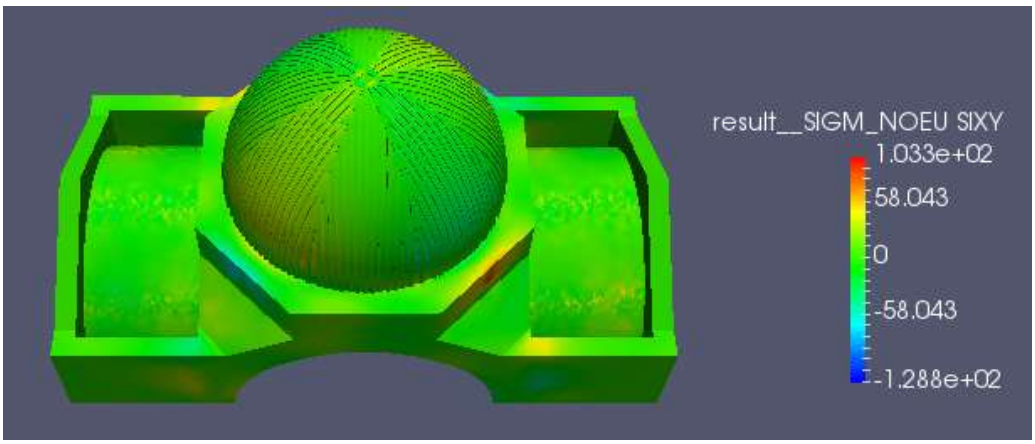


*Figure 137. Result of $\tau_{xy}$ stresses in the model B. Stage 1 – Step 3*

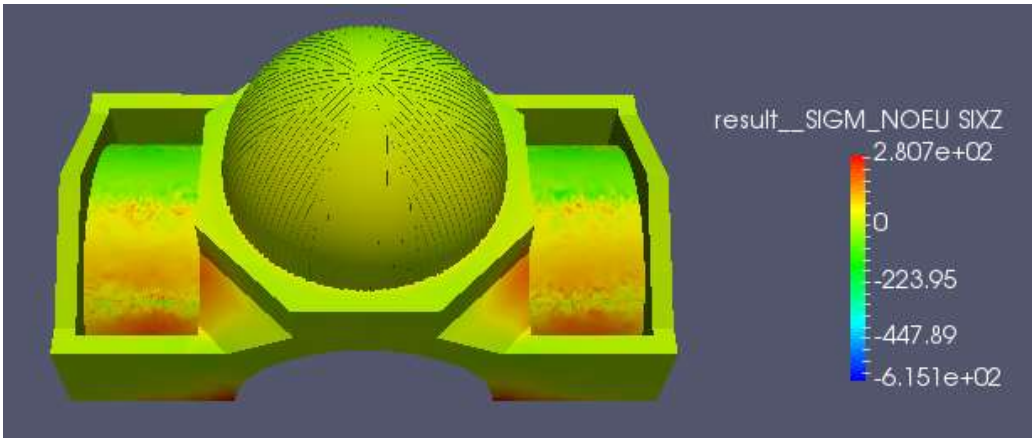


*Figure 138. Result of $\tau_{xz}$ stresses in the model B. Stage 1 – Step 3*

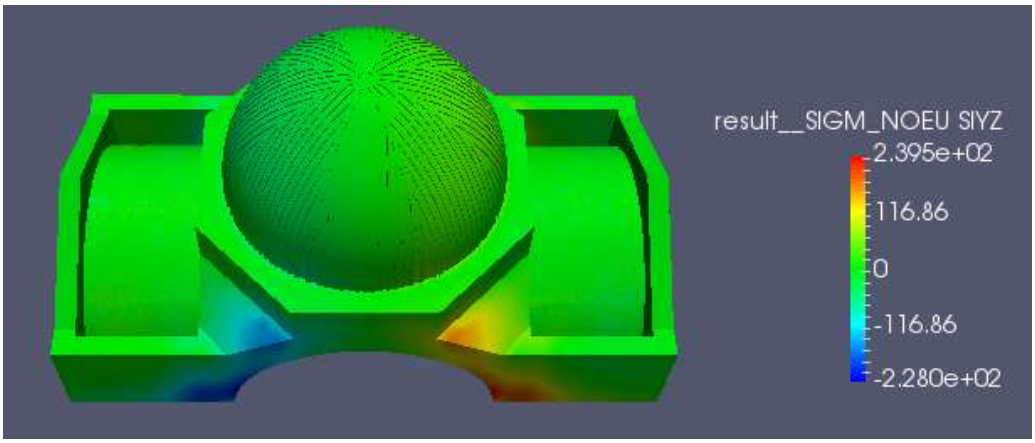


*Figure 139. Result of $\tau_{yz}$ stresses in the model B. Stage 1 – Step 3*